FOODBORNE PATHOGENS DETECTION WITH NANOPOROUS ANODIC ALUMINUM OXIDE MEMBRANE BASED BIOSENSOR

TAN FEI

M.Phil

The Hong Kong Polytechnic University

2012

The Hong Kong Polytechnic University

Department of Health Technology and Informatics

Foodborne Pathogens Detection with Nanoporous Anodic Aluminum Oxide Membrane Based Biosensor

TAN FEI

A thesis submitted in partial fulfillment of the requirements for the degree of Master of Philosophy

June 2011

CERTIFICATE OF ORIGINALITY

I hereby declare that this thesis is my own work and that, to the best of my knowledge and belief, it reproduces no material previously published or written, nor material that has been accepted for the award of any other degree or diploma, except where due acknowledgement has been made in the text.

TAN Fei

Abstract

This research investigated nanoporous anodic aluminum oxide membrane based immnuosensor for foodborne pathogenic bacteria detection by impedance spectrum. Polydimethylsiloxane (PDMS) based immnuobiosensors integrated with nanoporous alumina membrane were developed for detection of *E. coli O157:H7* and *Staphylococcus aureus* respectively and simultaneously. Firstly, antibodies to the targeted bacteria were covalently immobilized on the nanoporous alumina membrane via self assembled (3-glycidoxypropyl)trimethoxysilane (GPMS) silane. The successful covalent immobilization of silane monolayer on nanoporous membrane surface was characterized by X-ray photoelectron spectroscopy (XPS). The antibody immobilization on silane modified membrane was also confirmed by XPS and Atomic Force Microscopy (AFM). Then, single type bacteria detection system and simultaneous detection system for multiple type bacteria detection were developed for impedance measurement. For single type bacteria detection, impedance spectrum was first recorded for target bacteria samples using specific antibody immobilized nanoporous membrane with a frequency range from 1 Hz to 10,000 Hz. Impedance amplitude changes induced by target bacteria capturing with specific antibody modified membrane were found to increase with the bacteria concentrations. The sensing limit was around 10^3 CFU/ml. Cross experiments between antibody immobilized membranes and non-target bacteria were also performed to test the specificity of this device. No obvious impedance amplitude change was found for non-target bacteria samples. These results were also confirmed by sandwich type

fluorescence immunoassay. For the simultaneous detection system for multiple type bacteria detection, mixed bacteria samples with *E. coli O157:H7* and Staphylococcus *aureus*, and samples with only one type bacteria were tested. The impedance changes on *E. coli O157:H7* detection chamber and *Staphylococcus aureus* detection chamber showed the increase with related bacteria concentrations in the mixture samples, respectively. However, when only one kind of bacteria such as *E. coli O157:H7* or *Staphylococcus aureus* added into the system, only the specific antibody modified membrane side showed an increase of impedance amplitude change. For response time detection experiment, the detection assay for both *E. coli O157:H7* and *Staphylococcus aureus* could be completed in around 3 hours.

Acknowledgement

I would like to express my sincere and deepest gratitude to my supervisor, Dr. Mo Yang. His guidance and advice was invaluable to my research and thesis. His tolerance and encouragement supported me throughout my graduate studies.

I would like to thank Dr. LEUNG Hang Mei Polly for bacteria samples preparation and guidance, Mr Man Nin YEUNG from MRC for SEM experiment, Ms Winnie Wu from CSAR in Hong Kong Baptist University for the help of XPS and Dr. Shuangyi Liu from ME in University of Hong Kong for AFM experiment. I also want to express my thanks to HTI general office for their great support.

The assistance from my laboratory colleagues was also greatly appreciated. I would like to express my sincere thanks to our group members: Dr. XU Baojian, Dr. LIU Zongbin, Dr. YU jinjiang, Mr. POW Yu Fung, Mr. CHEN Xi, Mr. YUM Kee Him and Miss. QIN Xueshan.

Finally I want to express my great acknowledgment to my parents for their continue encouragement and support which has given me confidence and strength.

TAN Fei

Table of Contents

List of Figures

List of Tables

Chapter 1 Introduction

1.1 Diseases caused by Foodborne Pathogenic Bacteria

1.1.1 Foodborne Pathogenic Diseases

Foodborne illnesses are defined by World Health Organization (WHO) as diseases caused by agents that enter the human body from food. They are usually infectious or toxic in nature. The illnesses caused by presence of pathogenic bacteria or other species of microbes are infectious while the illnesses caused by the ingestion of toxins contained within the food are toxic. In recent decades, the foodborne diseases have emerged as major concerns of public and increasingly threaten the health of people. In the United States, there are 6 million to 81 million persons affected by foodborne diseases each year (Mead et al. 2000). In Hong Kong, many efforts have been spent on investigating all the foodborne diseases outbreak and promoting food safety knowledge, the number of people infected by foodborne diseases and the incidence of foodborne disease outbreaks are continuously increasing from 1996 to 2005 (Fig 1.1) (Chan and Chan 2008).

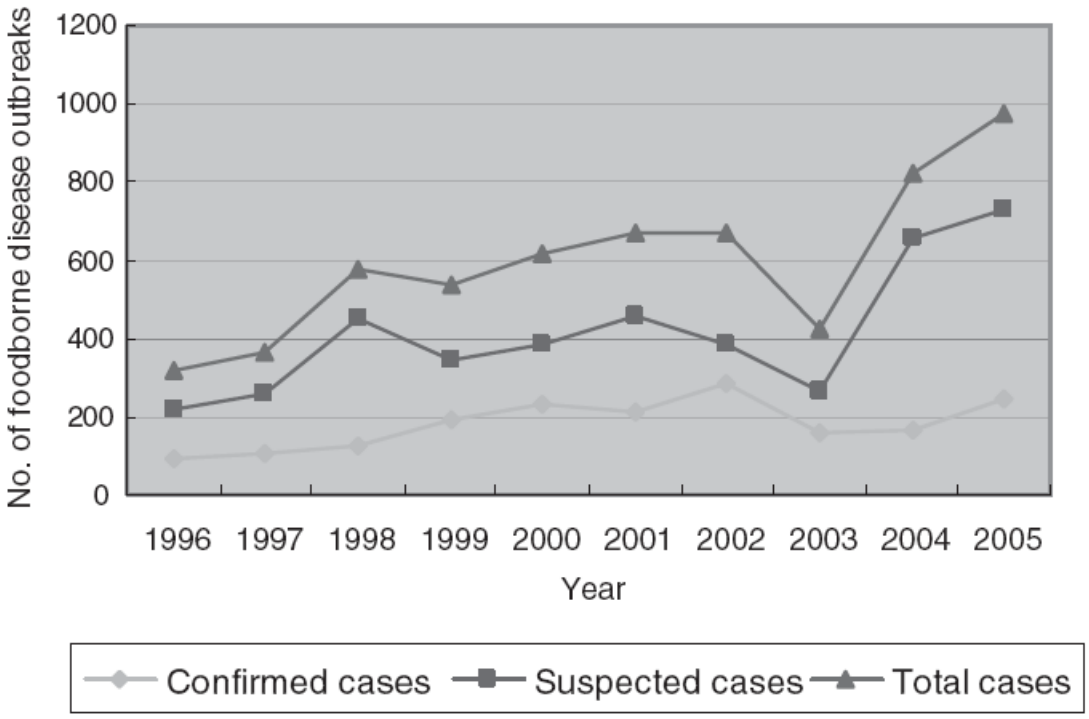

Fig 1.1 The number of foodborne diseases outbreaks in the Hong Kong Special Administrative Region increases from 1996 to 2005 (Department of Health 2006, The Government of the Hong Kong Special Administrative Region).

1.1.2 Foodborne Pathogenic Bacteria

Among the pathogenic microorganisms, including viruses, pathogenic bacteria, parasites, fungi, toxins and prions, which cause foodborne diseases, pathogenic bacteria are the most common foodborne pathogens, accounting for 91% of all outbreaks of foodborne diseases in the United States (Yang and Bashir 2008). Table 1.1 shows the types of important foodborne pathogenic bacteria with the caused disease, secreted toxins, infection sources and dose. The annual cost of human illness caused by six major pathogenic bacteria, including *Salmonella*, *Campylobacter jejuni*, *E. coli O157:H7*, *Listeria monocytogenes*, *Staphylococcus aureus* and *Clostridium*

perfringens, is estimated around $9.3-$12.9 billion in USA, among which 30%-50% are attributed to foodborne diseases. The six major pathogenic bacteria are characterized in Table 1.2 with their estimated annual cases, hospitalizations and deaths (Leonard et al. 2003).

Table 1.1 Important foodborne pathogenic bacteria (Leonard et al. 2003)

Bacteria	Disease	Toxin	Sources of infection	Infectious dose	Symptom onset time
Bacillus anthracis	Anthrax	Edema factor	Milk or meat	10^6 cells/g	6-15 h
Campylobacter jejuni	Diarrhea dysentry	-	Dairy products, meat, and mushrooms	400-500 cells	2-5 days
Clostridium botulinum	Botulism	Neurotoxin	Low acid and inadequate processed foods	Few nanograms of toxin	18-36 h
Escherichia coli O157:H7	Gasteroenteritidis	Enterotoxin	Meats, fish, milk, rice, vegetables	10 cells	12 h to 3 days
Salmonella typhi and *paratyphi*	Typhoid fever, paratyphoid	-	Eggs, mMilk, meats	15-20 cells	6-48 h
Shigella dysenteriae	Bacillary dysentry	Neurotoxin	Salad, milk, dairy products, poultry	10^1 - 10^2 cells	12-50 h
Staphylococcus aureus	Pneumonia	Entrotoxin	Meat, poultry, milk, dairy products	10^5 cells/g or 1 g toxin	Few hours
Streptococcus spp.	Fever, sore throat	-	Milk, dairy products, sausages	10^3-10^7 cells	1-3 days
Listeria monocytogenes	Listeriosis	-	Milk, dairy products, poultry, meats	400-1000 cells	>12 h

Table 1.2 A summary of estimated foodborne illnesses, hospitalizations and deaths caused six major pathogenic bacteria in the US annually as calculated by the USDA's economic research service (Leonard et al. 2003).

Bacteria	Estimated annual cases	Estimated annual hospitalisations	Estimated annual deaths
Salmonella	1,342,532	16,102	556
Listeria monocytogenes	2493	2298	499
Campylobacter spp.	1,963,141	10,539	99
Escherichia coli (0157:H7 and other types)	173,107	2785	78
Clostridium perfringens	248,520	41	7
Staphylococcus food poisoning	185,060	1753	2

1.1.3 *Escherichia* (*E. coli*) *O157:H7* and *Staphylococcus aureus*

Bacteria of *E. coli O157:H7* and *Staphylococcus aureus* are the most popular pathogenic bacteria which have attracted much of researcher's attention, and they are also usually appeared in our daily life, therefore, I choose them as the objects.

E. coli was first discovered by Escherich in 1885 as a Gram negative rod-shaped bacterium. *E. coli* is a typical inhabitant of the human intestinal tract and is often motile by means of flagella. The shape of *E. coli* is unicellular with about 1 micrometer in width and 2-4 micrometers in length. Most strains of *E. coli* are harmless, however, some strains such as serotype O157:H7 which is an enterohemorrhagic strain of the bacterium *E. coli*, can cause serious foodborne illnesses or deaths in the elderly, the very young or the immunocompromised patients. The "O" in the name means the somatic cell wall antigen number and the "H" means the flagella antigen, therefore, *E. coli O157:H7* expresses the 157th somatic antigen identified and the 7th flagella antigen. *E. coli O157:H7* was first recognized as a pathogen illness during two outbreaks of bloody diarrhea in Oregon and Michigan of United States in 1982 (Riley et al. 1983; Wells et al. 1983). In 1983, Karmali and his team found an association between *E. coli* strains (including O157:H7) which produced a cytotoxin lethal (Shiga toxin) and enteropathic haemolytic uraemic syndrome (HUS) which was characterized by thrombocytopenia, acute renal injury and microangiopathic haemolytic anaemia (Karch et al. 2005). Soon after this, the strain of O157:H7, the first of several strains recognized as enterohaemorrhagic *E.*

coli (EHEC) (Levine et al. 1987), which was transmitted to bodies from contaminated food such as raw milk and undercooked ground meat.

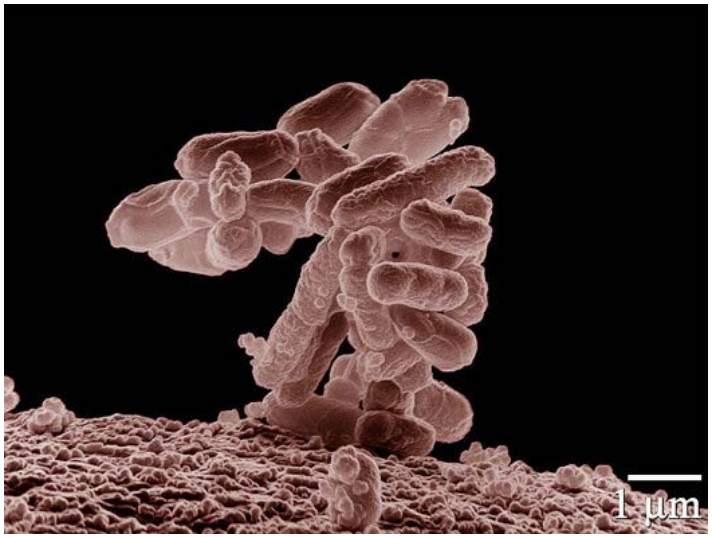

Fig 1.2 *E. coli O157:H7* at 10000x (POPSIC)

E. coli O157:H7 first attracted people's attention after the outbreak in 1993 in Seattle-Tacoma, where more than 700 persons infected from hamburger-associated food and 4 of them died (Obrien et al. 1993). After that, outbreaks of *E. coli O157:H7* infections were reported associated with roast beef (Rodrigue et al. 1995), unpasteurized apple juice ([Anon] 1996; Hilborn et al. 2000), Jerky made from deer meat (Keene et al. 1997), Mesclun Lettuce (Hilborn et al. 1999), white radish sprouts (Michino et al. 1999) and Genoa salami (Williams et al. 2000). In recent decades, the number of outbreaks caused by *E. coli O157:H7* increased dramatically. In 1999, several children were infected by *E. coli O157:H7* during swimming in Washington, United States (Bruce et al. 2003; Bopp et al. 2003). Large outbreaks have been reported from Europe (Dundas et al. 2001; Sartz et al. 2008), Japan (Ahmed et al. 2005), Canada (Ali 2004; MacDonald et al. 2004), United States (Kotewicz et al.

2008; Goode et al. 2009). In Hong Kong, there were also reports about *E. coli O157:H7* isolated from cattle and pigs in an abattoir (Leung et al. 2001).

Staphylococcus aureus (*S. aureus*) is a Gram-positive and non-motile bacterium which appears as grape-like clusters (*staphylo* means grape in greek) with a large, round and golden-yellow colonies. *S. aureus* was discovered by the surgeon Alexander Ogston in Scotland in 1880 in pus from surgical abscesses. It is a spherical cell with 1 micrometer in diameter and always hemolytic on blood agar. *S. aureus* can lead to different types of suppurative infections and toxinosis in human, such as boils and furuncle. Furthermore, with several virulent characteristics, *Staphylococcus aureus* causes more serious infectious diseases such as endocarditis, pneumonia and bacteremia. The *S. aureus* infections are usually blocked by normal host defenses at the portal of entry. However, if the host defenses are destroyed even by a minute needle-stick or a surgical wound, the bodies could be easily colonized by *S. aureus*, which makes it hard to control the infections. *S. aureus* could also colonize in human through respiratory tract and cause infections such as *Staphylococcal* pneumonia. Therefore, *S. aureus* is considered as a serious and important pathogen. Methicillin-resistant *Staphylococcus aureus* (MRSA) are strains of *Staphylococcus aureus* that could resist to beta-lactam antibiotics, including the penicillins and cephalosporins. MRSA always occurs in hospital among patients with invasive apparatus, trauma and weak immune systems. It commonly causes serious infections such as blood poisoning (septicemia) and heart valve infection.

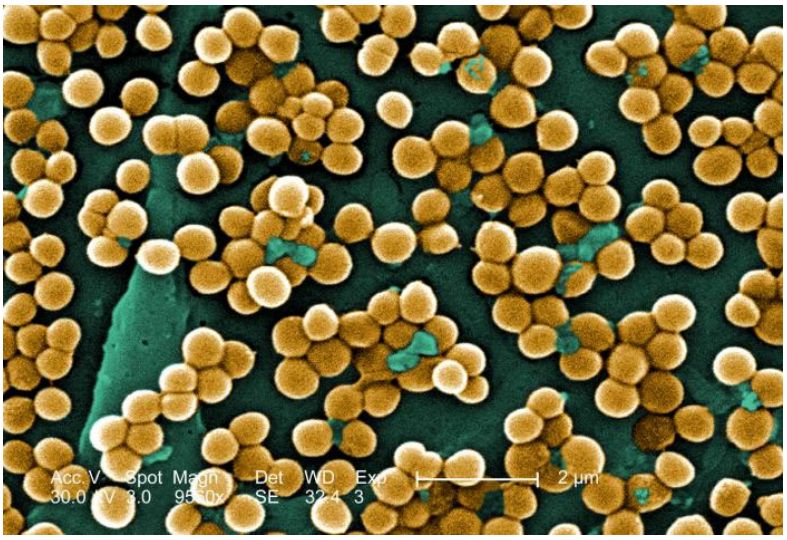

Fig 1.3 *Staphylococcus aureus* at 9500x (Center of Disease Control, CDC stock photo)

It was reported in the early 21st century that 14 patients were involved in the MRSA infection in the surgical departments of the Atrium Medical Center, Netherlands. Two months later, another MRSA outbreak happened involving 7 patients in the nursing home and five months later, one patient developed an MRSA infected after an abdominal surgery (Wagenvoort et al. 2000). Subsequent outbreaks were reported in southwestern Alaska caused by MRSA skin infections (Baggett et al. 2001), San Diego, United States (Campbell et al. 2004), France (Guerin et al. 2000), Australia (O'Brien et al. 2004), Norway (Larssen et al. 2005), Brazil (d'Azevedo et al. 2008) and Singapore (Chan et al. 2009).

MRSA is an epidemic and important pathogen in Hong Kong. It was first reported in Hong Kong in 2004 (Ho et al. 2004). Hong Kong is one of the regions which has the highest prevalence rates of MRSA among the whole Asia Pacific regions from previous studies (Bell et al. 2002; Ip et al. 2004). The Hong Kong Government soon

established monitoring group to surveillance MRSA with the help of Center of Health Protection (CHP) and the Center of Infection in the University of Hong Kong (Ho et al. 2007). All the hospital and university microbiologist of Hong Kong were encouraged to collect MRSA infection cases for this monitoring group since 2005 and the volunteers from all industries reported cases to CHP. The Hong Kong government also began a program which could collect wound swabs from patients with purulent skin infection for MRSA culture in 2006. MRSA infection was regarded as a statutory notifiable infection to help monitoring group for surveillance effectively. During the first half year of 2007, there were 70 persons who got MRSA infection in Hong Kong and the cases were evenly distributed geographically with 30% in Kowloon, 26% in New Territories West, 19% in New Territories East and 26% in Hong Kong Island (Tsang and Tsui 2007).

Staphylococcal enterotoxins (SEs) can be generated in some strains of *S. aureus*, which makes *S. aureus* the major pathogen for food poisoning. *S. aureus* could survive in a wide range of temperatures from 7℃ to 48℃ (Schmitt et al. 1990) and wide sodium chloride concentrations (up to 15%), which makes *S. aureus* difficult to control in food. The symptoms of staphylococcal food poisoning include nausea, abdominal cramps, vomiting and sometimes followed by diarrhea. Outbreaks of community-acquired foodborne illness caused by methicillin-resistant *Staphylococcus aureus* were also reported in 2002, where three children were confirmed to infected by MRSA after eating shredded pork and coleslaw from a convenience-market delicatessen (Jones et al. 2001). *Staphylococcus aureus* food

poisoning outbreaks were also associated with egg yolk (Miwa et al. 2001), spaghetti and meat sauce (Mouallem et al. 2003), and a snack made up of potato balls fried in vegetable oil (Nema et al. 2007).

1.2 Traditional Methods for Pathogenic Bacteria Detection

Pathogenic bacteria detection is one of the most important tasks for food safety and public health. To avoid diseases caused by pathogenic bacteria, the process of detection and identification is the first control step. Therefore, it is significantly necessary to control these bacteria in food and water supply by effective detection and inspection approaches. Traditional methods for bacteria detection mainly rely on microbiological and biochemical techniques. Culture and colony counting method and electron microscopy are generally based on counting bacteria cells. The method of immunology involves microbiological reaction between antibody and antigen and the method of polymerase chain reaction (PCR) is based DNA analysis (Velusamy et al. 2010).

1.2.1 Culture and Colony Counting Methods

The culture and colony counting method is the oldest and standard method for bacteria detection. It includes the procedures of microbiological culturing, isolation of pathogen and enrichment and plating. Then pathogenic bacteria can be detected by measuring physicochemical changes caused by their metabolic activities or growth

by optical methods (Swaminathan and Feng 1994). Although reliable, the procedure of this conventional method is labor intensive and excessively time-consuming, taking up to several days to yield confirmed results (de Boer and Beumer 1999). Therefore, it is not suitable for making timely assessments on food quality.

The fluorescent-antibody (FA) technique could be applied to count specific bacteria in situ. In general, fluorochrome labeled antibody binds with specific bacteria. If the bacteria cells present, the combined specific antibodies would cause them to fluoresce and the number of fluorescing cells is then counted by an epifluorescence microscope (Hobson et al. 1996). The most widely used fluorochrome is fluorescein, such as fluorescein isothiocyanate (FITC). The fluorescent-antibody technique is a simple and direct method for bacteria detection. However, most fluorochromes are prone to photobleaching which makes the detection process not stable.

1.2.2 Electron Microscopy Methods

Some traditional methods used for pathogenic bacteria identification focus on the morphology feature changes by bacteria metabolism with the help of microscopy techniques. Bacterial cells were counted and sized by scanning electron microscope (SEM) on membrane filters (Krambeck et al. 1981) and analyzed to measure the cell volume and dry weight by transmission electron microscope (TEM) (Borsheim et al. 1990; Loferer-Krossbacher et al. 1998).

Bacteria have also been detected by scanning probe microscopy (SPM). Howell et al. developed patterned antibody microarrays to study the ability for binding targeted bacteria. Pathogenic bacteria such as *E. coli O157:H7* and *Renibacterium salmoninarum* were detected by the microarrays with the help of high-resolution SPM imaging (Howell et al. 2003). The antibody microarrays were fabricated by the method of microcontact printing (μCP). The high specificity of bacteria binding to their specific antibody was observed by SPM compared with the low-binding selectivity to non-specific antibody. It demonstrated that the method of microarray coupled with high-resolution scanning probe was a sensitive and specific way for bacteria detection.

Huff et al. utilized surface changes of the high-resolution topographical imaging provided by Atomic Force Microscopy (AFM) to detect and characterize the viral particles and other pathogens (Huff et al. 2004). This AFM was capable of 2 nanometers lateral resolution and 1 nm vertical resolution, which could monitor the minute changes in topography. This pathogen detection system coupled with AFM could provide detailed 3-dimensional surface information and real-time data acquisition without need of signal amplification.

Microscope methods could obtain the morphology information in a direct, label-free manner and provide real-time data acquisition. Compared with fluorescent-based techniques, these label-free readout methods have the advantages of easy-operation (without multiple washing steps). Moreover, these methods could prevent the

complex labeling process which may change the morphological information of antibodies or other proteins and largely affect detection results. Meanwhile, problems such as photo bleaching and label stability could also be avoided (Huff et al. 2004). However, these microscopic techniques for bacteria detection require the high-cost instrumentations and always need skilled operators.

1.2.3 Polymerase Chain Reaction

Polymerase chain reaction (PCR) is a nucleic acid amplification technique which is widely used for bacteria detection by amplifying a piece of DNA sequence including the targeted bacteria's genetic material. It is based on thermal cycling which consists of cycles of denaturation by heating, polymerization and extension by cooling (Lazcka et al. 2007).

Ke et al. described using both conventional PCR and real-time PCR assays for detection Group B *Streptococci*. The conventional PCR assay could achieve sensitive detection with a high specificity. And the real-time PCR detection was comparable with conventional PCR in sensitivity and specificity. In addition, rapid thermal cycling for amplification time and real-time fluorescence monitoring were achieved (Ke et al. 2000).

Multiplex PCR was also used to detect different types of bacteria simultaneously by using multiple sets of primers and probes that were specific for bacteria. Hu et al.

described a simultaneous identification of serotype O157:H7 of *E. coli* and its virulence factors in a single reaction by multiplex PCR assay (Hu et al. 1999). *Salmonella spp.* and *Listeria monocytogenes* were also detected in food samples simultaneously following the procedures of culture enrichment and multiplex real-time PCR. Two designed sets of primers specific to *L. monocytogenes* and *Salmonella spp.* were used to compose the multiplex assay. Primers used for *L. monocytogenes* detection were complementary to a region of the *hly* gene while the primers to detect *Salmonella* were complementary to a region of the *bipA* gene. This multiplex real-time PCR achieved sensitive and specific detection of two kinds of bacteria simultaneously and shortened the assay time from 5-7 days to less than 2 days (Jofre et al. 2005).

Generally, the approach of PCR has a high sensitivity with a good specificity. However, it is largely restricted by assay time. In addition, the detection of bacteria with PCR is expensive and complex which requires skilled operators.

1.2.4 Immunology based Technique

The immunological detection has been successfully employed with the advantage of less assay time. The immunology-based methods are widely used to detect different kinds of foodborne pathogenic bacteria, such as *E. coli O157:H7* (Gehring et al. 2004), *Salmonella typhimurium*, *Listeria monocytogenes* (Chen and Durst 2006; Magliulo et al. 2007) and *staphylococcal enterotoxin* (Schlosser et al. 2007). The

immunology-based methods include enzyme linked immunosorbent assay (ELISA) (Johnson et al. 1995), enzyme-linked fluorescent assay (ELFA), enzyme-linked immunomagnetic chemiluminescence (ELIMCL) (Gehring et al. 2004), and immunomagnetic separation (Pyle et al. 1999).

Compared with traditional PCR and culture and colony counting method, the immunology-based methods are rapid. However, the sensitivity is low and could not be used for real-time detection. Therefore, there is an urgent need to develop a technique that could rapidly, simply, reliably detect pathogenic bacteria in real-time with high sensitivity and specificity. In addition, in view of future market, this technique should be portable and low cost.

1.3 Biosensors for Pathogenic Bacteria Detection

In the past decades, great efforts have been seen for the development of practical biosensors to offer new analytical platforms for applications in pharmaceutical industry, environmental diagnostics and food safety. A biosensing system is typically composed of a biological component and a physiochemical signal detection component to detect biological species such as nucleic acids, proteins, cells, virus, and tissues. The biological component could be microorganism, enzyme, cell, antibody, DNA or a biomimic, while the transducers may be optical, piezoelectric or electrochemical (Lazcka et al. 2007). The biosensor could be classified based on the employed transducer which plays a significant role in procedure of bacteria detection.

The transduction methods such as optical, piezoelectric and electrochemical are the most common methods used in today's research for bacteria detection (Velusamy et al. 2010).

1.3.1 Optical Biosensors

Optical biosensor is a rapid, sensitive and direct method in detection of bacteria via optical approaches. It detects the changes in optical properties of reagents, such as light adsorption, reflection, refraction, dispersion, chemiluminescence, fluorescence and light energy. Due to the high sensitivity, surface plasmon resonance (SPR) becomes the most popular technique in all optical biosensor techniques to detect bacteria. For example, Subramanian et al. used SPR biosensor to detect *E. coli O157:H7* with high sensitivity and specificity. With help of polyethylene glycol terminated alkanethiol mixed self-assemble monolayer (SAM), antibodies against *E. coli O157:H7* were immobilized on a sensor chip. Direct and sandwich assays were carried out to detect *E. coli O157:H7*. The surface of biosensor was monitored during detection by optical microscope. The detection limit was as low as 10^3 CFU/ml of *E. coli O157:H7* (CFU: Colony-Forming Unit), with high specificity against *Salmonella*. Meanwhile, the sensitivity was enhanced by 1000 times by using sandwich assay when compared with direct assay (Subramanian et al. 2006).

Waswa et al. used the Spreeta^{TM}, SPR-based biosensor to detect *E. coli O157:H7* in different food samples with specific antibody. Milk, apple juice and ground beef

patties spiked with various concentration *E. coli O157:H7* were injected on to sensor surface, and the light from an LED was reflect off a gold surface, the minimum measurable changes in refractive index (RI) caused by the antibody-antigen reaction was recorded as the detection limit. This assay demonstrated rapid and real-time detection with the sensitivity as high as 10^2-10^3 CFU/ml (Waswa et al. 2007).

1.3.2 Piezoelectric Biosensors

Piezoelectric biosensors which depend on the use of piezoelectric crystals are extremely appropriate for sensitive bacteria detection. Crystals such as quartz is made to oscillate at a specific frequency under the influence of an electric field. This frequency depends on the applied electrical frequency. Therefore, when bacterial cells bond to the surface of crystal due to the antibody-antigen reaction, the thickness of crystal changes, resulting in the frequency change of oscillation which can be detected electrically (Velusamy et al. 2010).

The piezoelectric biosensors were widely applied for rapid detection of pathogenic bacteria. Su et al. developed a piezoelectric immunosensor to monitor *E. coli O157:H7* in a short assay time based on the SAM modified surface of a quartz crystal Au electrode. The biosensor resonant frequency was decreased by the binding assay of antibody-bacteria during the detection, where the frequency shift was closely related to the concentration of *E. coli O157:H7*. By using this method, the

bacteria concentration ranging from 10^3-10^8 could be easily detected in 30-50 minutes (Su and Li 2004).

Quartz crystal microbalance (QCM) is the main type of piezoelectric biosensor. Due to the simplicity and low cost, it has been greatly applied for detection of DNA immobilization and hybridization (Caruso et al. 1997) and pathogenic bacteria (Mo et al. 2002). Mao et al. demonstrated a QCM-based DNA sensor for *E. coli O157:H7* detection based on the nanoparticle amplification. The sensor surface of QCM was modified by a thiolated single-strand DNA (ssDNA) which was specific to *eaeA* gene of *E. coli O157:H7*. The DNA hybridization between the ssDNA and the complementary DNA from *E. coli O157:H7* caused the frequency shift. Nanoparticles coated with streptavidin were used for frequency shift amplification. As a result, this QCM-based DNA sensor gave a detection limit of *E. coli O157:H7* as low as 2.67×10^2 CFU/ml (Mao et al. 2006).

1.3.3 Electrochemical Biosensors

Electrochemical biosensors are extremely important approaches for pathogenic bacteria identification and quantification. The main principle of electrochemical biosensors is that biochemical reactions produce ions and electrons or block the flow of ions and electrons, resulting in some measurable changes of the electrical property, which are detected by electrochemical instruments. Compared to optical and piezoelectric biosensor, electrochemical biosensor is portable which is amenable to

miniaturization and can be used to detect bacteria in *situ*. In addition, it allows the analyst to work in turbid media. Electrochemical biosensors can be classified by the measured transduction parameters, such as amperometric biosensor, potentiometric biosensor and impedimetric biosensor (Lazcka et al. 2007).

1.3.3.1 Potentiometric Biosensor

A potentiometric biosensor is based on ion selective electrodes. It consists of ion selective membrane bioactive materials such as enzyme. The species caused by enzyme-catalyst reaction are detected by the ion selective electrodes. The LAPS consists of an electrolyte-insulator-semiconductor structure, the potential changes caused by biochemical reaction are detected by the difference in charge distribution. A LAPS system measures the alternating photocurrent produced by light source, so that potential changes are converted to voltage (Leonard et al. 2003). The light addressable potentiometric sensor (LAPS) based filed effect transistor (FET) was reported to successfully detect pathogenic bacteria (Gehring et al. 1998; Ercole et al. 2003).

1.3.3.2 Amperometric Biosensor

The amperometric biosensor is a more sensitive method for bacteria detection compared with potentiometric biosensor. The amperometric biosensor is based on two-electrode or three-electrode system. The working electrode is generally

functionalized with bacteria antibody. A flow through immunoassay system based on amperometric technique coupled with high-dispersed carbon particles was developed to detect bacteria such as *E. coli Listeria monocytogenes* and *Campylobacter jejuni* (Chemburu et al. 2005). In this case, pathogenic bacteria cells were captured by specific antibodies immobilized with carbon particles served as solid phase, and then labeled by horseradish peroxidase (HRP) conjugated secondary antibodies to form a sandwich structure. When the peroxidase flowed through the biosensor, the amperometric signal was produced. This method provided bacteria detection limit as low as 50 cells/ml.

Amperometric technique combined with DNA hybridization and enzyme amplification is also used for *E. coli* detection. A micro-electromechanical system (MEMS) based amperometric detector for *E. coli* was designed. With the help of DNA hybridization and enzyme amplification, this assay was able to detect 1000 bacteria cells without PCR. In addition, a small sample volume on order of a few micro liters was another advantage of this system (Gau et al. 2001).

1.3.3.3 Impedimetric Biosensor

Impedimetric biosensor is a sensitive sensor in biological and chemical applications. It is based on the parameter of impedance which equals to voltage divided by current. Impedance has extended the concept of resistance into alternating current (AC). It not only describes the amplitude between voltage and current, but also the phase.

Impedance (Z) could be expressed in $R+jX$ and $Z_m\angle\theta$, where R is the real compartment, X is the imaginary compartment, Z_m is the absolute value and θ is the phase of impedance respectively. R is the resistance and the X is the reactance which is caused by the capacitance and inductance.

Impedance technique measures the electrical current when a sinusoidal voltage is applied to a system at different frequencies to get a spectrum which is called the electrochemical impedance spectroscopy. The impedance based biosensor attracts researchers' attention in application of bacteria detection for the advantage of convenience of miniaturization, easy-to-operation, inexpensive, real-time and label-free operation. More importantly, it is extraordinarily sensitive when bacteria cells attach to a substrate and alter the ionic conduction. The technique of impedance microbiology has been widely used in the application of bacteria detection and quantification in the 1990s. Impedance change in the medium is measured caused by the growth of bacteria, then the viable and dead bacteria cells is differentiated in 12 hours (Yang and Bashir, 2008).

Electrode system coupled with the equivalent circuit analysis has been developed based on the technique of impedance microbiology. Bacteria cells are cultured in medium in a chamber with microelectrodes. When the bacteria grow and adsorb on surface of electrode, the impedance amplitude of the microelectrodes change. Yang et al. demonstrated a three-electrode impedance system for bacteria of *Salmonella typhimurium* growth monitoring. By monitoring impedance spectrum, Yang et al.

found the change of double layer capacitance leaded to the impedance amplitude change at the frequency range lower than 10 kHz, which was caused by the bacteria cells adsorption on the electrode surface (Yang et al. 2003).

Due to the development of Micro Electronic Mechanical System (MEMS) technique, Interdigitated microelectrodes (IMEs) made by microfabrication technique has been developed for bacteria growth detection. An IMEs based impedance system was fabricated for *Salmonella typhimurium* growth monitoring by Electrical Impedance Spectroscopy (EIS) method (Yang et al. 2004b), in which the IMEs were applied to measure the impedance change caused by the bacteria growth. Compared with traditional methods, the response time of this technique was shorter and no pretreatments were needed in the experiment procedures.

Yang et al. integrated the indium-tin oxide IMEs into an immunobiosensor to rapidly detect the presence of *E. coli O157:H7.* Antibodies specific to *E. coli O157:H7* were immobilized onto the IMEs. The antibodies immobilization and the *E. coli O157:H7* cells binding to immobilized antibodies on IMEs caused the change of impedance which was monitored by electrochemical analyzer. This IMEs based impedance biosensor showed a detection limit of 10^6 CFU/ml (Yang et al. 2004a).

An impedance based biosensor with a microelectrode array as the transducer was also used to detect *E. coli O157:H7*. The density of the array was extremely high which enlarged the sensing area for bacteria bonding. As a result, the impedance

change was maximized because there were more bacterial cells captured on the electrode array. This biosensor provided a detection limit of 10^4 CFU/ml and could be further applied for other pathogens detection (Radke and Alocilja 2005).

In conclusion, the metal electrode-based impedance biosensor for bacteria detection is due to the impedance change of electrodes when bacteria cells adhere to the surface of electrodes. Compared with traditional methods, this technique has shortened the detection time. However, the sensitivity of metal electrodes is limited by the metal electrode polarization effect. Especially, when the size of electrodes decreases, the electrode impedance caused by the electrode polarization is much increased at the low frequency range. If the impedance related with bacteria is much smaller than this high electrode impedance, it is hard to extract the impedance component of bacteria information from total measured impedance. Moreover, most current electrode based impedance biosensor can only detect one type of bacteria at one time. So it is of great interest to develop an impedance based biosensor composed of substrate materials without polarization effect which can also be used for multiple bacteria detection simultaneously with a good sensitivity.

1.4 Nanoporous Anodic Aluminum Oxide (Alumina) Membrane

Nanoporous anodic aluminum oxide (alumina) membrane has attracted great attention as an excellent substrate in the biological research. It can be fabricated by the well established two-step anodization process. The highly ordered nanopores can be controlled by the anodization voltage. The properties of non-conductivity, well-defined nanopores, small pore diameter between 20 nm to 200 nm and high pore density ($1\times10^9/cm^2$), allow nanoporous alumina membrane to be an ideal biomaterial interface for biosensor applications. In the past decade, nanoporous membrane is of great interest as a popular platform for biosensing due to its high surface area ratio, enhanced sensitivity, biocompatibility and easy surface functionalization. Various applications of nanoporous membrane for biosensing are introduced as following.

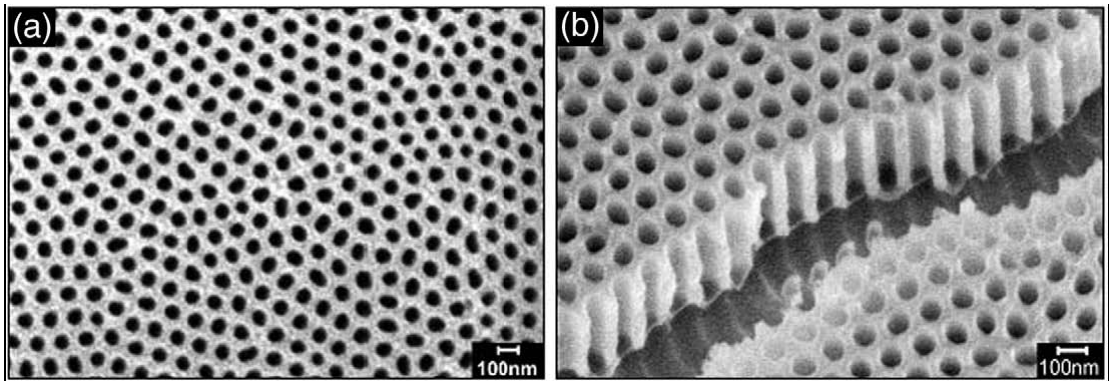

Fig 1.4 Nanoporous alumina membrane (a) top view, (b) cross-section view (Gultepe et al. 2007)

1.4.1 Support of Lipid Membrane for Single Molecule Analysis

A lipid bilayer is an artificial membrane composed of lipid molecules (usually phospholipids). It is an essential component of all biological membranes, including mammalian cell membranes. And it is important for the permeability properties of cell membranes. The functional coupling of lipid bilayer with inorganic solids became a very attractive topic in the past twenty years (Sackmann, 1996). Many efforts were spent to focus on fabricating artificial lipid membrane structures attached to a solid surface to allow for the insertion of functional transmembrane peptides for detection of transport activity, which is the prerequisite of a lipid membrane based biosensor (Romer et al., 2004). When biomolecules go through the embedded protein nanopores within the lipid membrane, the amplitude and current blockage duration are changed for the ion current (Akeson et al., 1999). Information about size, structure and sequence of small biomolecules can be derived by ion current analysis. The in vitro lipid membrane systems can be integrated with electrochemical or clamp signal measurements for ion transport study. The nanoporous membrane can be a good insulating platform to support protein embedded lipid layer for single molecule analysis. The nanopore size, pore surface chemistry, nanoporous membrane topography could be controlled in nanoscale during fabrication process of many materials. It makes possible to regulate analyte–surface interactions which has the potential to support the engineered pores for single-molecule detection and analysis (Bayley and Cremer, 2001).

1.4.2 Nanoporous Alumina Membrane for DNA Hybridization Detection

Nanoporous membranes can be fabricated with a regularly arranged hexagonal pattern of nanopores with controlled diameters. Such nanoporous membranes have high surface area which allows binding relatively large amounts of target molecules. In addition, due to the advantages of low auto-fluorescence, high porosity which allows for high flow rates through the membrane, good transparency as well as the small pore diameter which is comparable to the nucleic acid length, the nanoporous alumina membrane is widely used in for the application of DNA and RNA detection and sensing.

For the property of optical transparency in UV and IR regions, the nanoporous alumina membrane can be allowed to direct detect DNA molecules by method of optical adsorption. Vlassiouk et al used nanoporous alumina membrane to capture DNA molecules on amino silane modified surface Combined with the advantage of high surface area, the nanoporous alumina membrane was successfully used to detect and separate DNA molecules efficiently by optical and IR adsorption methods (Vlassiouk et al. 2004).

The current nano-manufacturing technique can fabricate the nanopores with comparable size with small biomolecules such as short DNA and RNA. It makes it possible to detect DNA molecules using nanoporous membrane by monitoring ionic conductivity change in the nanopores. Vlassiouk et al. used nanoporous alumina

membrane to monitor DNA hybridization process via electrical measurements. Single stranded DNA (SS-DNA) was first immobilized on the inside walls of nanopores. The ionic current was blocked through the nanopores once the target DNA was captured after DNA hybridization. The ion current change can then be monitored by cyclic voltammetry and impedance spectroscopy (Vlassiouk et al. 2005). Wang et al. used surface charge effect to modulate ionic conductance for label-free DNA sensing. A mixture of neutral silanes and morpholinos (neutral analogues of DNA) was optimized to modify nanopore surface. Upon DNA binding, a strong effect will be generated for ion conductance change (Wang and Smirnov 2009).

A capacitance sensor based on a nanoporous alumina structure was fabricated for DNA hybridization sensing (Kang et al. 2010). The membrane served as a template and the gold nanowires made by depositing gold film on surface of membrane were used as the working and counter electrodes respectively. The capacitance of the sensor decreased greatly when the complementary DNA molecules were captured.

Kim et al. described a microfluidic system made of polydimethylsiloxane (PDMS) with nanoporous alumina membrane embedded with it for DNA extraction from blood sample. The permeation rate was used to measure the extraction efficiency. A low permeation rate indicates that the DNA was captured on the membrane and not allowed to pass through the membrane. The eluted DNA from blood sample was further amplified by PCR (Kim and Gale 2008).

1.4.3 Nanoporous Alumina Membrane for Cellular Detection

In the last decade, cell based biosensor is of particular interest for cell monitoring methods due to their simplicity, sensitivity, and low cost. The cell based biosensor use the whole cell as sensing element to detect agents with physiological effects to the cells. For this purpose, it is of great interest to develop an ideal interface to control the cell surrounding microenvironment for the study of cell response to various agents.

It is important to design a biocompatible nanoporous membrane with multiple functions with long term physical and chemical stability for biosensing applications. Especially, efforts have focused on tuning surface chemistry to regulate cellular and tissue responses for implantable nanoporous membrane biosensors. Wolfrum et al. designed biohybrid system based on nanoporous alumina membrane which served as a biological interface to control the biochemical environment (Wolfrum et al. 2006). Swan et al. fabricated nanoporous alumina with uniform pore size and distribution based on the two-step anodization process. Osteoblast adhesion and morphology on different diameters of nanopores (30-80 nm) were studied by monitoring the cell morphology and adhesion. SEM images showed the cell extending into the nanopores. The advantages of using nanoporous alumina membrane with proved biocompatibility for improvement of cell response have been demonstrated (Swan et al. 2005).

The nanoporous alumina membrane was also used as a substrate for cancer cell studies. Yu et al. used nanoporous alumina membrane for the study of anti-cancer drug effect of retinoic acid (RA) on human esophageal squamous epithelial KYSE30 cancer cells with impedance spectroscopy. The sensing mechanism was based on nanopore blocking effect by adherent cells cultured on membrane surfaces. During impedance measurement, the applied electric field generated ion current through the insulated membrane but without polarization effects. This device was successfully used to monitor cancer cell adhesion, proliferation and anti-cancer drug induced change by impedance spectroscopy. Liu et al. further developed a PEG cell based microarray on nanoporous alumina membrane with cell micropatterning and controlled drug delivery to cytotoxic effects of cisplatin (Yu et al. 2009).

1.5 Scope and Outline of Thesis

The purpose of this project is to develop a PDMS based chip integrated with specific antibody immobilized nanoporous anodic aluminum oxide membrane for the detection of *E. coli O157:H7* and *Staphylococcus aureus* (most popular bacteria which appeared in our daily life) respectively and simultaneously. The detailed objectives are listed as following:

1 Immobilization of specific antibodies on nanoporous alumina membranes. Nanoporous alumina membrane is firstly modified with self assembled silane

monolayer. Then, specific antibodies are covalently grafted on the membranes via the self assembled silane monolayer.

2 Fabrication of PDMS based micro chip integrated with functionalized nanoporous alumina membrane. A PDMS based microchip is fabricated by soft lithography technique. Nanoporous alumina membranes modified with specific antibodies is integrated into PDMS based biosensor. Two types of system are developed for single type bacteria detection and simultaneous detection system for multiple type bacteria detection.

3 Single type bacteria detection with impedance measurement. The *E. coli O157:H7* and *Staphylococcus aureus* with different concentrations are detected with specific antibody modified membranes by impedance analyzer at different frequencies. The response time is measured for the two bacteria samples using specific antibody modified membranes with various concentrations which is defined as the time from adding the bacteria samples for the sensor signal response (impedance change) to reach 75% of its total value. Cross bacteria experiments are also performed to testify the specificity. Sandwich type immunoassay with fluorescence labeling is also used to determine the specificity.

4 Multiple bacteria detection using simultaneous detection system. *E. coli O157:H7* and *Staphylococcus aureus* are detected simultaneously with parallel antibody modified alumina membranes and the independent impedance monitoring units with mixed bacteria samples. Samples with only one type of bacteria were also used to testify the specificity of the system.

Chapter 2 Methodology

2.1 Surface Modification of Nanoporous Alumina Membrane

2.1.1 Silane Modification

In order to covalently immobilize the antibodies on the nanoporous alumina membrane, the surface of the membrane should be functionalized first. Silane modification method is used in this project, which employs the hydroxyl groups on the alumina membrane surface to react with (3-glycidoxypropyl)trimethoxysilane (GPMS) for consequent antibody immobilization (Fig 2.1). Silane of (3-glycidoxypropyl)trimethoxysilane (GPMS) (≥98wt.%) bought from Sigma-Aldrich is chosen with $-SiO_3$ head group and epoxy end group. The group of $-SiO_3$ can react with the hydroxyl groups (-OH) on the nanoporous membrane surface after boiling in peroxide (H_2O_2), meanwhile, the functional group of epoxy can react with amino groups in antibody for covalently bonding. Based on this bonding mechanism, the specific antibodies could be chemically and stably linked onto nanoporous alumina membrane surface.

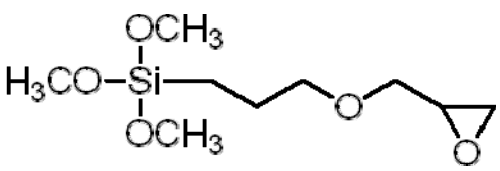

Name: (3-glycidoxypropyl)trimethoxysilane (GPMS)
Molecular Formula: $C_9H_{20}O_5Si$
Molecular Weight: 236.34

Fig 2.1 Information of GPMS silane for surface modification

The detailed silanization process is described as following. First of all, nanoporous alumina membranes (100 nm pore diameter, 60 μm thickness) were treated with 10% boiling hydrogen peroxide (H_2O_2) for about 30 min to remove any contaminants and generate reactive hydroxyl group (-OH) on the surface. Subsequently, these membranes were boiled again in deionized water for 15 min to completely clean the surface. The treated nanoporous membranes were dried by nitrogen blowing and then immediately immersed into the toluene solution with 1% GPMS overnight. GPMS silane molecules were then self-assembled onto the membrane surface. Subsequently, the membranes were rinsed 3 times with pure toluene followed by anhydrous ethanol to remove the physically absorbed GPMS molecules away from the membrane surfaces. Finally, the membranes were gently dried by nitrogen gas blowing, and stored in the environment of nitrogen for further application. The modification process of GPMS grafting onto alumina membrane is shown in Fig 2.2. The formation of GPMS silane on membrane surface was further confirmed by water contact angle measurement and X-ray photoelectron spectroscopy.

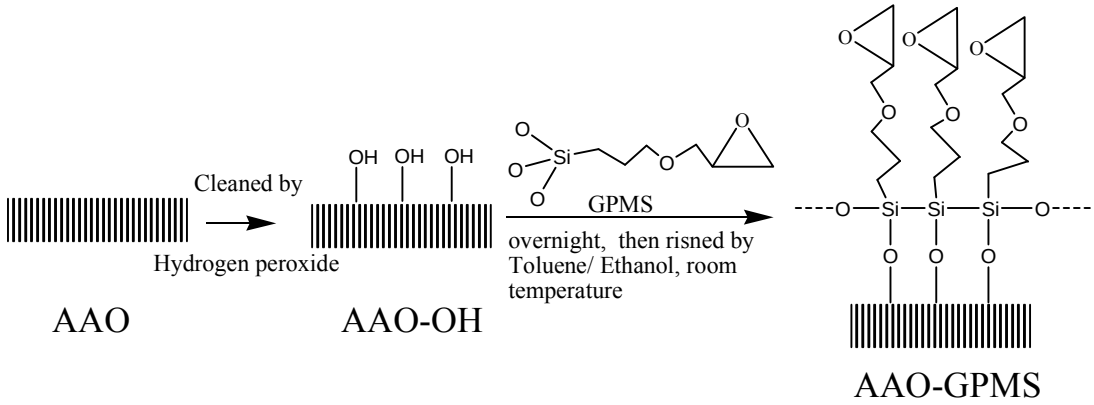

Fig 2.2 Schematic illustration of surface modification by GPMS silane

2.1.2 Antibody Immobilization

Since the active epoxy groups of the silane molecule were exposed on the surface of membrane, the antibodies with amino head groups were immobilized firmly on the silane modified nanoporous alumina membrane through covalent bonding. Antibodies for both *E. coli O157:H7* and *Staphylococcus aureus* were purchased from Abcam Ltd. Purified antibodies specific to *E. coli O157:H7* and *Staphylococcus aureus* were dehydrated and diluted with PBS solution to a concentration of 50 μg/ml, and then added onto surface of nanoporous alumina membranes respectively. Afterwards, these membranes were incubated for 24 hours in fridge at 4℃ which was appropriate to keep the activity of antibody. The antibody immobilized nanoporous alumina membranes were rinsed with PBS solution for 3 times to remove the physical and unspecific adsorbed antibodies away from the surfaces. Finally these membranes were dried with nitrogen gas. The process of antibody immobilization on GPMS silane modified nanoporous alumina membrane was shown in Fig 2.3.

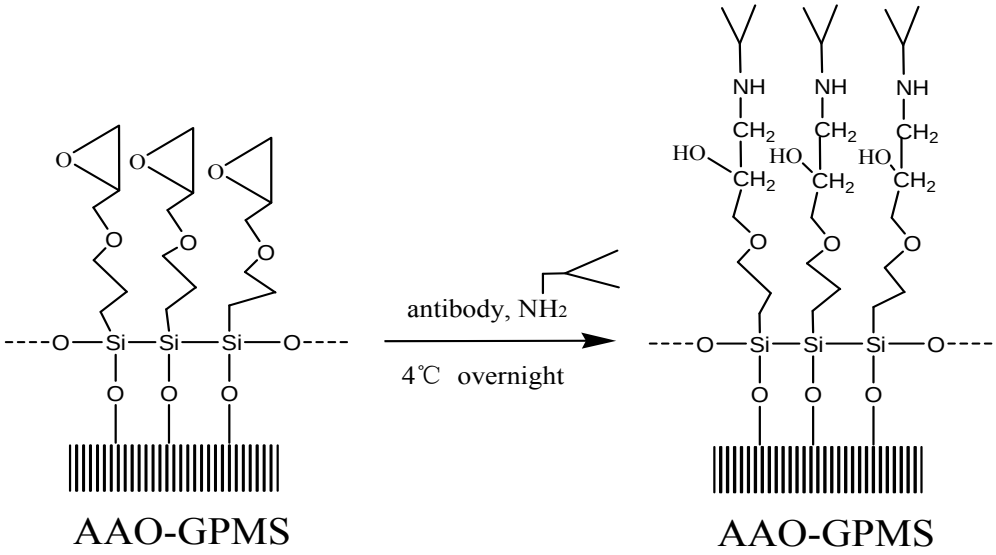

Fig 2.3 Schematic illustration of specific antibody immobilized on nanoporous alumina membranes

2.2 Surface Characterization

After surface modification, the surface of nanoporous alumina membrane was characterized to confirm the silane modification and the antibody immobilization. Water contact angle measurement, X-ray photoelectron spectroscopy (XPS), scanning electron microscopy (SEM) and atomic force microscopy (AFM) were used as the surface characterization methods.

2.2.1 Water Contact Angle Measurement

The wettability is the ability of a droplet of liquid to spread on a solid surface. It is defined as the contact angle between droplet of liquid and solid surface, which determines whether the solid surface is hydrophilic or hydrophobic. For the water

contact angle measurement, a droplet of liquid was deposited on a horizontal and flat surface of solid substrate. The water contact angle measurements measure the angle between a droplet of liquid, usually deionized water and a solid substrate when interface of liquid contacts with the surface of solid in thermal equilibrium. The surface of solid material is hydrophilic when the water contact angle is between 0° to 90°, or hydrophobic when the water contact angle is between 90° to 180°. The water contact angle depends on the solid surface properties. Therefore, if the properties of solid surfaces are altered by surface modification, the water contact angle of the surface will be changed. The water contact angle was described by the following equation, where W_A is the work of adhesion, γ_L is the surface free energy of liquid, and θ is the contact angle.

$$W_A = \gamma_L (1 + \cos\theta) \tag{2.4.1}$$

Fig 2.4 shows the contact angle goniometer (Rame-Hart 250-F1 standard goniometer, NJ, USA) used for static contact angle measurement. It includes 3 parts, luminous source, water droplet injector and camera with high resolution. 10 μL deionized water droplet was deposited onto the membrane surface and profile images captured by camera was analyzed by software of DROPiamge Advanced 2.1. The recorded data were then averaged for 10 independent measurements.

Fig 2.4 Rame-Hart goniometer contact angle equipment.

2.2.2 XPS Measurement

The GPMS covalent bonding on nanoporous membrane and the antibody immobilization were analyzed by XPS. Fig 2.5 shows the XPS equipment of a Sengyang SKL-12 electron spectrometer equipped with a VG CLAM 4MCD electron energy analyzer. Al Kα source (1253.6 eV) operated at 10 kV and 15 mA. The XPS experiments were taken in the Centre of Surface Analysis and Research of the Hong Kong Baptist University.

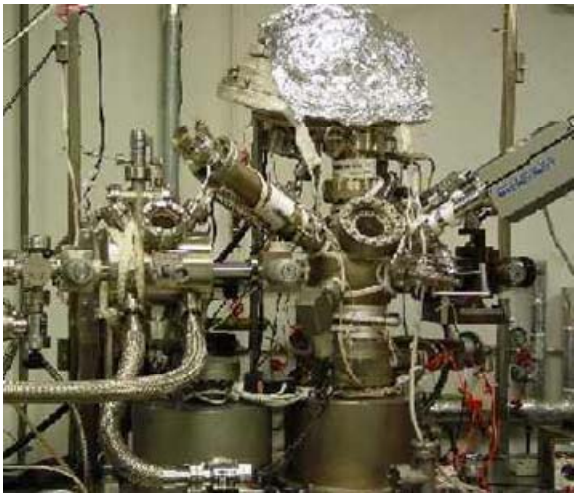

Fig 2.5 SKL-12 multi-technique surface analysis system.

Binding energy of emitted photoelectrons was tested by concentric hemispherical analyzer. Binding energy spectra from 0-1100 eV were collected and high resolution spectra were collected from 275-300 eV to detect the peaks of C1s and analyze the change of chemical bond. The hydrocarbon C1s 285.0 eV binding energy was set as reference for all spectra. The peak fit and chemical composition percentage analysis was performed by software of XPSPEAK 4.1.

2.2.3 SEM and AFM Measurements

Scanning electron microscope (JEOL Model JSM-6490) was used to take surface images of nanoporous alumina membrane with and without bacteria cells in Material Research Centre of the Hong Kong Polytechnic University. Atomic force microscope (AFM, Veeco, diMultiMod V) images were taken in the department of mechanical engineering of the University of Hong Kong for analysis of the surface morphology and thickness of nanoporous alumina membrane with antibody molecules and bacteria cells.

Atomic force microscopy (AFM) is a powerful tool for high resolution scanning. The resolution of AFM is on the order of a nanometer or even smaller, which is higher than electron microscopy. Unlike SEM which produces a two-dimensional image of a material surface, a surface profile of three-dimensional is provided by the AFM. In addition, the SEM always needs pretreatments to the samples such as gold coating which may largely damage the sample surface, and it also extremely requires a

vacuum environment when testing. However, the AFM can perform perfectly without any pretreatments and can work at room temperature in an ambient air. Therefore, AFM is especially appropriate for analysis of biological molecules or even living organisms.

2.3 Fabrication of PDMS Device with Nanoporous Membranes

PDMS devices integrated with nanoporous alumina membranes were developed for the detection of *E. coli O157:H7* and *Staphylococcus aureus*. Commercially available nanoporous alumina membranes were purchased from Whatman Ltd. with pore size of 100 nm and thickness of 60 μm for food pathogen detection and integrated into the PDMS based chip. The PDMS device with antibody immobilized nanoporous alumina membrane bonded between two PDMS compartments is shown in Fig 2.6.

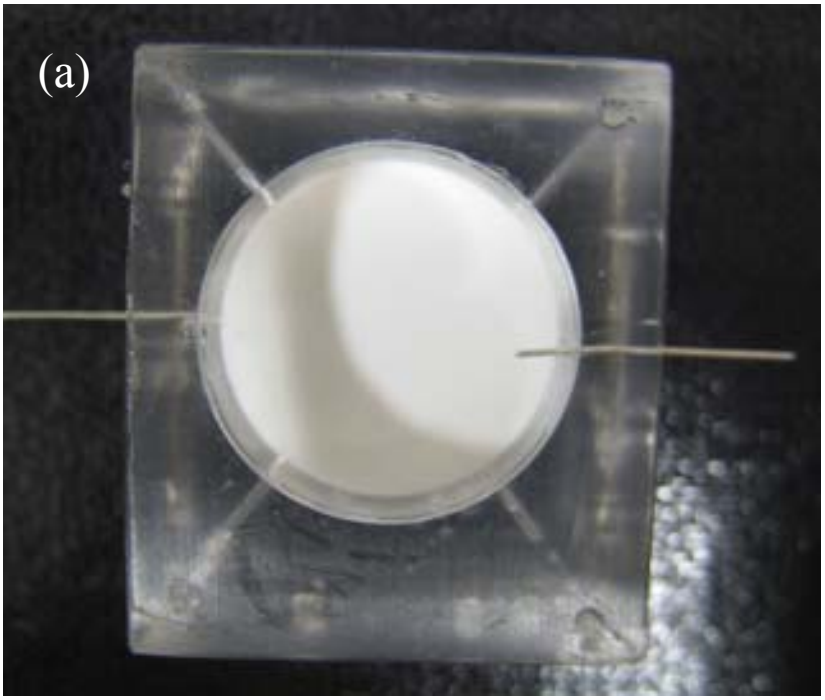

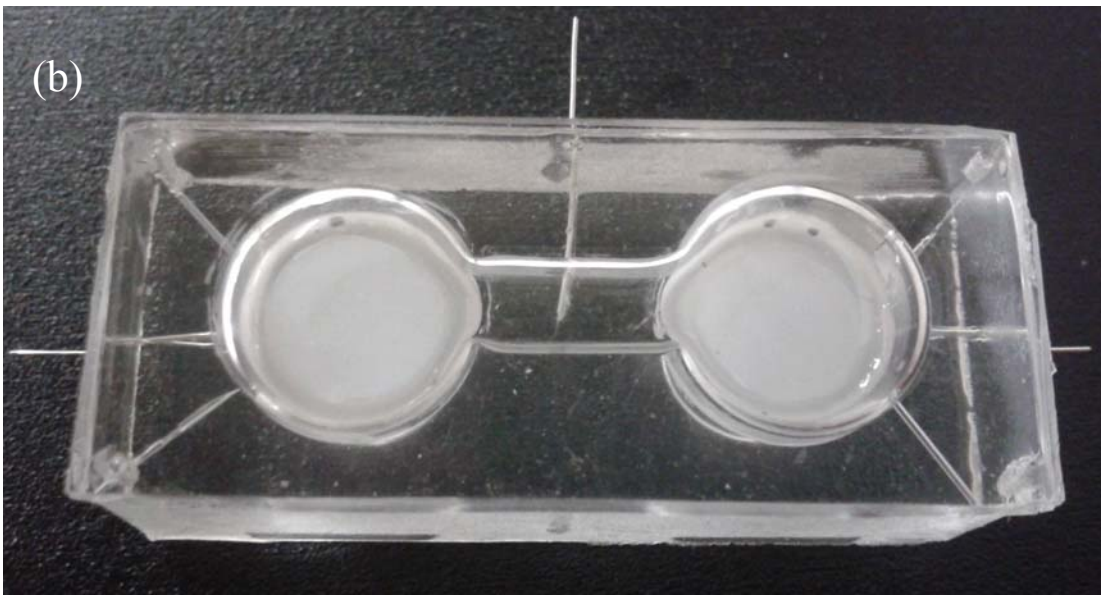

Fig 2.6 The photo of PDMS device for (a) single bacteria detection and (b) simultaneous detection of two types of bacteria

Upper and bottom compartments were fabricated by PDMS and separated by nanoporous alumina membrane. To make the PDMS compartments, silicon elastomer and curing agent were added into a clean petri dish with the ratio of 10:1, and then they were mixed together evenly by stirring. A vacuum pump was applied to pump the bubbles out of silicon elastomer and curing agent. This procedure was important to avoid the bubbles trapped in the PDMS elastomer after curing. After vacuumization, the mixed silicon elastomer and curing agent were poured into the designed mold and incubated in a oven for curing at the temperature of 75℃ for about 2 hours. After the PDMS elastomer was cured, it was cleaned with ethanol followed by deionized water. Finally, it was dried with air blowing. Afterwards, the PDMS compartments were pretreated by plasma cleaner PDC-32G shown in Fig 2.7. The purpose to perform plasma treatment was to create hydroxyl group (-OH) on the surface and change hydrophobic surface to hydrophilic surface. The hydrophobic surface could physically adsorb protein or other particles and affect the bacteria detection experiment.

Fig 2.7 Plasma cleaner PDC-32G

Fluidic channels in the upper and bottom compartments were punched using gauge needles with diameter of 0.5 mm. The platinum wires served as the working electrode and counter electrode were located into the upper and bottom compartments respectively. The microwire electrodes were further connected with the impedance analyzer. AB glue was used to seal the nanoporous alumina membrane with PDMS device to prevent electrolyte leakage.

2.4 Bacteria Capturing

Staphylococcus aureus or *E. coli O157:H7* were taken from stock culture and plated on a nutrient Luria–Bertani (LB) agar respectively for overnight incubation (20–24 h) at a 37^0C incubator before usage. The bacteria were then diluted to different concentrations in PBS solution. To prevent the non-specific adsorption, bovine serum albumin (BSA) was added as the backfilling agent. Before the bacteria detection experiment, both lower and upper chambers of the microfluidic chip were filled with PBS solution. Then the PBS solution in the upper chamber was replaced by bacteria samples and incubated for about 3 hours at 37^0C. After the binding reaction between antibodies and bacteria antigen, PBS solution was injected into upper compartment to further wash the membranes 3 times to remove the unspecific absorption of bacteria from the surface before impedance measurement. The target bacteria captured on the complimentary antibody modified membrane were confirmed by sandwich type immunoassay using fluorescent isothiocyanate (FITC)-labeled antibody. After the bacteria cells captured by specific antibodies on

the functionalized nanoporous alumina membrane, 50 μL, 0.5mg/ml fluorescein (FITC) conjugated anti-*E.coli O157:H7* and anti-*Staphylococcus aureus* antibodies (Abcam) were used to form a sandwich structure. After incubated at room temperature for 30 minutes, the membrane was rinsed by phosphate-buffered saline (PBS) solution (0.01M, PH=7.4) for three times to remove physically adsorbed FITC antibodies from the membrane surface. A fluorescence microscope (Nikon Eclipse 80i fluorescence microscope, Nikon, Japan) was used to take images.

2.5 Single Type Bacteria Detection with Impedance Measurement

The mechanism of impedance sensing system of the nanoporous membrane based impedance biosensor for single type bacteria detection is shown in Fig 2.8. After the injection of bacteria samples, bacteria cells are anchored by specific antibody immobilized on the silane modified nanoporous alumina membrane. Since the bacteria cell size is of the bacteria cell is around 1-3 μm, which is much larger than the nanopore size around 100 nm, the nanopores would be covered by the anchored bacteria. Therefore, the electrolyte current is blocked and the impedance amplitude will increase, which can be monitored by the impedance analyzer.

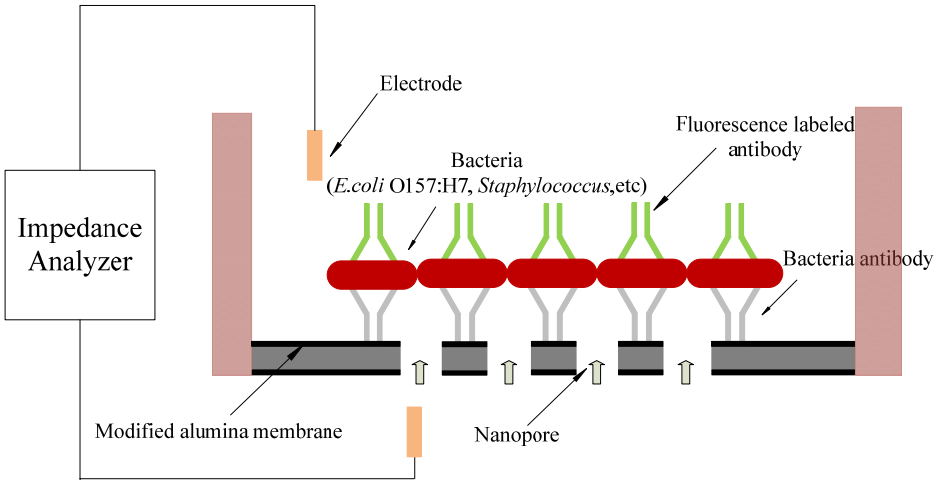

Fig 2.8 Mechanism of nanopore based bacteria impedance sensing

In the experiments, after specific antibodies were successfully immobilized onto the nanoporous alumina membrane, the left GPMS silane monolayer which did not react with antibodies were blocked by 1% bovine serum albumin solution (BSA) in PBS (Sigma-Aldrich) at 37℃ for 1 hour. Various concentrations of bacteria were then injected into the upper compartment and incubated for about 3 horus at 37℃. After the binding reaction between antibodies and bacteria antigen, PBS solution was injected into upper compartment to further wash the membranes 3 times to remove the unspecific absorption of bacteria from the surface before impedance measurement.

A platinum (Pt) wire electrode with diameter of 0.5 mm and purity of 99.95% was immersed into the upper compartment as the working electrode and another platinum electrode was placed in the lower compartment of the chip as the reference electrode. The whole testing system was connected with the electrochemical impedance

analyzer VersaSTAT3 (METEK). For all the impedance experiment, a sinusoidal alternating current (AC) with potential of 50 mV was applied during the bacteria detection procedure. The measured magnitude of impedance and phase angle between voltage and current from frequency range from 1 Hz to 10^5 Hz were recorded by the software V3-Studio (Princeton Applied Research). The temperature was maintained at 25℃ and all other environmental conditions were kept the same between experiments to prevent influence by other factors.

After the impedance spectrum was recorded by V3-Studio software, the data of impedance were extracted and analyzed. The normalized impedance change (NIC) was used to show the difference of magnitude of impedance with respect to the control data. The value of NIC was given by following equation:

$$NIC = \frac{Z_{sample} - Z_{control}}{Z_{control}} \times 100\% \qquad (2.4.2)$$

where $Z_{control}$ is the magnitude of impedance for control sample, and Z_{sample} is the magnitude of impedance for bacteria samples.

The software of ZSimpWin V3.21 (Princeton Applied Research) was used for the equivalent circuit model analysis from the measured impedance spectrum. The components of equivalent circuit model were chosen according to nanoporous membrane surface electrochemistry. The software was run iteratively to find the best

fitting of measured impedance spectrum. For this purpose, the chi-square (χ^2) value was used to determine the fitting of a given model to the experiment data. According to references, a χ^2 which was comparable with the order of 1×10^{-3} or below was accepted for an equivalent circuit (Cui and Martin 2003).

2.6 Simultaneous Detection of Two Types of Bacteria with Impedance Measurement

The principle of simultaneous bacteria detection for two types of bacteria was shown in Fig 2.9. This system was used to detect two kinds of bacteria including *E.coli O157:H7* and *Staphylococcus aureus* simultaneously. This PDMS based device was separated by the functionalized nanoporous alumina membrane with *cis* and *trans* sides. Each chamber underneath the nanoporous membrane worked as an independent *trans* compartment full of PBS solution, while the upper chamber worked as the common *cis* compartment. Three platinum microelectrodes were inserted into the two *trans* compartments and the common *cis* compartment, respectivley. As a result, each *trans* compartment could work independently with its own planar working electrode and the common reference electrode without influencing the other *trans* compartment. For example, when nanoporous membrane on *trans* (1) cpatured specific bacteria 1, the impedance between common *cis* chamber and *trans* (1) would increase due to the blocking of electrolyte current. The "open' or "close" status of nanopores of trans (2) with capturing of bacteria 2 will

not affect the impedance signals in trans (1). Both trans (1) and trans (2) could work independently with the independent planar working electrodes.

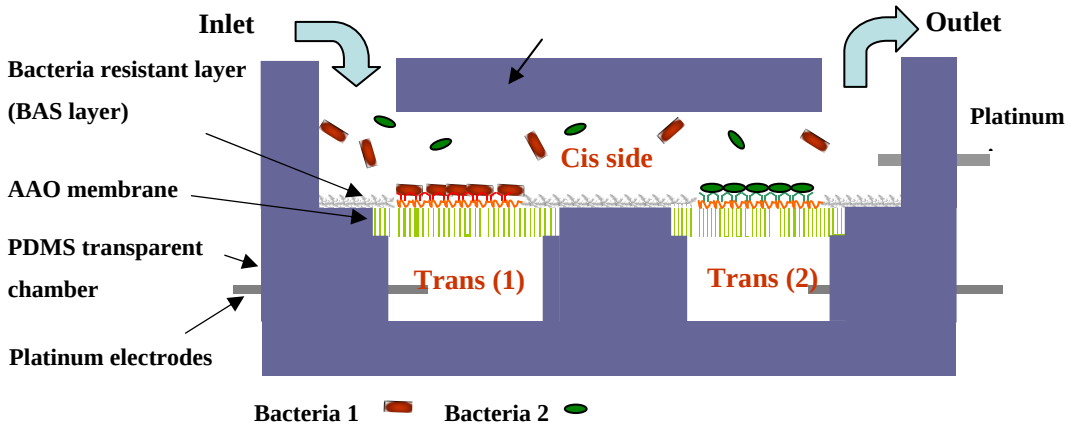

Fig 2.9 Working mechanism for multiple bacteria sensing system

The membranes on trans (1) and trans (2) were modified by anti-*E.coli O157:H7* and anti-*Staphylococcus aureus*, respectively. Two relays were connected with the two platinum microelectrodes in *trans* chambers with the common terniaml connected with the impedance analyzer. For the impedance measurement, pure PBS was first injected into *trans* compartments. Samples of mixed *E. coli O157:H7* and *Staphylococcus aureus* with different concentrations were then injected into the common *cis* compartment. To testify the specificity of this simultaneous detection system, samples of only *E. coli O157:H7* or only *Staphylococcus aureus* were also added for testing. The other impedance measurement procedures were similar to the single type bacteia detection experiment.

Chapter 3 Results

3.1 Silane Modification on Nanoporous Alumina Membrane

3.1.1 Characterization by Water Contact Angle

The surface wettability of the nanoporous alumina membranes were tested by the water contact angle measurement with a Ramie-Hart goniometer (NJ, USA) equipped with a video camera. The static contact angle images of water on different surfaces were captured by the video camera. The water contact angle was measured on both unmodified nanoporous alumina membrane and GPMS silane modified nanoporous alumina membrane to investigate the surface property change of the nanoporous membrane before and after silane modification.

Fig 3.1(a) shows the image of a droplet of 10 μL deionized water on the surface of unmodified nanoporous alumina membrane. The droplet of deionized water spread out quickly and completely on the membrane surface. The average contact angle value shown in Table 3.1 is 14.59°±0.51° (n=10), which means the surface of unmodified nanoporous alumina membrane is very hydrophilic. However, as shown in Fig 3.1(b), the droplet of deionized water didn't spread well on the GPMS silane modified membrane surface and formed a semi-microsphere shape. The average contact angle value, shown in Table 3.1 (b), is 84.52°±0.01° (n=10). Compared with the surface of unmodified alumina membrane, the GPMS silane treated surface was

more hydrophobic due to GPMS monolayer on the interface between the water droplet and the solid surface.

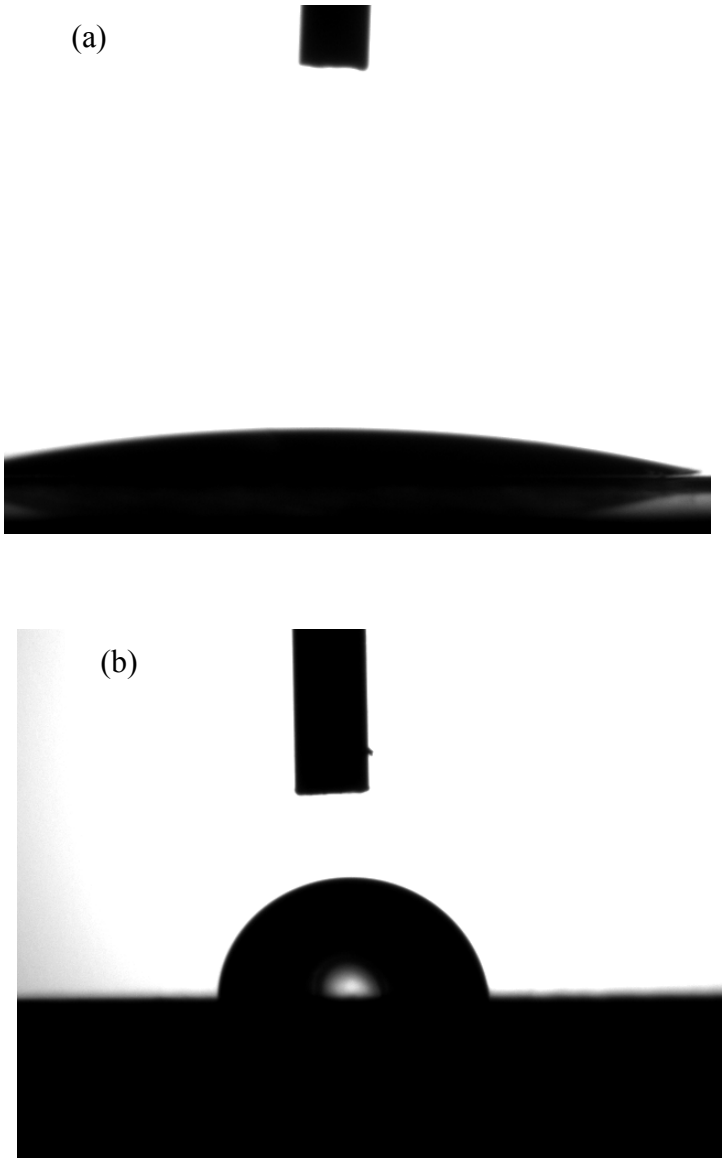

Fig 3.1 Images of deionized water droplets on (a) unmodified nanoporous alumina membrane, and (b) GPMS silane modified nanoporous alumina membrane

Table 3.1 Water contact angle values for unmodified alumina membranes and GPMS silane modified alumina membranes

Unmodified alumina membranes	1	2	3	4	5	6	7	8	9	10	Mean±SD
	14.4	14.5	14.4	15.6	14.3	15.0	15.2	14.0	14.3	14.2	14.59±0.51

GPMS modified alumina membranes	1	2	3	4	5	6	7	8	9	10	Mean±SD
	84.6	84.5	84.6	84.5	84.5	84.5	84.5	84.5	84.5	84.5	84.52±0.04

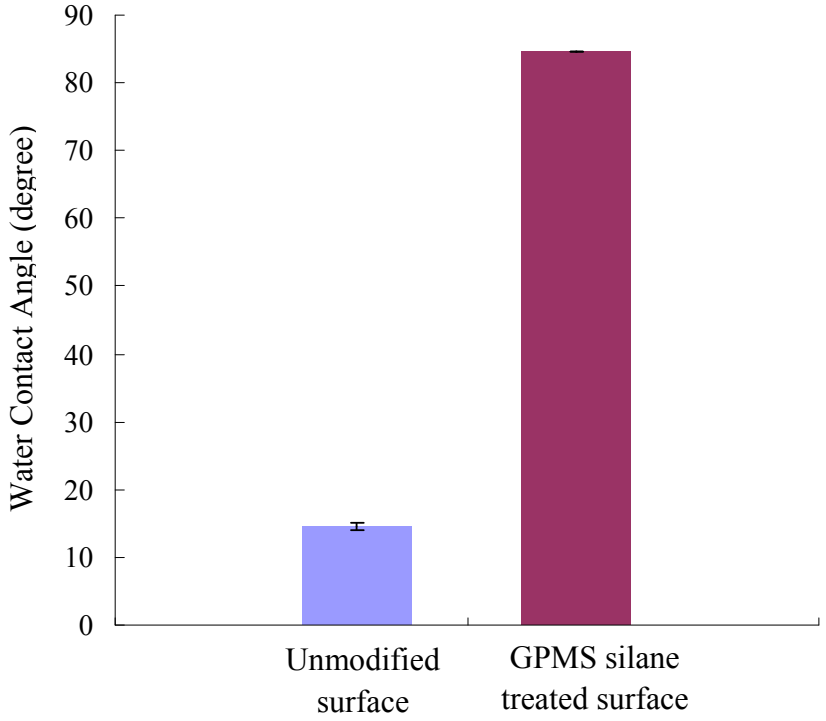

Fig 3.2 Comparison of water contact angle between unmodified and GPMS silane modified surfaces of nanoporous alumina membrane

The water contact angle comparison histogram is also shown in Fig 3.2. Before silane treatment, the bare alumina membrane is ultra-hydrophilic, with contact angle of 14.59±0.51°. However, after GPMS silane treatment, the contact angle increased to 84.52±0.04°, which indicates the GPMS silane treatment made the surface more hydrophobic. The difference for water contact angels before and after GPMS silane treatment is mainly due to the change of surface chemical groups. There were many hydrophilic hydroxyl groups on the unmodified nanoporous alumina membrane, which caused the surface ultra-hydrophilic (Xiong et al. 2005). After GPMS silane

modification, the silane monolayer covalently linked onto the membrane surface, the epoxy groups at the end of the GPMS monolayer changed the surface property that resulted in a much larger contact angle (Liechti et al. 1997). Compared with bare membrane surface, this GPMS treated membrane could render the surface epoxy group for antibody immobilization for the following experiments.

3.1.2 XPS Characterization for Silane Modification

X-ray photoelectron spectroscopy (XPS) is used to measure the surface chemical composition of materials. The surface properties after surface treatment such as silane modification, scraping and cleaning off surface contamination by ion beam etching can be analyzed by XPS. It is especially precise to measure the elemental composition at the top surface with 1-10 nm range. To confirm the GPMS silane grafting on the nanoporous membrane, the chemical composition of both bare nanoporous alumina membranes and GPMS epoxysilane modified membranes were analyzed by XPS.

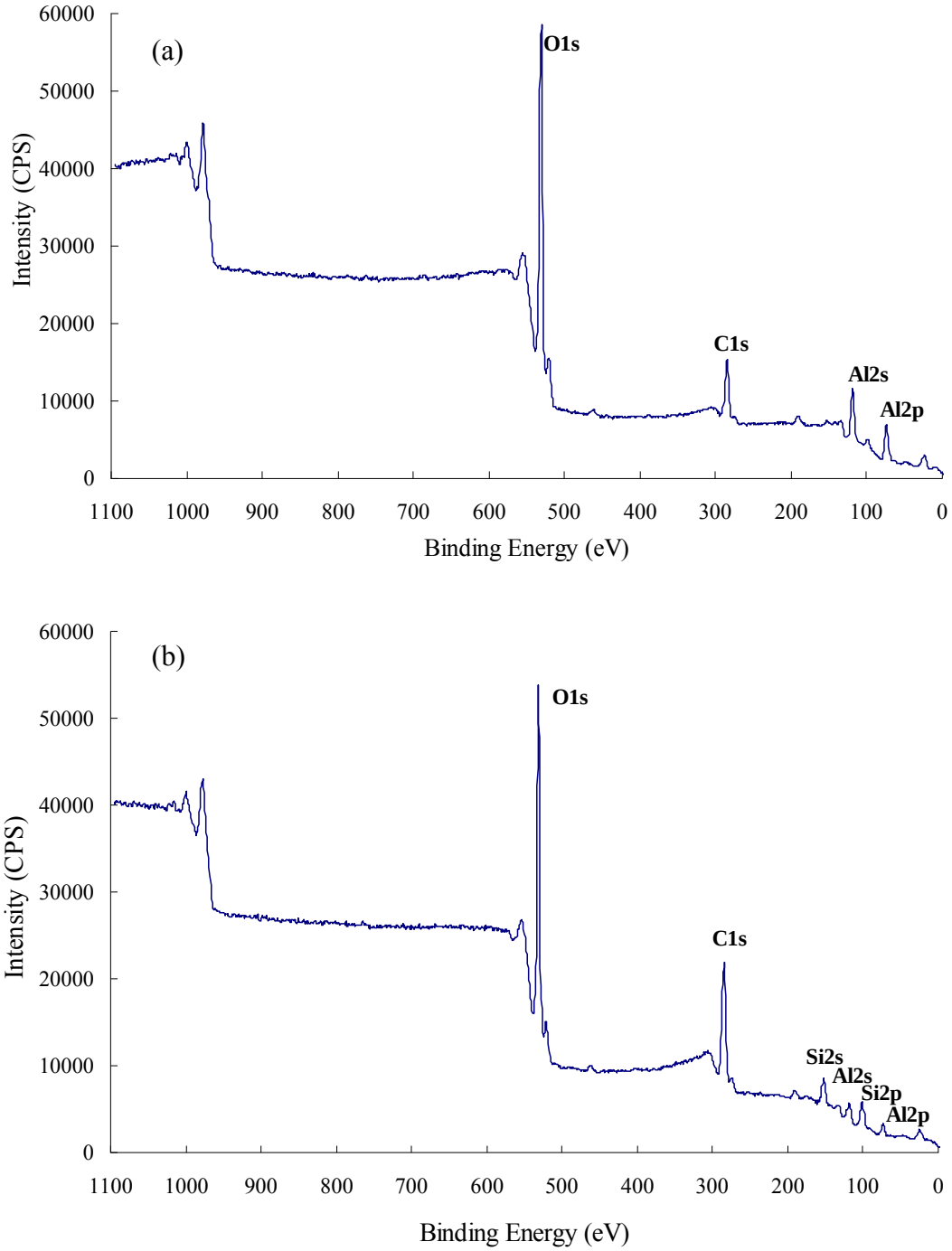

Fig 3.3 XPS wide scan spectrum for (a) unmodified nanoporous alumina membrane, (b) GPMS silane modified nanoporous alumina membrane

Table 3.2 Surface elemental composition of different nanoporous alumina membranes

Element percentage	unmodified surface	GPMS treated surface	Change
C_{1s}	17.134%	34.899%	17.765% ↑
O_{1s}	69.565%	55.808%	13.757% ↓
Al_{2p}	13.301%	3.834%	9.467% ↓
Si_{2p}	/	5.460%	5.460% ↑

Fig 3.3 (a) and (b) show the XPS wide scan spectra of unmodified nanoporous alumina membrane and GPMS silane modified nanoporous alumina membrane. The long band that ranged from 0 eV to 1100 eV was a general band including all the elements on the surface. In Fig 3.3 (a), the highest peak between the binding energy of 535 eV to 540 eV represents O_{1s}. The peak in the range from 70 eV to 80 eV, and from 110 eV to 120 eV illustrated the presence of aluminum (Al_{2p} and Al_{2s}). These results were consistent with the compositions of nanoporous alumina membrane (Al_2O_3). The presence of carbon in the binding energy of 285-290eV (C_{1s}) is mainly caused by the remaining of oxalic acid (HOOC-COOH) during the nanoporoua alumina membrane fabrication process. Fig 3.3 (b) showed the XPS spectrum of GPMS modified nanoporous alumina membrane. Similar to the unmodified one, O_{1s}, C_{1s} Al_{2p} and Al_{2s} can be found from the spectrum. Additional peaks in binding energy from 95 eV-105 eV and 145 eV-155 eV showed the presence of silicon element (Si_{2p} and Si_{2s}). The existance of silicon element was from the GPMS silane, whose chemical formation is $C_9H_{20}O_5Si$ during the procedure of surface modification.

The comparison between unmodified and GPMS silane modified nanoporous alumina membranes demonstrated the succesful grafting of GPMS silane on the membrane surfaces.

Table 3.2 showed the comparison of nanoporous alumina membrane surface elemental composition before and after silane modification. The comparision showed the appearnce of 5.460% of silicon on the silane modified surface which was from grafted GPMS monolayer. In addition, a 17.765% increase in carbon and a 9.467% decrease in aluminum also confirms the existence of GPMS silane monolayer, because the GPMS molecule contains the hydrocarbon chains but no aluminum.

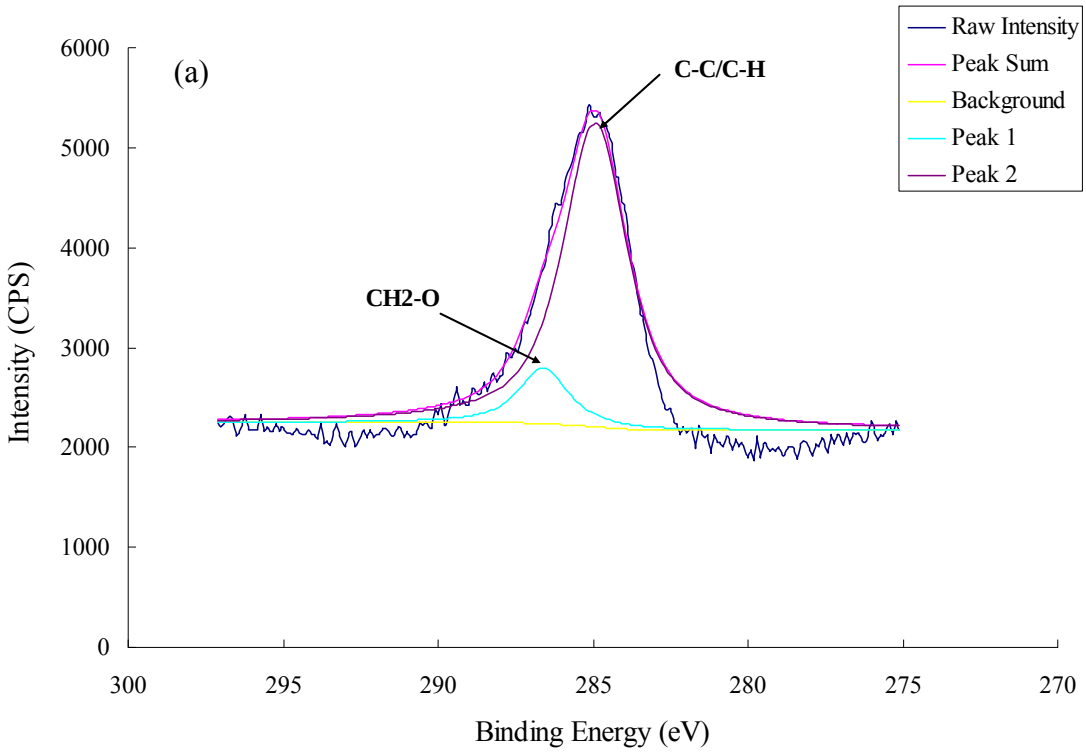

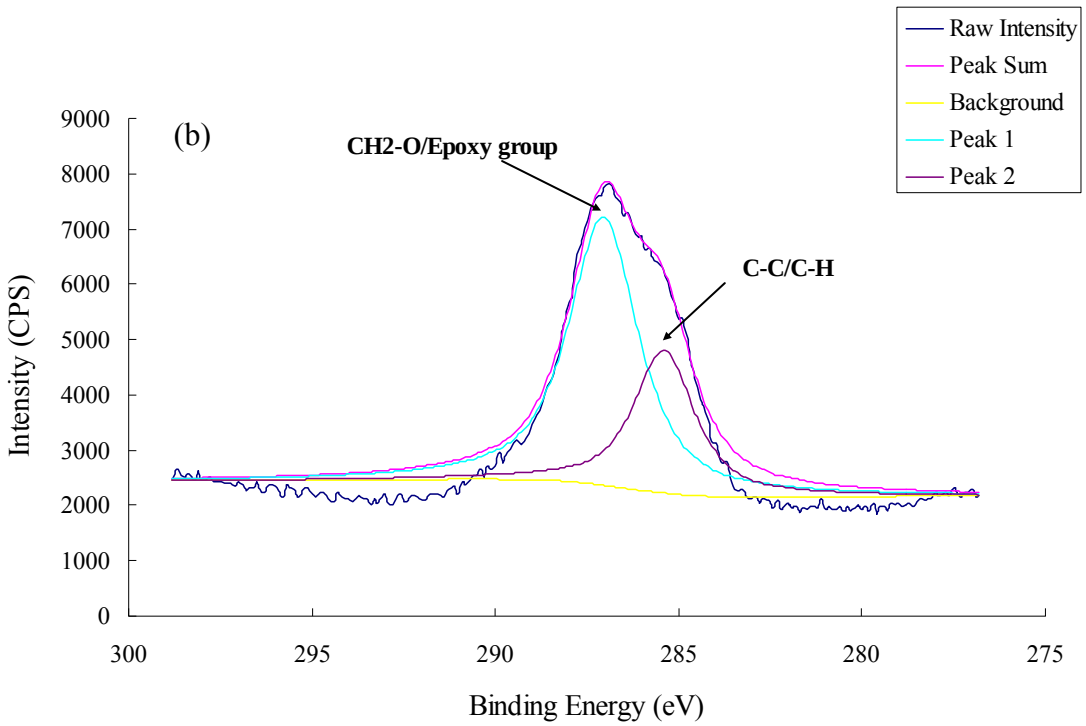

Fig 3.4 High-resolution XPS spectrum for C_{1s} peak of (a) unmodified nanoporous alumina membrane, (b) GPMS silane modified nanoporous alumina membrane

To further support the covalently gafting between nanoporous alumina membrane and GPMS silane molecules, high resolution XPS spectrum of C_{1S} peak was performed and the results were shown in Fig 3.4. The peaks at 285.2 eV were the hydrocarbon (C-C/C-H), while the peaks at 286.8 eV represented alkoxy group (C-O). As shown in Fig 3.4 (a), almost all of the carbon were in the formation of C-C/C-H at 285.2 eV and there was only a small peak at 286.8 eV introduced by the remaining oxalic acid (HOOC-COOH) during nanoporous alumina membrane fabrication process. However, after GPMS silane treatment, there was a great percentage increase at the peak of C-O shown compared with the peak of C-C/C-H in Fig 3.4 (b). This increase of oxygen-containing carbon was attributed to the epoxy groups (CH_2O_2) in the GPMS silane monolayer. The XPS result of the ratio

(C-C/C-H) : (C-O) in GPMS modified alumina membrane was 13:7, which did not agree with that ratio in GPMS molecules. Because the C was also introduced by oxalic acid during the fabrication of nanoporous alumina membrane, not only from the GPMS molecules. However, from the change tendency of (C-C/C-H): (C-O) ratio, we could confirm the GPMS had been successfully linked onto alumina membrane.

3.2 Antibody Immobilization on Nanoporous Alumina Membrane

3.2.1 XPS Characterization for Antibody Immobolization

After the GPMS silane grafting on nanoporous alumina membrane, the specific bacteria antibodies were deposited onto the surface and incubated in fridge at 4 ℃ for 24 hours. Since the active epoxy groups of GPMS could easily react with amino groups ($-NH_2$) of antibody, the antibody molecules could be firmly grafted onto the silane modified nanoporous alumina surface. The wide scan of XPS was used to determine the gafting of antibody molecules on GPMS modified surface.

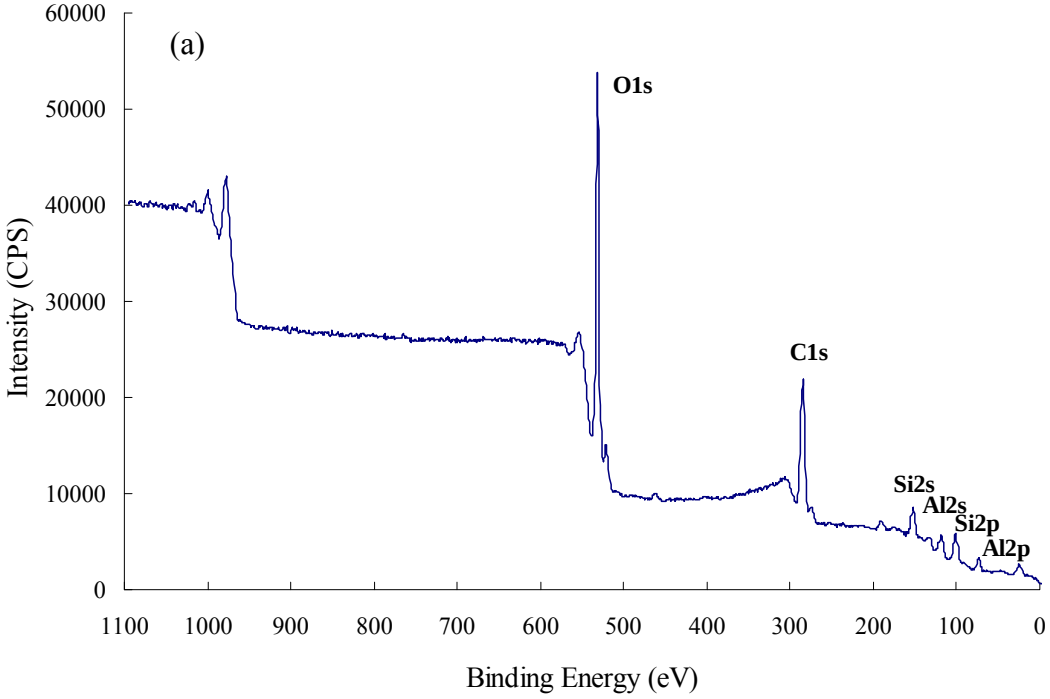

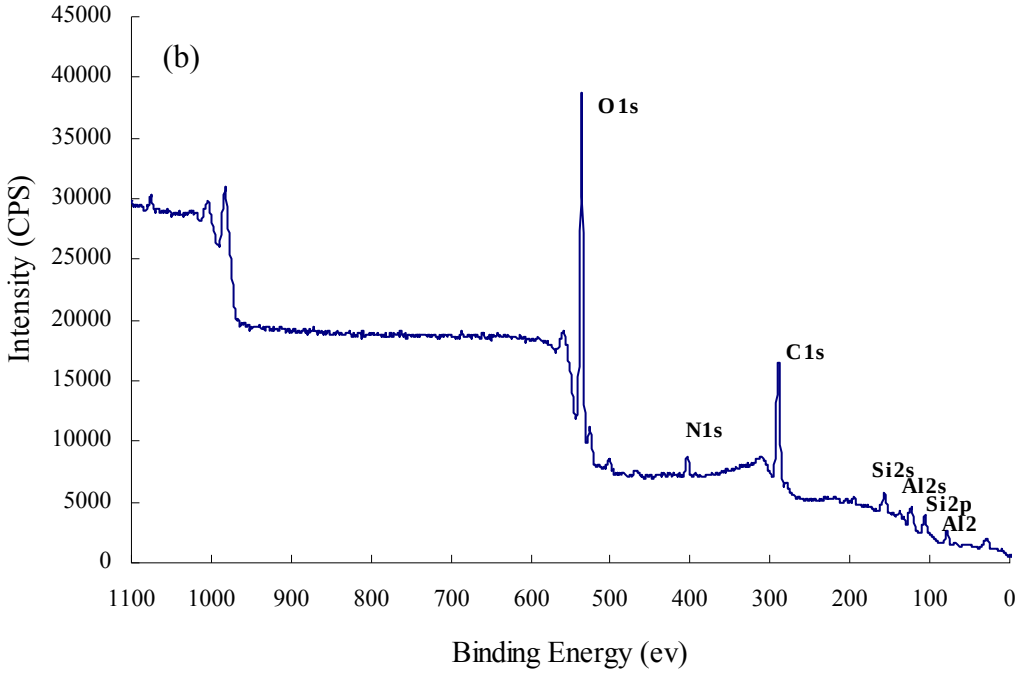

Fig 3.5 XPS wide scans for (a) GPMS silane modified nanoporous alumina membrane, (b) antibody modified nanoporous alumina membrane

Compared with GPMS modified surface shown in Fig 3.5(a), there was an additonal peak of N_{1s} representing appearance of nitrogen element for antibody gafted surface in Fig 3.5(b). The element of nitorogen was induced by amino group ($-NH_2$) from antibody during the reaction between epoxy groups of GPMS silane molecule and the amino groups in antibody. This comparision could conform that the antibody molecules were successfully grafted onto nanoporous alumina membrane.

3.2.2 Comparison between TPM and GPMS Silane Modification for Antibody Immobilization

Generally, there are two ways to immobilize antibody on solid substrate including physical adsorption and chemical grafting methods. In this project, we chose chemically grafting bacteria antibody on nanoporous membrane via GPMS silane monolayer. The advantage was to increase the stability and binding efficiency antibody on nanoporous membranes. To confirm this, we compared 3-(Trimethoxysilyl)propyl methacrylate (TPM) silane and GPMS silane modified nanoporous alumina membranes for antibody affinity study. The end group of TPM silane is vinyl group which will not react with antibody. However, the hydrophobic property of TPM silane monolayer can increase antibody physical adsorption. Therefore, TPM silane modified membranes were used as physical adsorption group and GPMS silane modified membranes were treated as chemical grafting group. The solution with fluorescence (FITC) labeled *E. coli O157:H7* antibody was added onto

the different types of surface. The fluorescence intensity was quantified using the imaging analysis software Image Pro Plus 6.0.

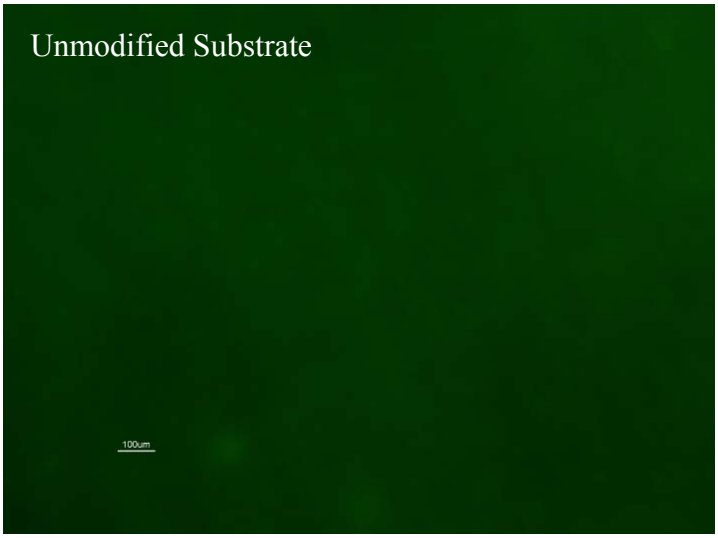

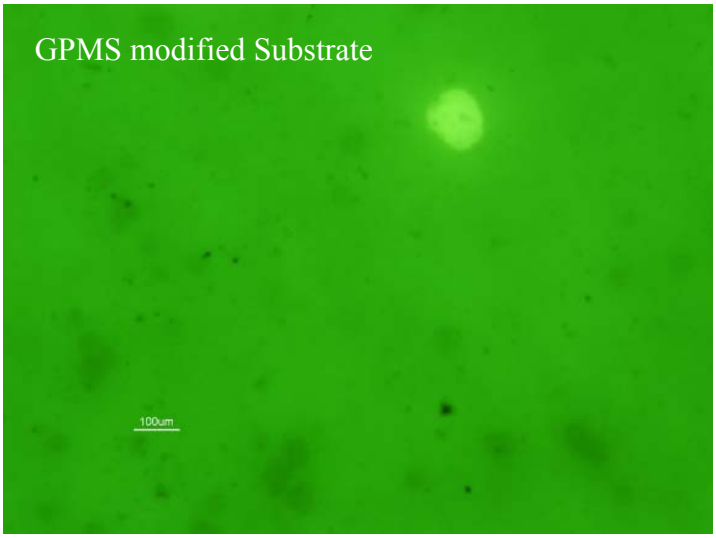

Fig 3.6 Comparison of antibody affinity among bare, TPM (1% in toluene) and GPMS (1% in toluene) modified membrane surface using 0.5 mg/ml FITC labeled *E. coli O157* antibody PBS solution

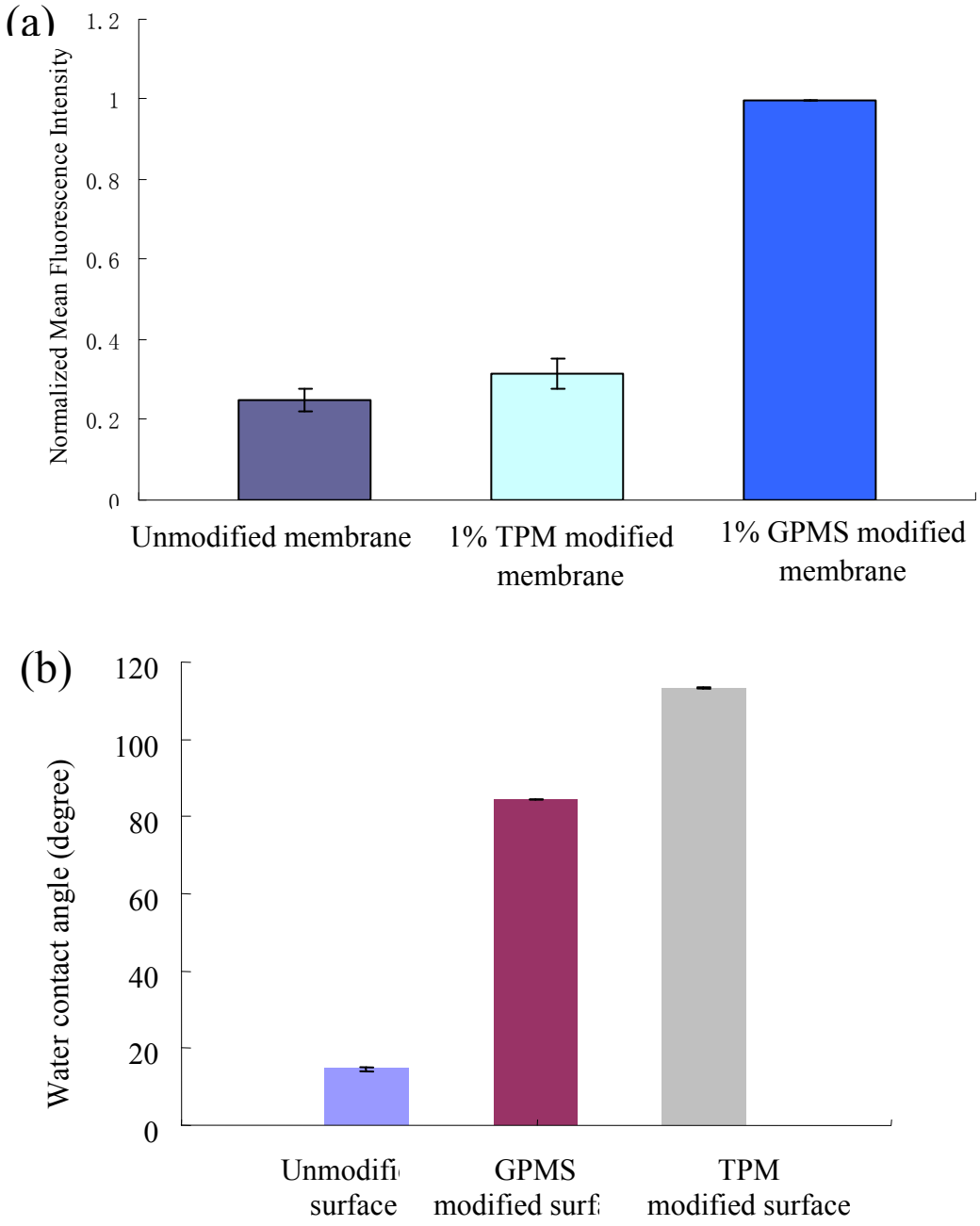

Fig 3.7 (a) Relative fluorescence intensity analysis of unmodified, TPM and GPMS modified nanoporous alumina substrate. The intensities of all samples were normalized using GPMS modified membranes as 100%. (b) Water contact angle for unmodified, TPM and GPMS modified nanoporous alumina substrate

Fig 3.6 showed the fluorescence images of 0.5 mg/ml FITC labeled *E. coli O157:H7* antibody solution adsorption on three samples including unmodified, TPM (1% in toluene) and GPMS (1% in toluene) modified nanoporous alumina membrane surfaces. After 24 hours immersion, all the samples were washed with PBS solution three times. There was no obvious fluorescence intensity increase for TPM modified surface compared with unmodified membrane. However, there was an obvious fluorescence intensity increase for GPMS modified membranes.

Fig 3.7(a) showed statistical analysis of antibody intensity for the three samples. The intensities of all samples were normalized using GPMS modified membranes as 100%. The unmodified membrane showed the lowest value of 24.9±3%, while the TPM modified membrane surface showed the intensity of 31.5±4%. Fig 3.7(b) showed the water contact angle measurement for the three samples. It could be seen that TPM modified nanoporous alumina membrane was very hydrophobic.

Without any modification, the antibody molecules could only physically adsorb onto membrane surface. Since the surface of unmodified alumina membrane was hydrophilic to resist protein adsorption, there was almost no antibody adsorbed on the surface. For the TPM silane modified membrane, the surface became hydrophobic due to the C=C bond at end of TPM molecule. However, there was no reaction between C=C and antibody, thus the antibody molecules could only physically adsorb on the membrane surface. Since the hydrophobic TPM modified surface was easy to adsorb antibodies, the intensity was a little higher than

unmodified membrane. For GPMS modified membranes, the fluorescence labeled antibody were chemically bonded with the GPMS modified surface due to the reaction between active epoxy group and amino group of antibody. Therefore, it was difficult to wash away the chemical bonded fluorescence antibody. The fluorescence intensity of GPMS modified surface was much higher than those of bare and TPM modified alumina membranes. It could be concluded that the chemical grafting method for antibody immobilization was much better than physical adsorption.

3.2.3 GPMS Concentration Effect on Antibody Immobilization

Three concentrations of GPMS silane in toluene solution were used to explore the concentration effect on antibody immobilization efficiency. Fig 3.8 showed the fluorescence images of 0.5 mg/ml FITC labeled *E. coli O157* antibody PBS solution adsorption on GPMS concentrations of 0.1%, 1% and 2% modified nanoporous alumina membranes. Fig 3.9 showed the relative intensity analysis for these three types of samples. The intensities of FITC labeled antibodies on the membranes were normalized using 2% GPMS modified membranes as 100%. In Fig 3.9, 0.1% concentration showed relatively lowest intensity with average value of 72.5±9.1%. It was due to no sufficient GPMS molecules to cover the whole surface for 0.1% concentration to capture antibody. When GPMS concentration increased to 1 %, the average intensity increased to 137.4±15.7 %. However, when GPMS concentration increased to 2.0%, the intensity did not increase further and there was a slight decrease to 100%. It might be explained by the competition among too close

neighbor silane molecules due to steric hindrance effects. Therefore, the optimal concentration of GPMS in toluene used in the experiment was 1% to achieve the best antibody immobilization efficiency.

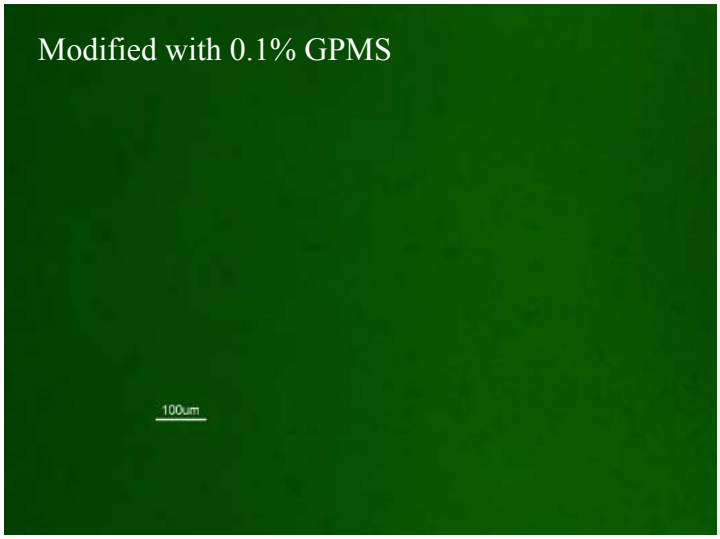

Fig 3.8 Comparison of antibody affinity among 0.1%, 1% and 2% GPMS modified membrane surfaces using 0.5 mg/ml FITC labeled *E. coli O157:H7* antibody PBS solution

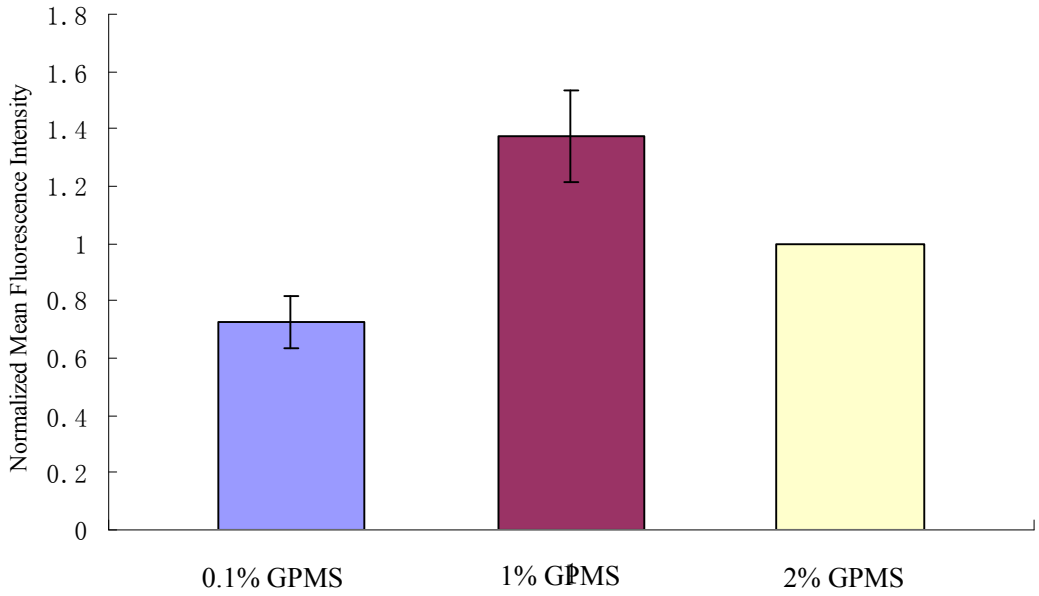

Fig 3.9 Normalized fluorescence intensity of antibody immobilization for 0.1%, 1% and 2% GPMS modified nanoporous alumina substrate using 0.5 mg/ml FITC labeled *E. coli O157:H7* antibody PBS solution

3.3 Bacteria Capturing on Antibody Immobilized Nanoporous Membrane

3.3.1 Fluorescence Microscopy Analysis

After bacteria antibody were successfully immobilized on nanoporous alumina membrane surfaces, bacteria solutions with different concentrations were then added for bacteria capturing experiments. The target bacteria captured on the complimentary antibody modified membrane were confirmed by sandwich type

immunoassay using fluorescent isothiocyanate (FITC)-labeled antibody shown in Fig 3.10. The specific fluorescence labeled antibodies served as the secondary antibody were conjugated onto the bacterial cells which were captured on the nanoporous membrane surface by primary antibodies to form a sandwich structure shown in Fig 3.10.

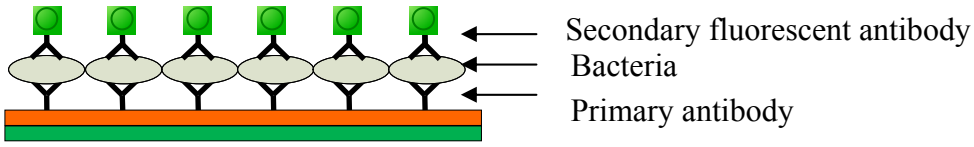

Fig 3.10 Sandwich structure of bacteria immobilized on nanoporous alumina membrane

Fig 3.11(a) showed the fluorescence images of *E. coli O157:H7* with a concentration of 10^6 CFU/ml captured on the nanoporous alumina membranes modified with anti-*E. coli O157:H7* antibodies. The property of low auto-fluorescence of the nanoporous alumina membrane made fluorescence labeled bacteria cells easy to bed distinguished. In Fig. 3.11(a), there were many green dots which represented many bacteria cells conjugated with fluorescence labeled secondary antibodies. To testify the specificity of this biosensor, a sample of *Staphylococcus aureus* with the same concentration of 10^6 CFU/ml added onto the anti- *E. coli O157:H7* antibody modified alumina membrane. Then, the fluorescence labeled secondary anti-*Staphylococcus aureus* antibody was added following by PBS solution washing three times. As shown in Fig 3.11 (b), there were few green dots on the membrane surface, which meant few *Staphylococcus aureus* cells were captured by *E. coli O157:H7* antibody modified nanoporous membranes. This result indicated that the

anti- *E. coli O157:H7* antibody modified nanoporous alumina membrane was specific for *E. coli O157:H7* detection and *Staphylococcus aureus* could not be captured onto the surface after washing procedures.

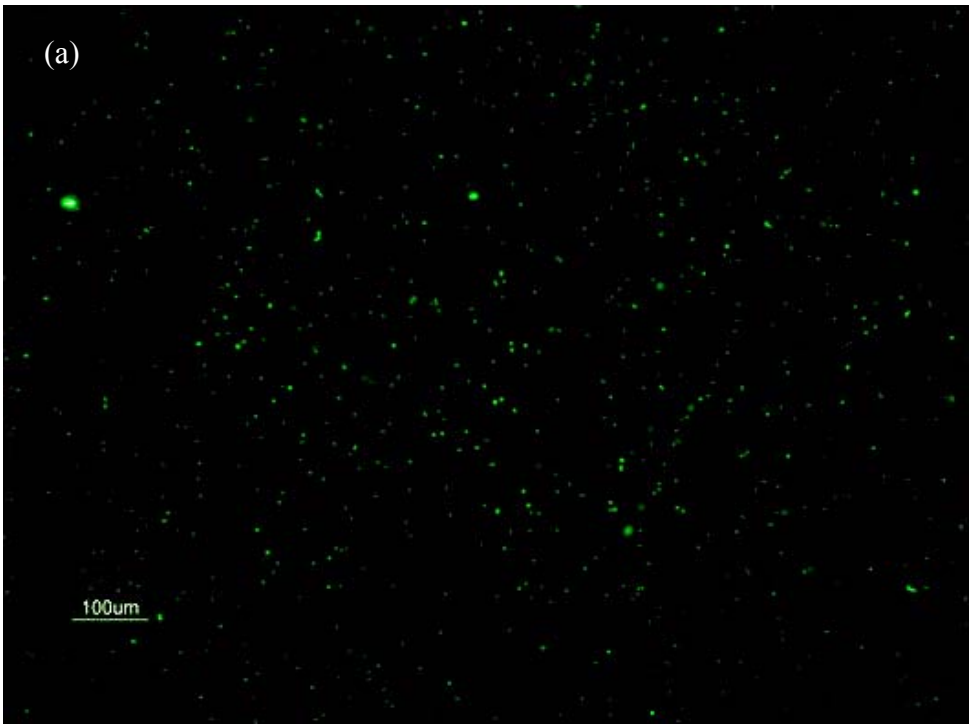

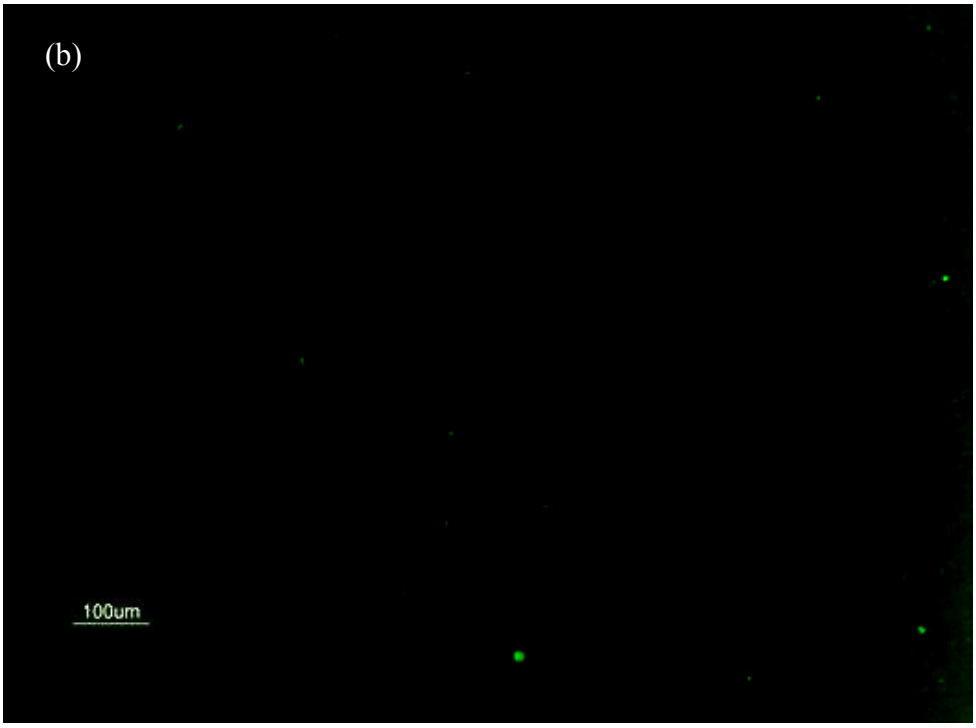

Fig 3.11 Fluorescence images of anti- *E. coli O157:H7* antibody modified membranes with samples of (a) *E. coli O157:H7*, (b) *Staphylococcus aureus* cells at a concentration of 10^6 CFU/ml

A similar experiment was performed with the anti-*Staphylococcus aureus* antibody modified membranes. Two kinds of bacteria solutions with the same concentration of 10^6 CFU/ml were added onto the membrane surfaces. After the specific secondary fluorescence antibody conjugated with bacteria cells with PBS solution washing, these membranes were analyzed under fluorescence microscope. The fluorescence images were shown in Fig 3.12.

The bacteria cells represented by the light green dots were firmly captured by the specific primary antibody after rinsing with PBS solution. Several green dots lighter than normal ones were bacteria cell clusters. Bacteria cells might gather together to form the cluster structure. When the bacteria clusters were conjugated by fluorescence antibodies, they might be lighter than normal single one. Fig 3.12(b) showed the images of fluorescence labeled *E. coli O157:H7* immobilized on the anti-*Staphylococcus aureus* antibody modified surface. Compared with the specific binding images in Fig 3.12 (a), there were few green dots on the membranes, which indicated *E. coli O157:H7* were not captured on the anti-*Staphylococcus aureus* antibody modified surface. This result indicated that the anti-*Staphylococcus aureus* antibody modified nanoporous alumina membrane was specific for *Staphylococcus aureus* detection and *E coli O157:H7* could not be captured onto the surface after washing procedures.

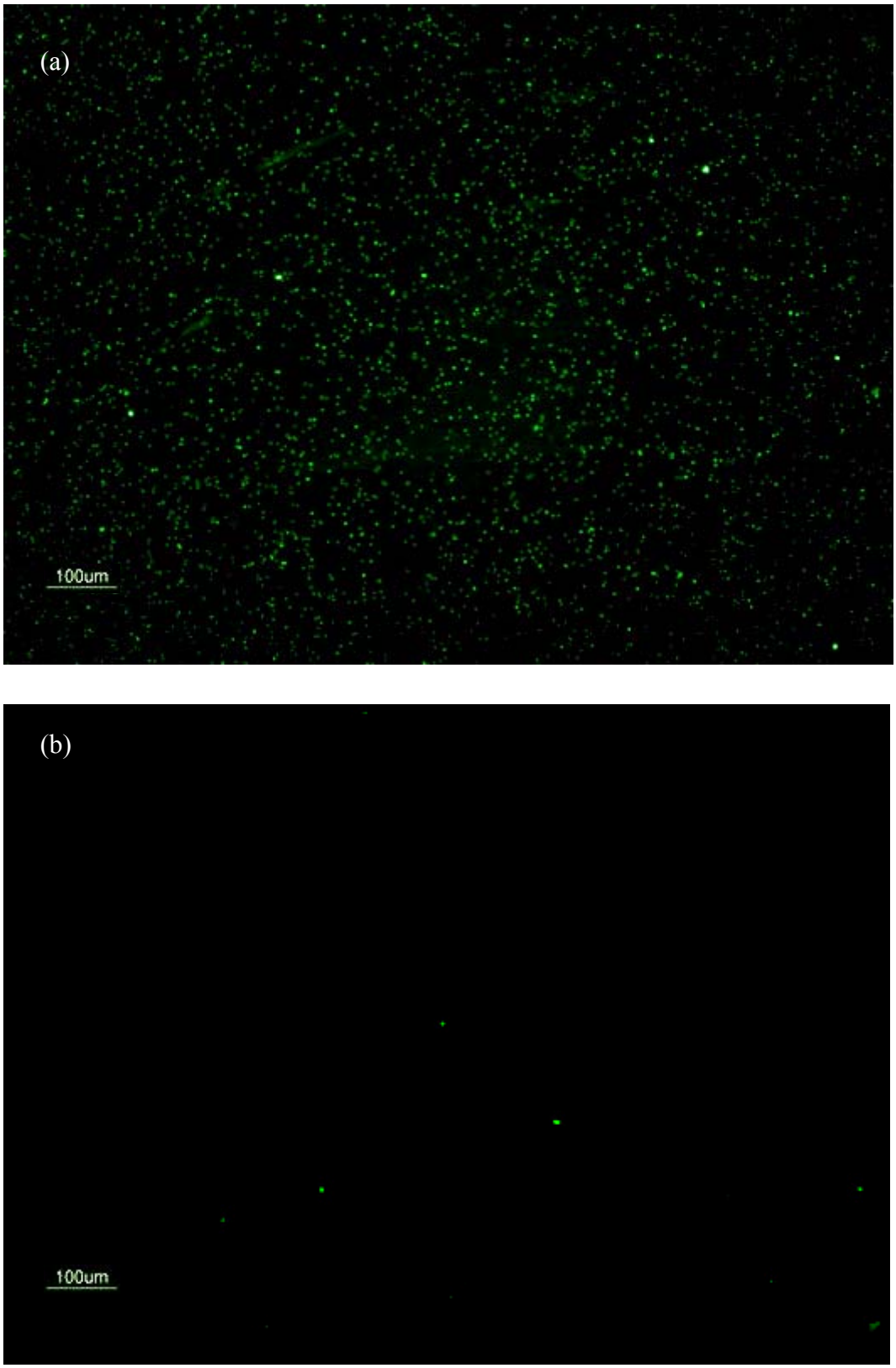

Fig 3.12 Fluorescence image of anti-*Staphylococcus aureus* antibody modified membranes with samples of (a) *Staphylococcus aureus*, (b) *E. coli O157:H7* cells at concentration of 10^6 CFU/ml

Fig 3.13 showed the fluorescence images of *E. coli O157:H7* captured on the specific anti- *E. coli O157:H7* antibody immobilized membrane surface with different concentrations from 10^2 to 10^7 CFU/ml. From Fig 3.13, it clearly showed that when the concentration increased, the density of bacteria cells captured also increased. This result showed that the number of captured bacteria cells were correlated with bacteria concentrations.

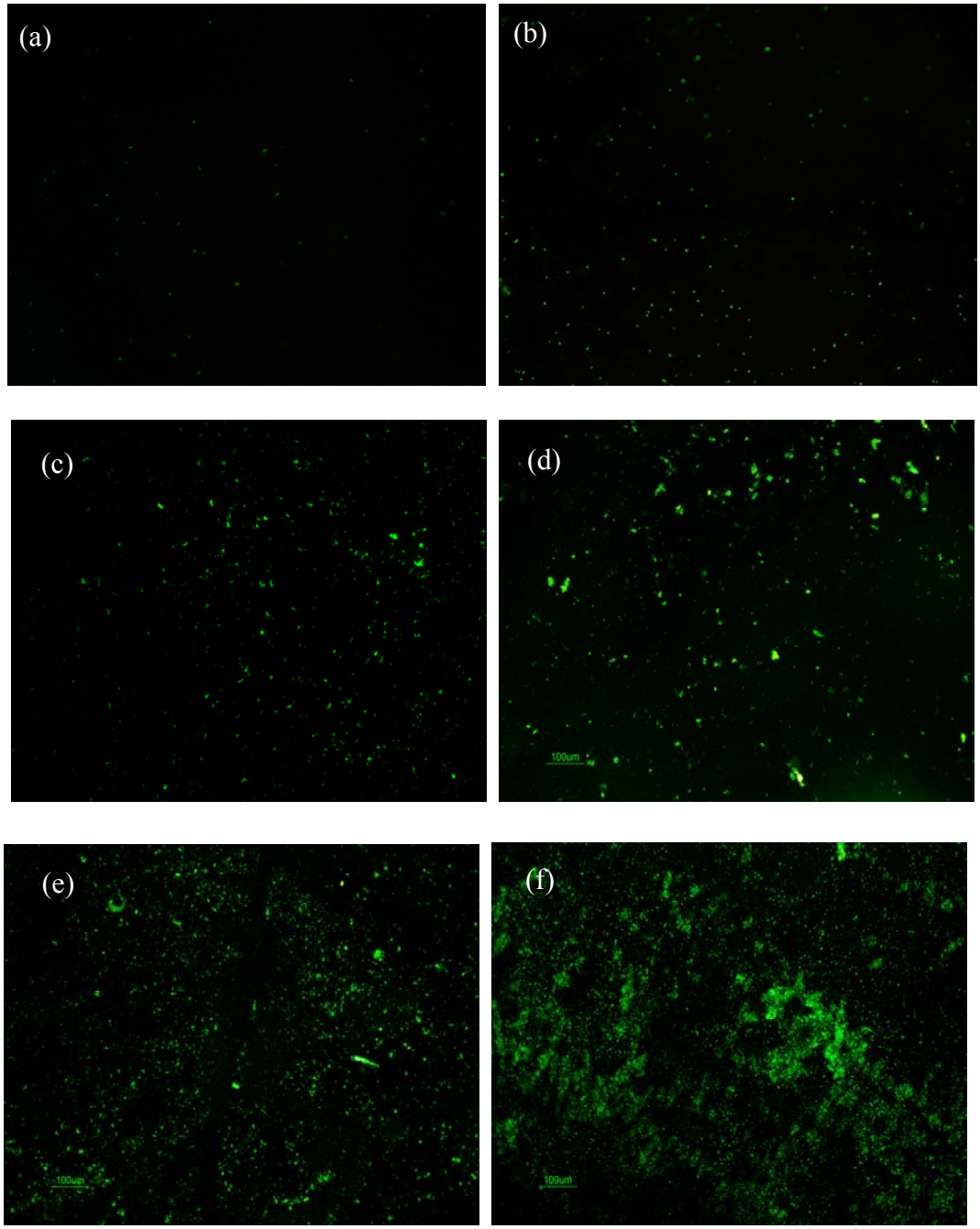

Fig 3.13 *E.coli O157:H7* cells in PBS with concentrations range from (a) 10^2 to (f) 10^7 CFU/ml

3.3.2 Atomic Force Microscopy Analysis

AFM was used to analyze the nanoporous alumina membrane surfaces with GPMS silane monolayer, antibody molecules and bacteria cells. Fig 3.14 (a) presented the tomography of nanoporous alumina membrane after GPMS silane monalayer gafting. The epoxysilane generated a homogeneous self-assembled monolayer that was dense and complete on the nanoporous membrane. This uniform and smooth monolayer was appropriate for furthur antibody immobilization experiment. Theoretically speaking, the head groups (silane) of GPMS were compactly linked onto the surface of nanoporous membrane with hydroxyl group, while the functional groups (epoxy) of GPMS were exposed for next surface modification step. These silane molecules were regularly grafted onto the nanoporous alumina membrane and this formation was beneficial for antibody immobilization.

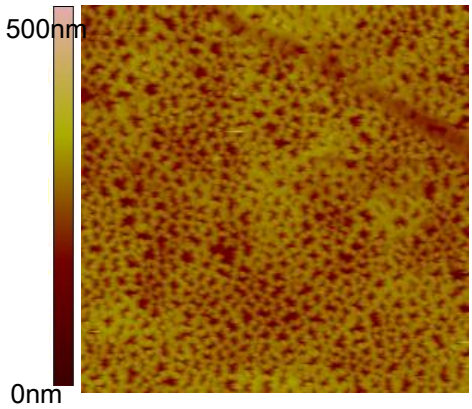
500nm
0nm

(a)

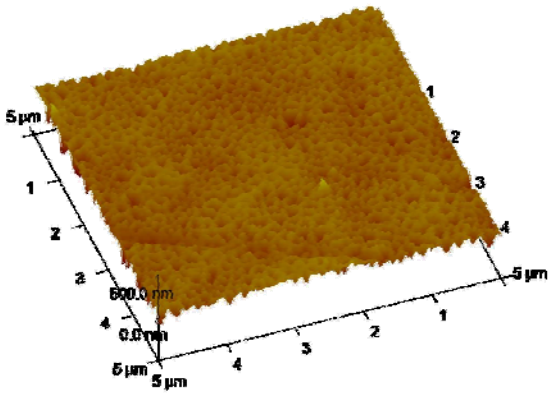

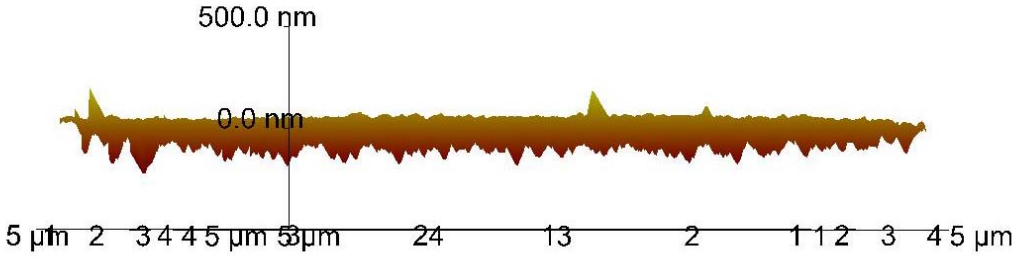
500.0 nm
0.0 nm
5 µm 2 3 4 4 5 µm 5 µm 24 13 2 1 1 2 3 4 5 µm

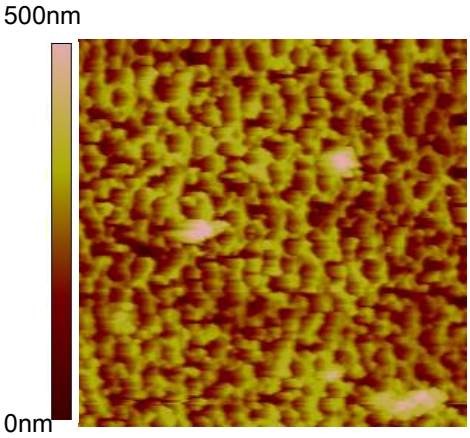
500nm
0nm

(b)

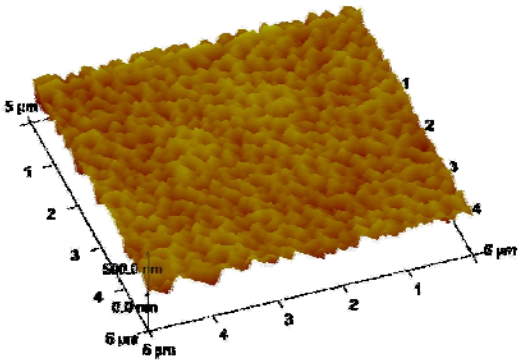

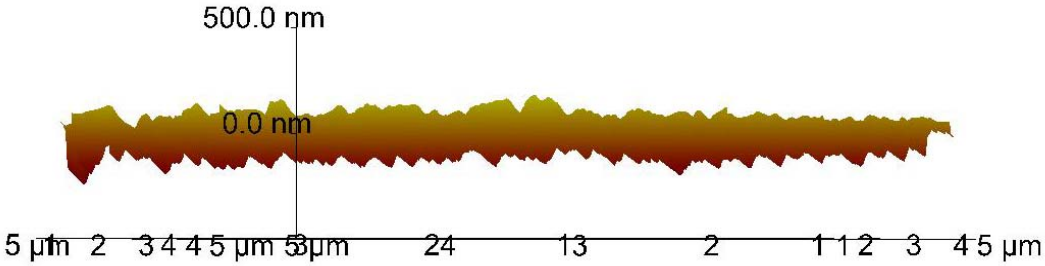
500.0 nm
0.0 nm
5 µm 2 3 4 4 5 µm 5 µm 24 13 2 1 1 2 3 4 5 µm

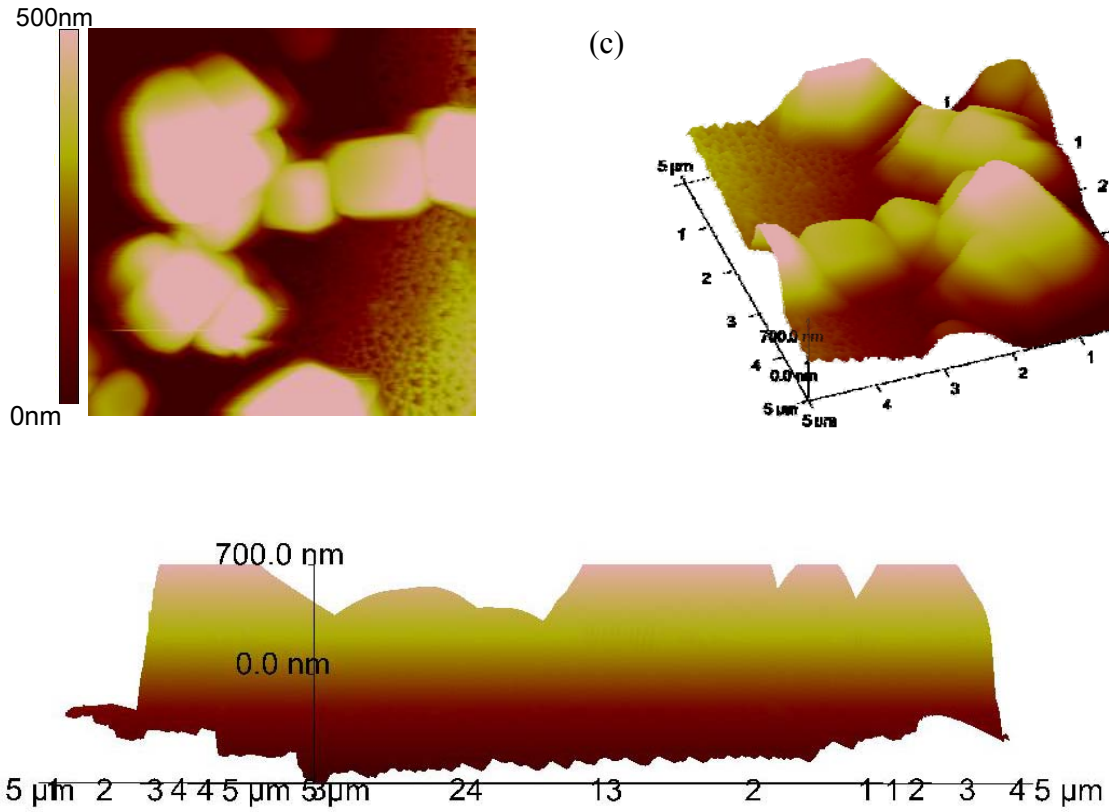

Fig 3.14 The 2D and 3D (scan size 5µm×5µm) AFM images of (a) GPMS epoxysilane modified nanoporous alumina membrane, (b) anti- *E. coli O157:H7* antibody immobilized on silane modified nanoporous alumina membrane, and (c) bacteria of *E. coli O157:H7* captured by antibody on the nanoporous alumina membrane

Fig 3.14(b) showed the topography of anti- *E. coli O157:H7* antibodies immobilized on the GPMS self-assemble monolayer on nanoporous alumina membrane after reacting with active epoxy group for 24 hours. It could be seen that the antibody molecules formed an irregular appearance with some aggregates which were caused by the non-completely monolayer structure. However, these aggregates are only tens of nanometers height which were much smaller than the measured height of *E. coli* bacteria cells that typically larger than 500 nm. Therefore, the presence of aggregates

would not influence the detection of bacteria binding. It was important for the reproducibility and sensitivity of biosensors. A distinctive difference in the topography of surface could be observed by comparing epoxysilane molecules and anti- *E. coli O157:H7* antibody molecules on membrane surface in Fig 3.14(a) and Fig 3.14(b). The antibody molecules showed bigger size and more global structure for their protein nature compared with Fig 3.14(a). Meanwhile the average surface height of Fig 3.14(b) was 3 nm larger than the height of Fig 3.14(a), which means the average surface height of anti-*E. coli O157:H7* antibody was about 3 nm (lighter color means higher surface) and this result was also consistent with previous studies about antibody molecules.

Fig 3.14(c) showed the AFM image of antibody modified nanoporous membrane after incubation with bacteria solution of *E .c*oli *O157:H7* at a concentration of 10^9 CFU/ml for 3 h. It could be seen that the bacteria cells of *E. coli O157:H7* were firmly captured by antibody on the nanoporous alumina membrane with an average height of 1.6 micrometers. In this figure, the binding density of *E coli O157:H7* on the 5 μm×5 μm scan area was 0.2 μm^{-2} and the total binding bacteria number on the whole membrane surface (diameter of 13 mm) would be 2.6546×10^7 cells. It was estimated 13.27 % *E. coli* bacteria cells were captured when 200 μl of 10^9 CFU/ml bacteria solution was dropped on the surface.

3.3.3 Scanning Electron Microscopy Analysis

Besides fluorescence microscopy and AFM, scanning electron microscopy (SEM) was also used for the characterization. Fig 3.15(a) showed the SEM image of a bare nanoporous alumina membrane with pore size of 100 nm. The bare nanoporous alumina membrane had regular nanopores and the pore size was uniform. In addition, it had a high porosity and pore density which led to a high surface area which could be functionalized easily and completely. Fig 3.15(b) and Fig 3.15(c) showed bacteria cells of *E.coli O157:H7* and *Staphylococcus aureus* with a concentration of 10^6 CFU/ml captured by specific antibodies immobilized on nanoporous alumina membranes, respectively. It could be seen that *E. coli O157:H7* showed a rod shape with the length around 3 μm and the width around 1 μm. Compared with *E. coli O157:H7*, *Staphylococcus aureus* had a round shape similar to grape cluster with a radius of 1 μm.

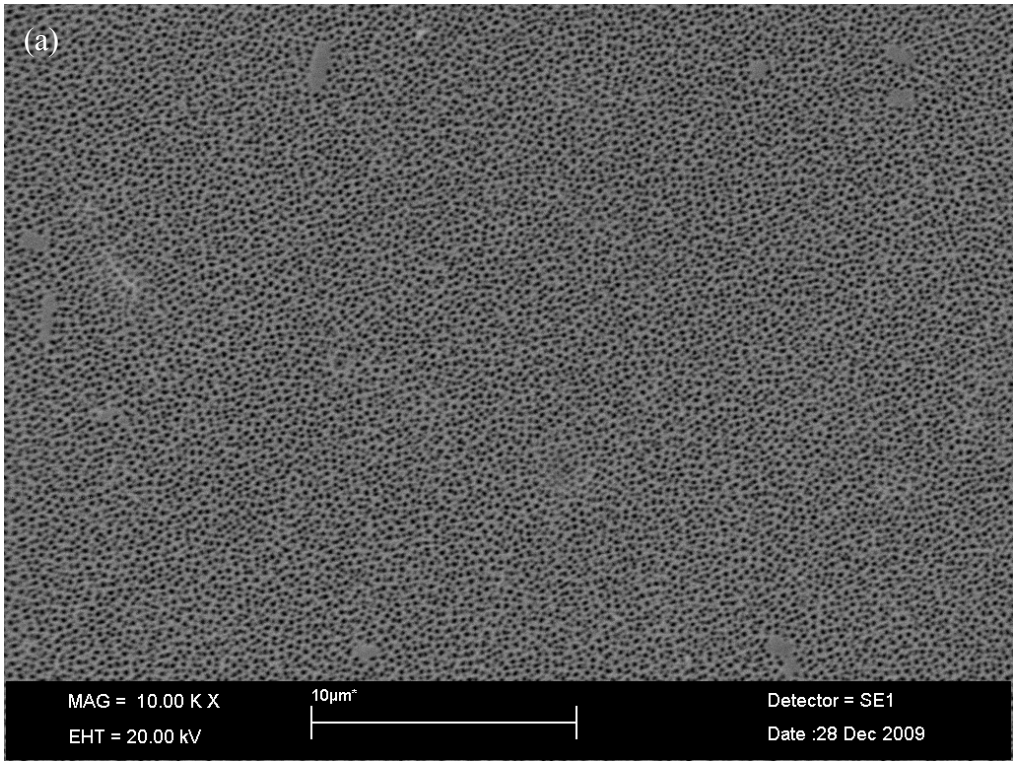
(a)
MAG = 10.00 K X
EHT = 20.00 kV
10μm
Detector = SE1
Date :28 Dec 2009

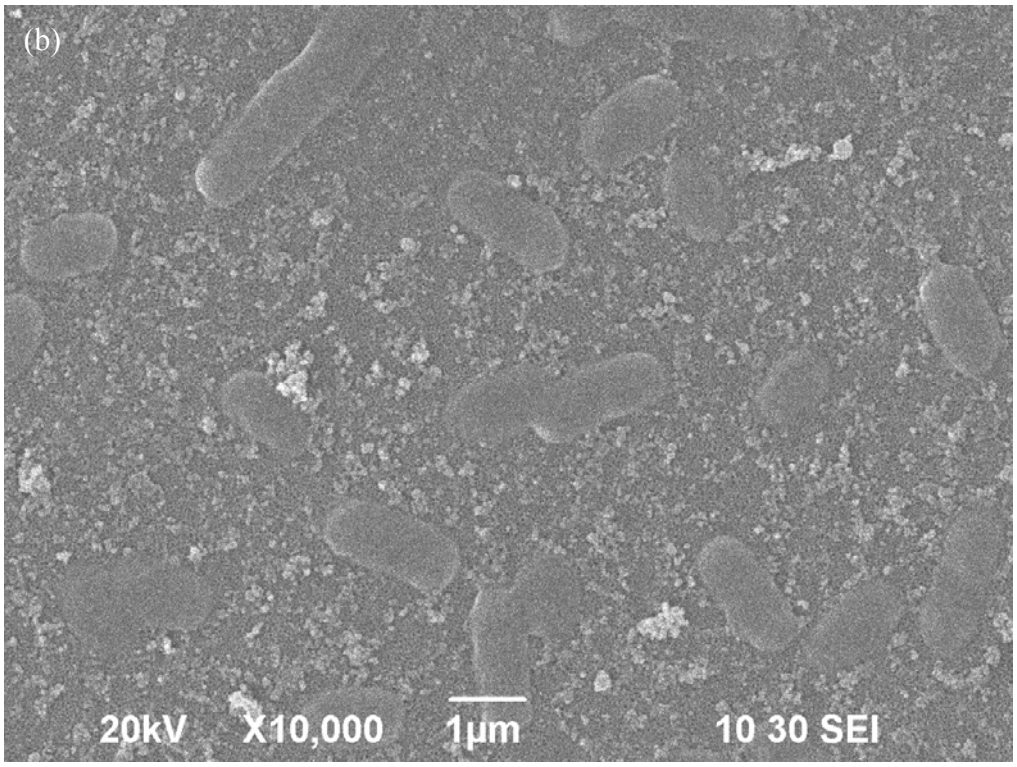
(b)
20kV X10,000 1μm 10 30 SEI

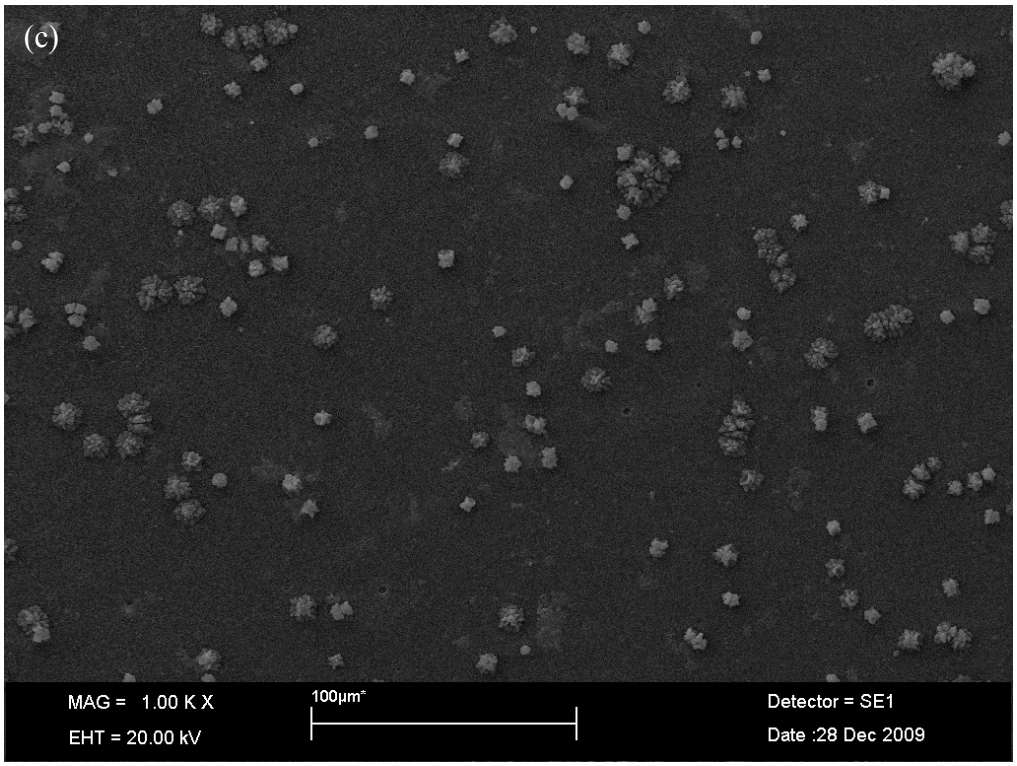

Fig 3.15 SEM images of the top view of nanoporous alumina membrane (a) bare, (b) with *E.coli O157:H7* cells captured by immobilized anti-*E.coli O157:H7* antibodies, (c) with *Staphylococcus aureus* cells captured by anti-*Staphylococcus* antibodies

The membrane surfaces in Fig 3.15 (b) and (c) were not covered by bacteria cells completely, which demonstrated that the binding of bacteria cells to the nanoporous alumina membrane was different from the adsorption of small molecules such as proteins and chemical reagents. The affinity and orientation of antibody molecules during the surface modification procedure, as well as the biological immuno-reaction between antibody and bacteria would largely influence the binding efficiency (Yang and Li 2005).

3.4 Impedance Spectrum for Single Type Bacteria Detection

After specific antibodies modified nanoporous alumina membrane were integrated into the PDMS based chip, .the electrical impedance spectrum measurements were performed to detect the presence of bacteria and the relationship between the concentrations of bacteria and the impedance amplitude change. The impedance of phosphate buffer solution (PBS) in upper compartment without bacteria was used as the control group.

The impedance data is always analyzed by Nyquist Plot when the redox probes are used in the electrochemical impedance experiment (Ruan et al. 2002). However, when studying the relationship between frequency and impedance to monitor the presence bacteria cells or analyze impedance change caused by different bacteria concentrations, the Bode Plot is appropriate (Gawad et al. 2004). In this experiment, the Bode plot was used for the analysis of impedance amplidue and phase angle with frequency.

3.4.1 Impedance Spectrum Monitoring for Bacteria Detection

To monitor the impedance changes before and after the bacteria captured by specific antibodies on nanoporous alumina membrane, the impedance spectroscopy method was adopted. After bacteria capturing, PBS solution was used to wash away the unbinded bacteria before the impedance measurement. The electric behavior of

nanoporous alumina membrane impedance sensor could be represented by the equivalent circuit model shown in Fig 3.16(a). The impedance change caused by bacteria cells captured on nanoporous alumina membrane was contributed to the parameters alteration of electrochemical components in the equivalent circuit. The equivalent circuit shown in Fig 3.16(a) consisted of three components, where R_S represented the electrolyte resistance of bulk solution, Z_{CPE} represented the constant phase element of interfacial double layer effect on the membrane surface, and R_C and C_C represented resistance and capacitance related to nanoporous membrane. The CPE is commonly used to replace a simple capacitor to represent electrode double layer (Gawad et al. 2004). R_C and C_C in parallel are used to represent the cell layer (cell wall, cell membrane and cell cytoplasm).

Fig 3.16(b) showed the Bode Plot of measured and fitted data of impedance and phase angle before and after *Staphylococcus aureus* captured on the membrane with a concentration of 10^4 CFU/ml. During the experiment, impedance spectrum is monitored from 1 Hz to 10 kHz which covered the main frequency range of bacteria substrate impedance change. The fitting curves using the equivalent circuit were also shown in Fig 3.16(b) which matched the measured data well. As shown in Fig. 3.16(b), there was a significant increase of impedance ampiltude after capturing bacteria sample of *Staphylococcus aureus*, which was mainly due to the captured bacteria covering on the nanoporous membrane and blocking the electrolyte current.

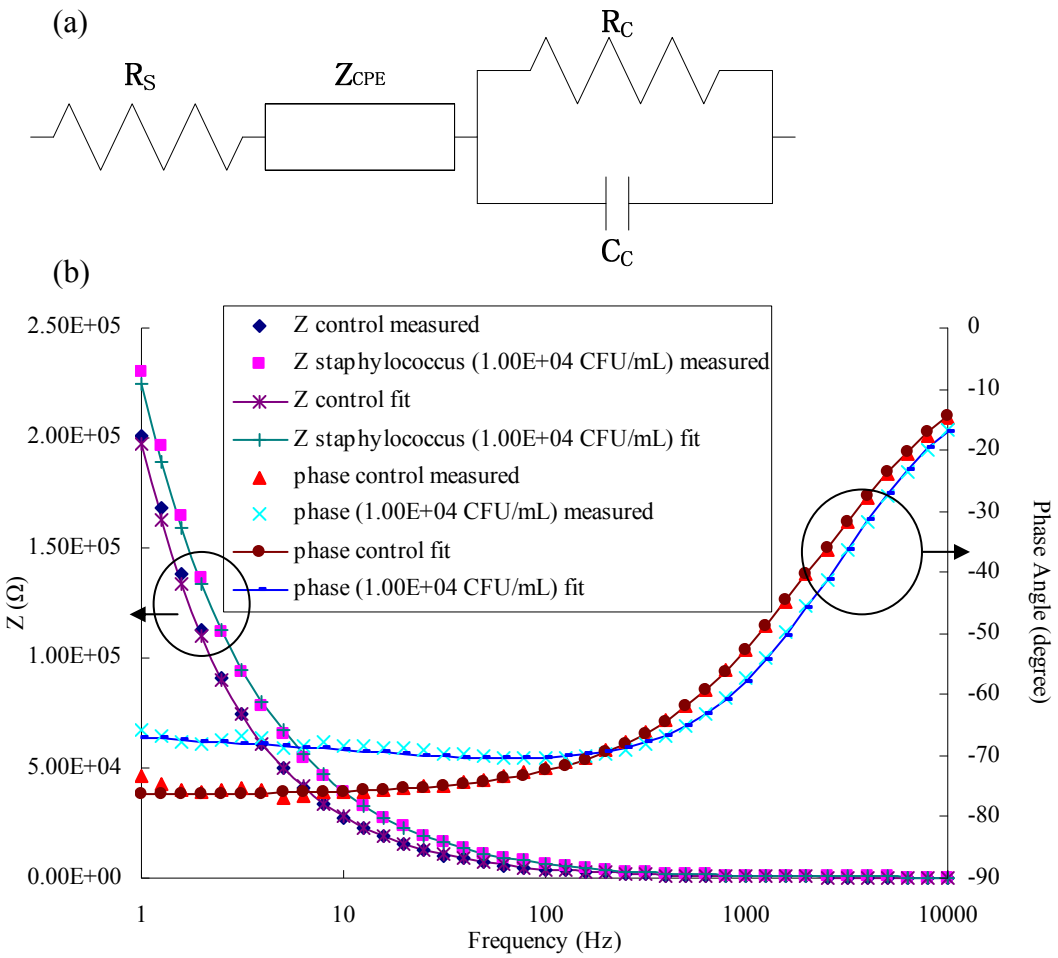

Fig 3.16 (a) Equivalent circuit for impedance measurement system based on nanoporous alumina membrane for detection of bacteria; (b) Bode diagram of measured and fitted data of impedance and phase angle of both PBS solution and *Staphylococcus aureus* with concentration of 10^4 CFU/ml

Table 3.3 Fitted equivalent circuit model parameters

Parameters	R_S (ohm)	C_C (F)	$Z_{(CPE)}$	R_C (ohm)
Control	284	9.51E-8	1.065E-06	192.9
10^4 cfu/ml	297	9.02E-8	1.069E-06	220.4

Fig 3.16(b) showed the measured and fitted curves of both impedance magnitude and phase angle. Bacteria sample of *Staphylococcus aureus* with concentration of 10^4 CFU/ml was captured by specific antibodies on the nanoporous alumina membrane. In order to validate the equivalent circuit for the impedance sensing system, impedance spectrum data measured by V3-Studio was analyzed by software of Zsimpwin V3.2.1 (Princeton Applied Research) and applied to generate a fitted curve. It could be seen that the fitted curves were highly in agreement with the measured data for both impedance amplitude and phase angle. The chi-squares were on the order of 10^{-4} which were greatly smaller than 10^{-3}. The chi-square value was acceptable on the order of 10^{-3} or below for an equivalent circuit (Cui and Martin 2003). Therefore, it could be concluded that the proposed equivalent circuit was suitable for impedance data fitting for this nanoporous membrane based biosensor. Table 3.2 showed the equivalent cuircuit prametrs of fitting models for impedance curves of both before and after bacteria capturing.

In Fig 3.16(b), the frequency ranging from 1 Hz to 10 kHz was separated into three sections obviously, which is largely related to the electrochemical components in the equivalent circuit. In the low frequency region from 1 Hz to about 10 Hz, the impedance magnitude was dominated by the electrode double layer capacitance which was represented by Z_{CPE}. In this region, the impedance amplitude decreased sharply with the increasing of frequency. In the high frequency region from 1 kHz to 10 kHz, the impedance was mainly determined by the electrolyte resistance of bulk solution Rs. In this region, the impedance amplitude became stable with the increase

of frequency due to the independence of resistor to frequency (impedance of resistor, $Z_R = R_S$). In the frequency region between 10 Hz and 1 kHz, the impedance was determiend by Rc and Cc together.

Fig 3.16(b) also showed the change of phase angle with frequency. For the phase angle of control group, the phase angle was close to -90° in the low frequency range from 1 Hz to 10 Hz and gradually approached to 0° in the high frequency range from 1 kHz to10 kHz. Because the phase angle would be shifted by -90° regarding to applied voltage when electrolyte current flowing through a capacitor. In contrast to capacitor, the phase angle of current sould stay in phase with voltage when going through a resistor. Therefore the phase angle in the regions between 1 Hz to 10 Hz was determined by Z_{CPE}, while the bulk solution resistance Rs dominated in the range between 1 kHz to 10 kHz.

3.4.2 Impedance Measurement for Different Concentrations of *E.coli O157:H7* and *Staphylococcus aureus*

Fig 3.17 showed the impedance spectrum of nanoporous membrane after bacteria capturing in *E. coli O157:H7* and *Staphylococcus aureus* PBS solution with concentrations from 10^2 to 10^6 CFU/mL by scanning the frequency from 1 Hz to 10 kHz. The impedance amplitude difference due to electrolyte current blocking by captured bacteria cells increased with the increasing of bacteria concentrations. At low frequency range, the bacteria cell behaved as an insulator and the current could

not flow through the cell. However, when the frequency was high, the polarization effect made the bacteria cell electrically "invisible" when current going through. In the experiment, the current could not pass through the bacteria cell easily at the low frequency range. Therefore, the impedance change caused by captured bacteria could be observed.

In Fig 3.17, with bacteria concentration increased, the impedance spectrums had an upper shift, which meant the increase of impedance amplitude at the whole frequency range, espcically in the low frequency range. It is because that samples with higher bacteria concentrations had more bacteria cells bond to the nanoporous alumina membrane which could lead to more nanopores blocking by the bacteria cells and hence increase the impedance amplitude. The impedance difference could also be represented by normalized impedance change (NIC) shown in the equation below.

$$NIC = \frac{Z_{sample} - Z_{control}}{Z_{control}} \times 100\%$$

As shown in Fig 3.18, NIC first increased from 1 Hz to about 100 Hz and then decreased from 300 Hz to 10 kHz. The maximum impedance amplitude change was in the region of 80-300 Hz and mostly around 100 Hz. So, NIC at 100 Hz was used as an indicator to describe the trend of impedance change caused by different bacteria concentrations. As shown in Fig. 3.19(a), the NIC at 100 Hz for *E. coli O157:H7* concentration of 10^2 CFU/ml was 4.62±0.23%. Then it increased to 16.77±0.80% for concentration of 10^3 CFU/ml, 45.46±2.27% for concentration of 10^4 CFU/ml, then it decreases little to 39.78±3.38% for concentration of 10^5 CFU/ml

and finally increased to 78.12±5.47% for concentration of 10^6 CFU/ml. In Fig. 3.19(b), the NIC at 100 Hz for *Staphylococcus aureus* with concentrations of 10^2 CFU/ml is 49.12±2.95%. Then it increased to 61.15±2.45% for concentration of 10^3 CFU/ml, 62.36±4.37% for concentration of 10^4 CFU/ml, 77.32±3.87% for concentration of 10^5 CFU/ml and 111.52±5.02% for concentration of 10^6 CFU/ml. As shown in Fig 3.19, a correlationship was found between bacteria concentraions and NIC% change for both *E. coli O157:H7* and *Staphylococcus aureus*. The regression equation for NIC versus *E. coli O157:H7* concentrations from 10^2 to10^6 CFU/ml is y=7.3832x-31.052 with R^2=0.8955, where y is the value of NIC and x is the concentration of *E. coli O157:H7* in Log CFU/ml. The similar regression equation for presence of *Staphylococcus aureus* with concentrations from 10^2 to10^6 CFU/ml is y=6.0084x+16.78 with R^2=0.9083.

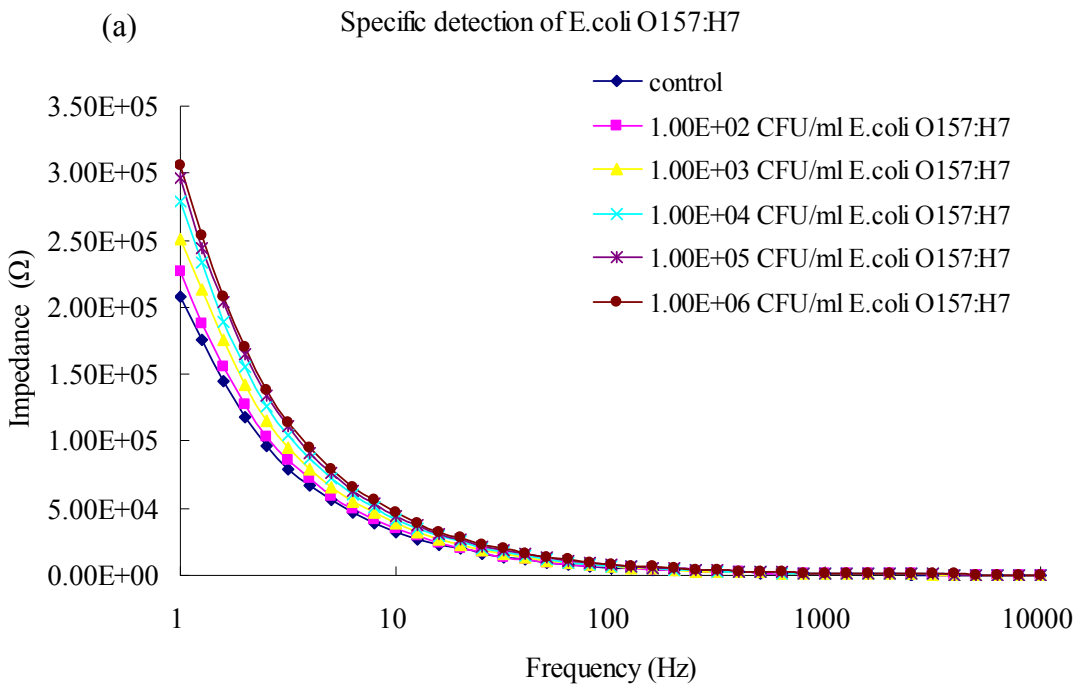

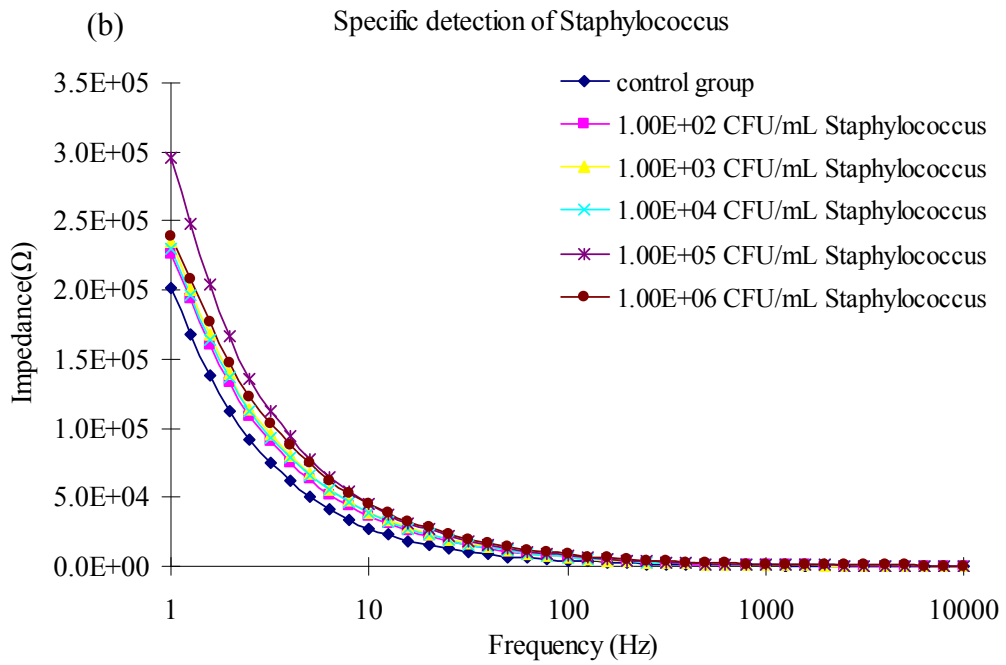

Fig 3.17 Impedance spectra of bacteria samples with concentrations from 10^2 to 10^6 CFU/mL, along with only PBS as control group, (a) *E. coli O157:H7*, (b) *Staphylococcus aureus*

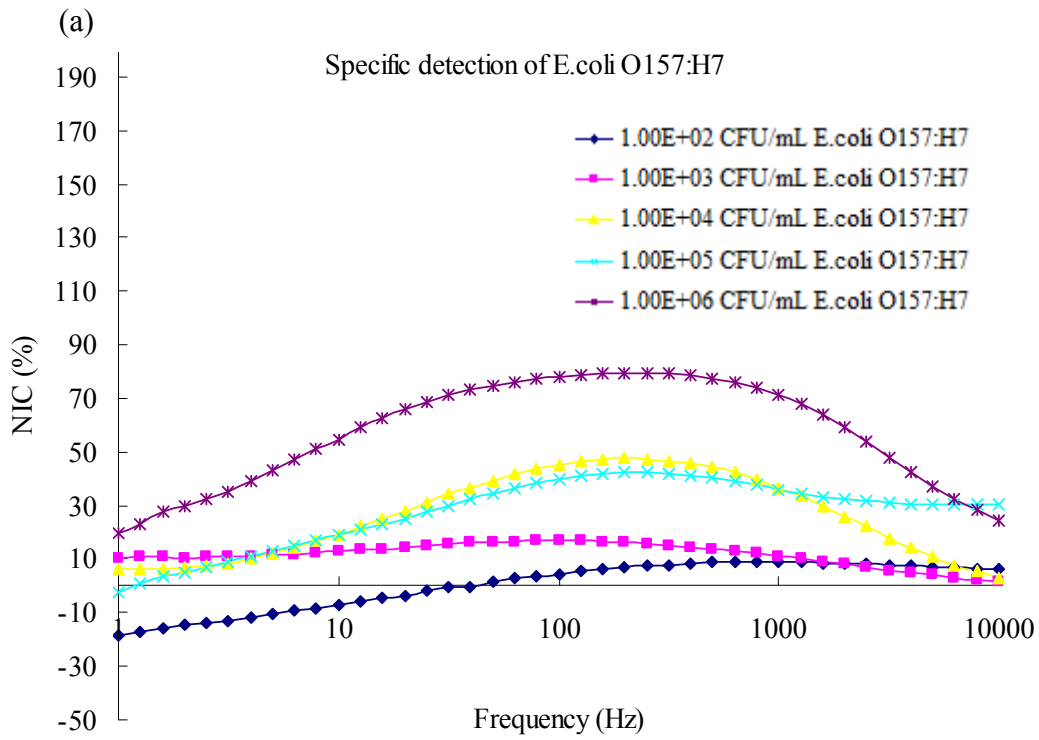

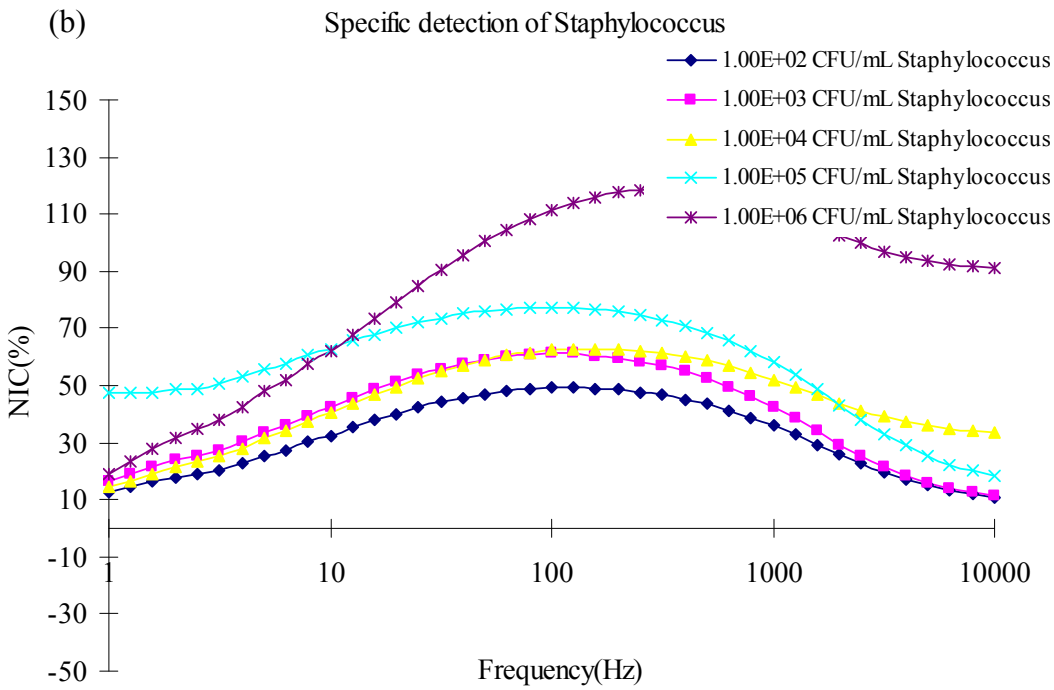

Fig 3.18 Normalized impedance change (NIC) from 1-10^5 Hz with different concentrations of (a) *E.coli O157:H7*, (b) *Staphylococcus aureus*

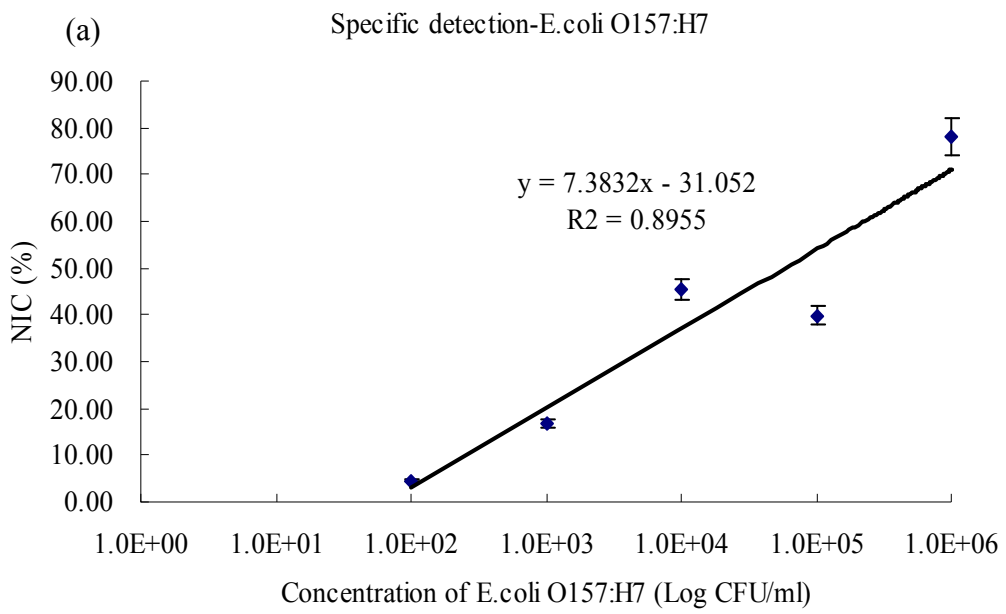

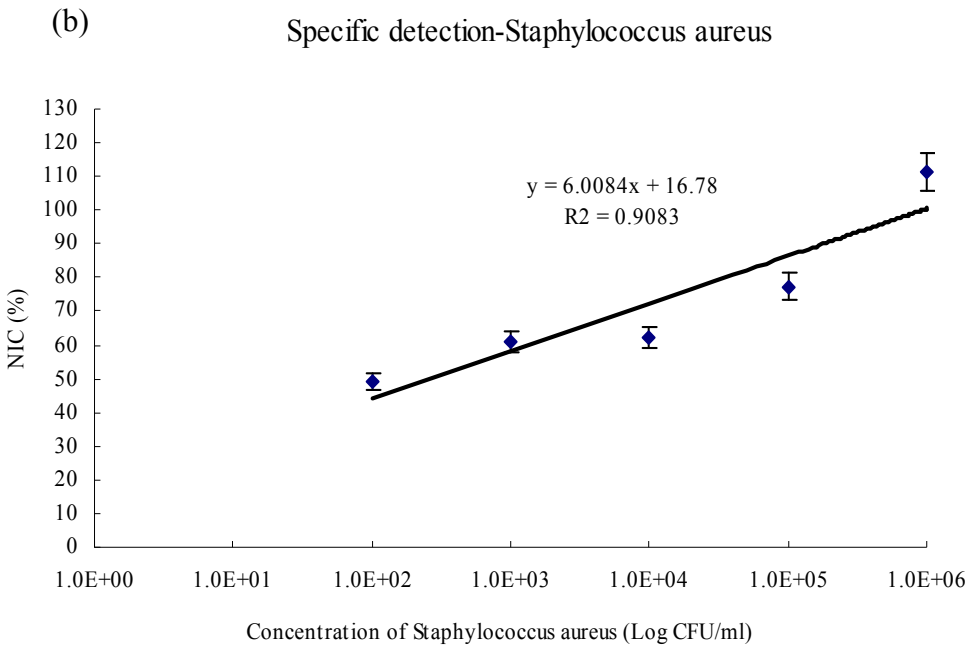

Fig 3.19 NIC at 100 Hz with different bacteria concentrations (a) *E. coli O157:H7*, (b) *Staphylococcus aureus* with respect to the control group. Spots indicate the experimental data, while the solid line means the regression line

The response time is an important indicator for the performance of biosensor. To analyze the response time of specific antibody modified membrane to target bacteria, both *E. coli O157:H7* and *Staphylococcus aureus* samples with various concentrations from 10^3-10^6 CFU/ml were used for testing. The impedance spectrum was recorded at time points of 0, 5, 10, 15, 20, 25, 30, 35, 45, 60, 90, 120 and 180 minutes and the normalized impedance change (NIC) at 100 Hz was plotted versus time. The response time was defined as the time from adding the bacteria samples for the sensor signal response (impedance change) to reach 75% of its total value (Ronkainen et al. 2010).

Fig 3.20 showed real-time response curves of anti- *E. coli O157:H7* modified membrane to samples of *E. coli O157:H7* with concentrations from 10^3-10^6 CFU/ml. As shown in Fig 3.20, the NIC did not change much in the first 20 minutes for 10^3-10^5 CFU/ml, but increased sharply for 10^6 CFU/ml. Then the normalized impedance change of all concentrations kept growing and increased rapidly by 12.0% for 10^3 CFU/ml, 19.0% for 10^4 CFU/ml, 33.3% for 10^5 CFU/ml and 80.4% for 10^6 CFU/ml at 2 hours, which accounted for 77.6%, 81.7%, 76.5% and 97.76% of the total impedance change from 0-180 minutes. However, in the next 60 minutes, the impedance magnitude increased only 22.4% for 10^3 CFU/ml, 18.3% for 10^4 CFU/ml, 23.5% for 10^5 CFU/ml and 2.3% for 10^6 CFU/ml of total impedance change within the 3 hours.

Generally, after *E. coli O157:H7* samples were added to the anti-*E.coli O157:H7* antibody modified membrane surface in the first 2 hours, these bacteria cells would react with the specific antibody and were captured on the membrane surfaces with a quick and relative large impedance change. With more and more bacteria cells captured on the membranes, the free bacteria in the sample solution were hindered from immobilization by captured bacteria. Finally, the captured bacteria on the anti-*E.coli O157:H7* antibody modified membrane was saturated and could not capture any more *E.coli O157:H7*.

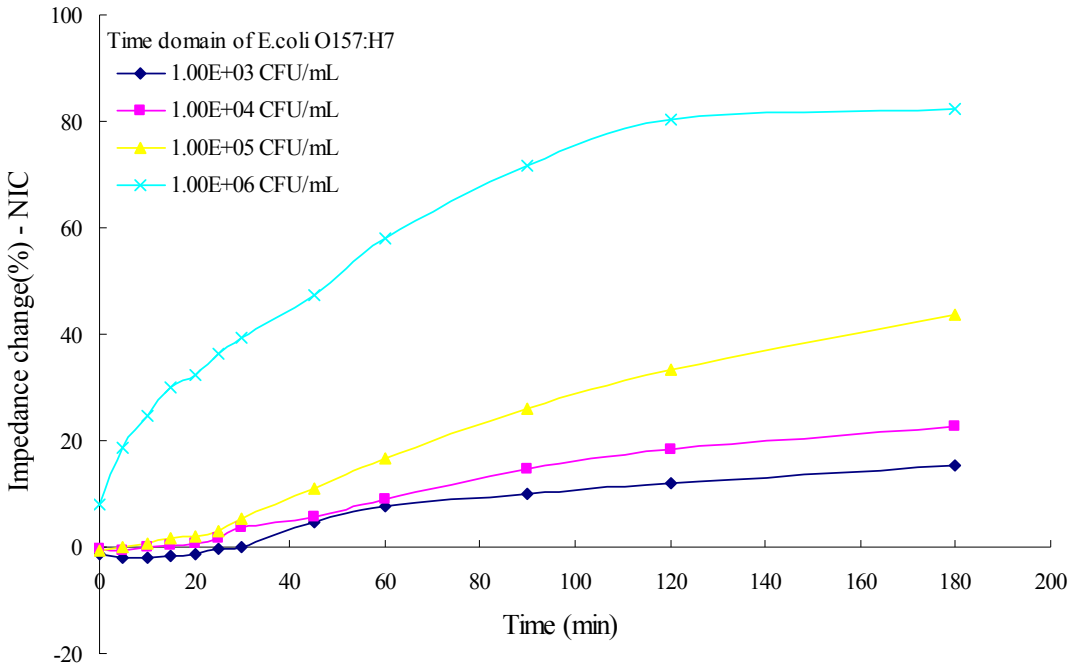

Fig 3.20 Time domain by impedance change with *E.coli O157:H7* for various concentrations

The reponse time experiments were also performed for *Staphylococcus aureus* with concentrations of 10^3-10^6 CFU/ml for 3 hours. As shown in Fig 3.21, the NIC at 100 Hz increased by 32.06% for 10^3 CFU/ml, 41.25% for 10^4 CFU/ml, 49.15% for 10^5 CFU/ml and 68.45% for 10^6 CFU/ml at 2 hours, which accounted for 83.3%, 87.0%, 85.8% and 96.4% of the total NIC change of the whole 3 hours. This big impedance change of the first 2 hours was mainly due to the large available sensing area on nanoporous alumina membrane at the beginning. In the final one hour, the membrane was almost saturated with only 4%-15% of total impedance change, which meant *Staphylococcus aureus* cells were difficult to be captured on nanoporous alumina membrane.

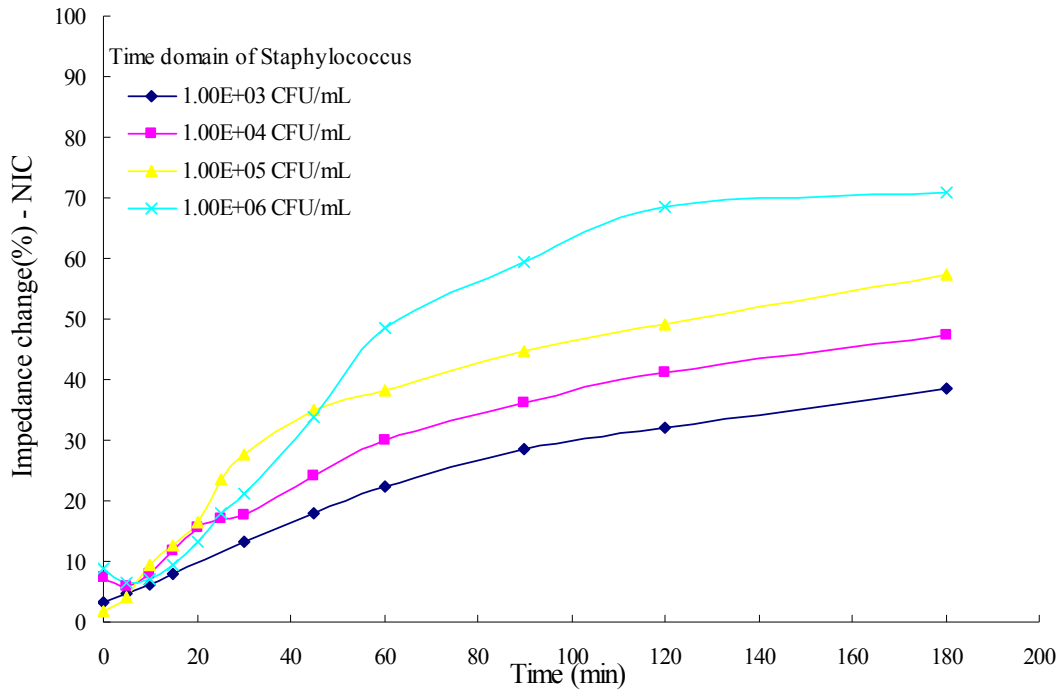

Fig 3.21 Time domain by impedance change with *Staphylococcus aureus* with various concentrations

From the above analysis, it could be concluded that for both *E.coli O157:H7* and *Staphylococcus aureus*, 2-3 hours are enough for the reaction of antibody-antigen to immobilize bacteria cells on functionalized nanoporous alumina membrane. The response time for both *E. coli O157:H7* and *Staphylococcus aureus* with all concentrations are between 2-3 hours.

3.4.3 Impedance Measurements for Cross-Bacteria Detection

The cross-reactivity in antibodies was an important concern in immunoassays. To assess the specificity of this bacteria detection system, the cross-bacteria detection experiments were studied to explore if there was a cross reaction between antibody and unspecific bacteria.

(a) Cross-bacteria detection of E.coli O157:H7 with S.a modified membrane

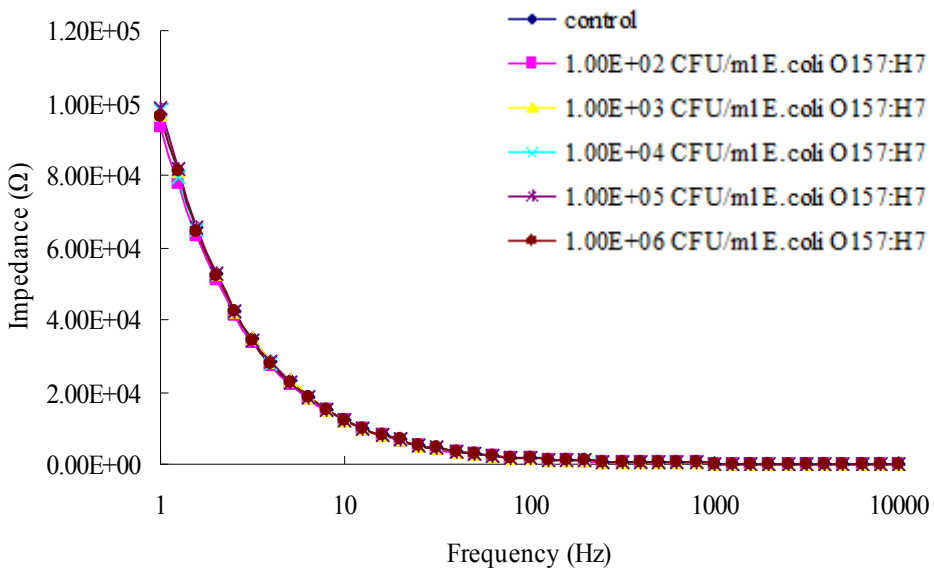

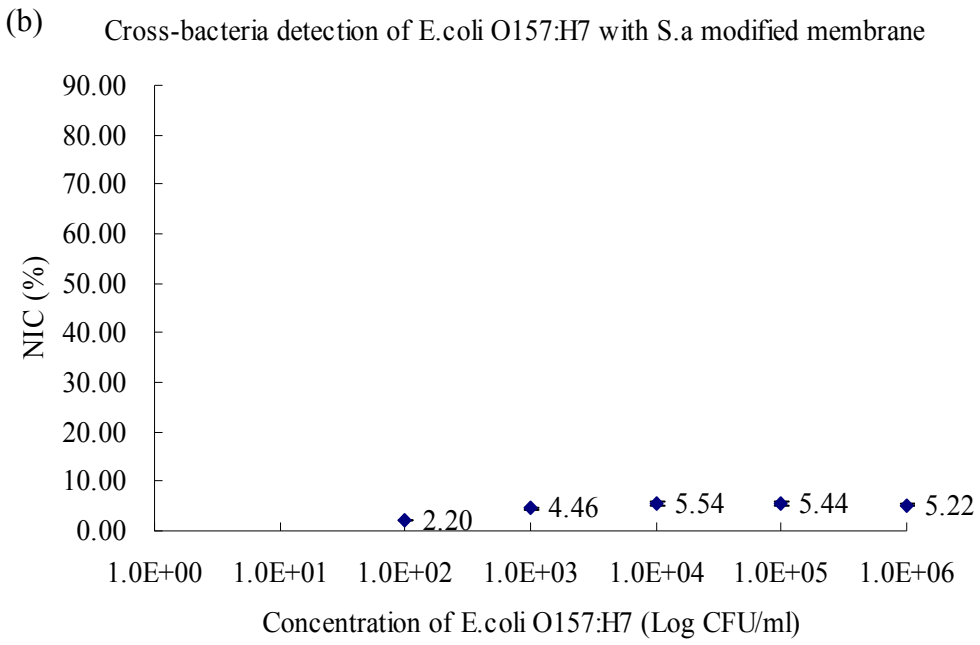

Fig 3.22 Impedance spectra (a) and NIC (b) of sample of *E .coli O157:H7* with anti-*Staphylococcus aureus* antibody modified membrane

The anti-*Staphylococcus aureus* antibody was grafted onto the GPMS modified alumina membrane, and samples with different concentrations containing *E.coli O157:H7* were added from 10^2 to 10^6 CFU/mL. Membranes were rinsed with PBS and the impedance spectrum was monitored to see if there was any *E.coli O157:H7* captured on the nanoporous membrane. Fig 3.22(a) showed that impedance amplitude change was undetectable between the PBS control group and bacteria samples with various concentrations. Compared with the specific antibody-bacteria reaction, there was no obvious impedance amplitude change. As shown in Fig 3.22(b), the NIC at frequency of 100 Hz is 2.20±0.19% for concentration of 10^2 CFU/ml, 4.46%±0.20% for the concentration of 10^3 CFU/ml, 5.54%±0.39% for the concentration of 10^4 CFU/ml, 5.44%±0.30% for the concentration of 10^5

CFU/ml and 5.22%±0.25% for concentration of 10^6 CFU/ml. In this experiment, the low impedance change around 5% or below for each concentration was believed to be caused by the non-specific bacteria adsorption that was failed to be washed away.

Figure 3.23 showed the cross bacteria experiments for *Staphylococcus aureus* detection using anti- *E. coli O157:H7* antibody immobilized nanoporous membrane based biosensor. Different concentrations from 10^2 to 10^6 CFU/ml of *Staphylococcus aureus* were tested. There was no obvious impedance amplitude change for all *Staphylococcus aureus* concentrations As shown in Fig 3.23(b), the NIC at frequency of 100 Hz is 2.93±0.11% for concentration of 10^2 CFU/ml, 4.71±0.27% for concentration of 10^3 CFU/ml, 5.30±0.63% for concentration of 10^4 CFU/ml, 5.99±0.29% for concentration of 10^5 CFU/ml and 6.79±0.33% for concentration of 10^6 CFU/ml. It confirmed that no obvious cross reaction happened between anti-*E. coli O157:H7* antibody and *Staphylococcus aureus*. The cross bacteria experiments demonstrated the high specificity of this biosensor for *E. coli O157:H7 and Staphylococcus aureus* detection.

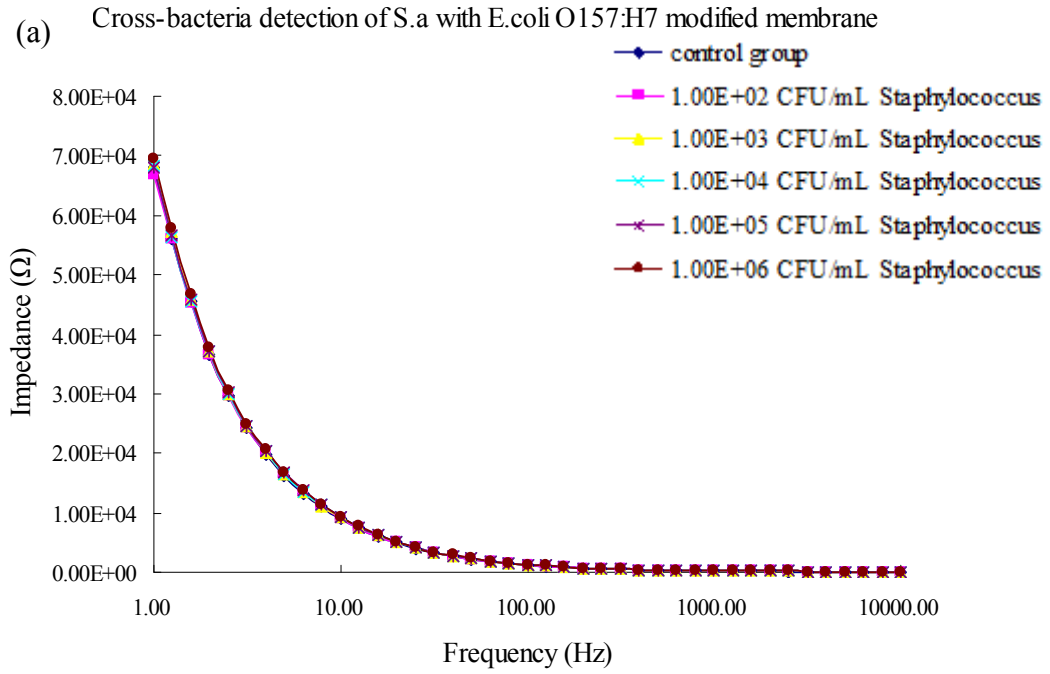

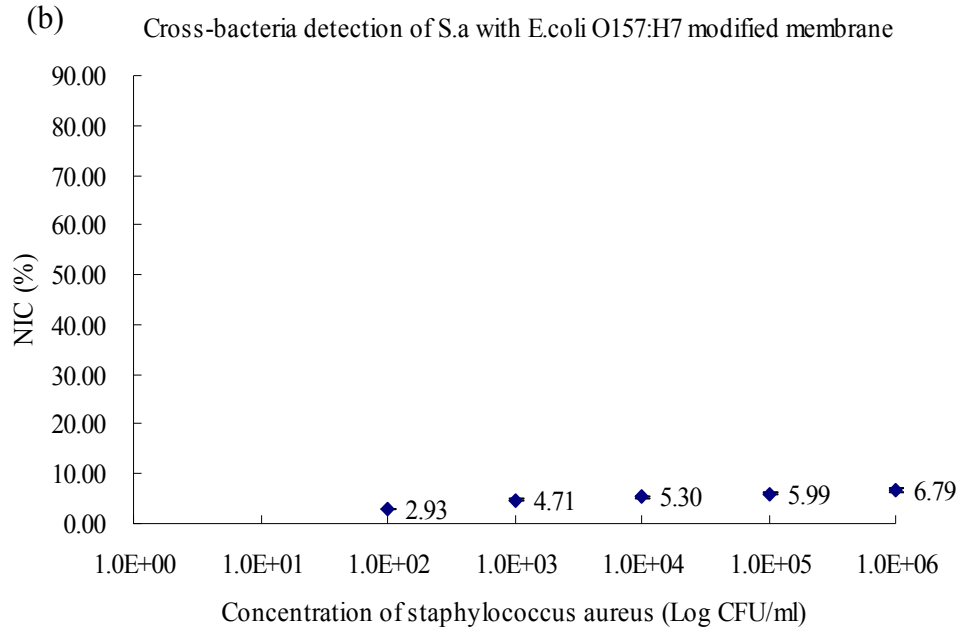

Fig 3.23 Impedance spectra (a) and NIC (b) of sample of *Staphylococcus aureus* with anti-*E.coli O157:H7* antibody modified membrane

3.5 Simultaneous Detection of Multiple Type Bacteria via Impedance Spectrum

The PDMS based chip for simultaneous detection of two types of bacteria was developed. Two nanoporous alumina membranes immobilzed with anti-*E. coli O157:H7* antibodies and anti- *Staphylococcus aureus* antibodies respectivley were integrated with this PDMS based chip. The mechanism was described in Chapter 2. Different samples were used to testify the functionality of this chip including 1) mixture of *E. coli O157:H7* and *Staphylococcus aureus* with different concentrations in PBS solution with the ratio1:1; 2) *E. coli O157:H7* with different concentrations in PBS solution; 3) *Staphylococcus aureus* with different concentrations in PBS solution and 4) Pure PBS solution as the control group.

3.5.1 Detection for Samples with only *E.coli O157:H7*

In order to test the specificity of this multiple bacteria sensing system, samples with only *E.coli O157:H7* or *Staphylococcus aureus* with different concentrations were injected respectively. Fig 3.24 showed the setup for samples with only *E. coli O157:H7* in the multiple bacteria detection system.

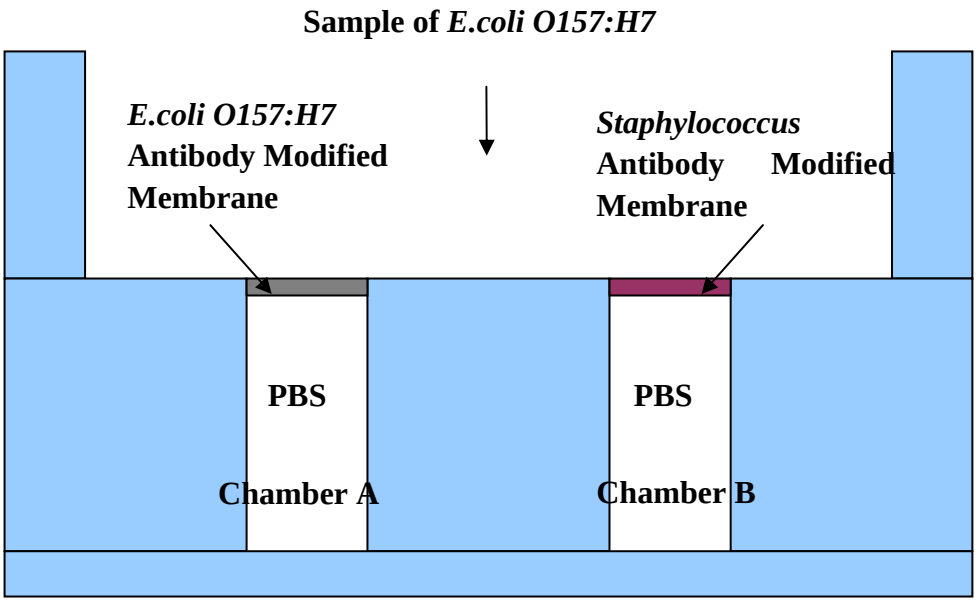

Fig 3.24 Setup of multipe type bacteria detection system for sample with only *E.coli O157:H7*

Fig 3.25 showed the measured impedance spectra and calculated NIC at 100 Hz with anti-*E.coli O157:H7* antibody modified membrane in chamber A for samples with only *E.coli O157:H7*. The impedance spectra were recorded in the frequency range from 1 Hz to 10,000 Hz with *E.coli O157:H7* concentration from 10^3 to 10^6 CFU/ml. As shown in Fig 3.25(a), the impedance spectra of anti-*E.coli O157:H7* modified membrane showed a regular upper shift with the increasing of *E.coli O157:H7* concentrations. In Fig 3.25(b), the NIC at 100 Hz was 7.36±0.87% for 10^3 CFU/ml, and then increased to 19.13±0.77% for 10^4 CFU/ml, 37.88±1.10% for 10^5 CFU/ml and finally to 60.06±0.97% for 10^6 CFU/ml, respectivley. The regression equation of NIC at 100 Hz for samples with *E.coli O157:H7* of 10^3-10^6 CFU/ml is y=7.6805x-48.475 with R^2=0.9826.

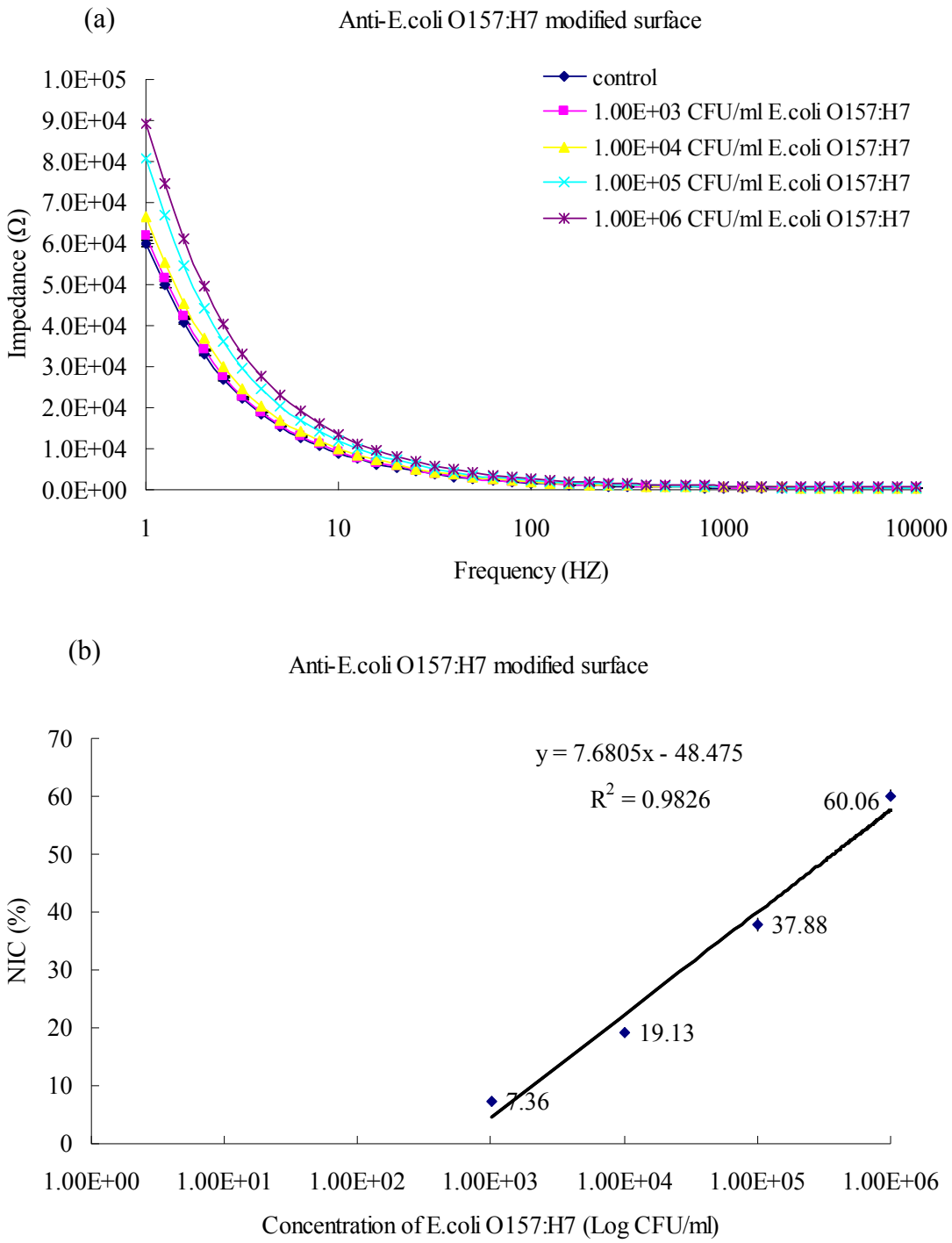

Fig 3.25 (a) Impedance spectra and (b) NIC of samples with only *E.coli O157:H7* from 10^3 to 10^6 CFU/ml on anti- *E. coli O157:H7* antibody modified nanoporous membrane

For furthur analysis of impedance change for bacteria capturing on nanoporous membrane, the impedance spectra were fitted with the equivalent circuit shown in Fig 3.16. In order to analyze the changes caused by bacteria cells on membrane, the resistance of bulk solution was fixed at value of 278.5 (R_s=278.5 ohm), which was derived from the fitting data for impedance spectra of control group. The impure capacitance of constant phase element (CPE) was represented by Q_{CPE} including Q_{Yo} and n. The parameter of n is between 0 and 1. If it is closer to 1, the CPE is more similar to a pure capacitance.

$$Q_{\mathbf{CPE}} = \frac{1}{Q_{Y0}(j\omega)^n}$$

Where Q_{Yo} is numerically equal to the admittance (1/|Z|) at ω = 1 rad/s.

Fig 3.26 showed the fitted parameters of equivalent circuit for impednace data from Fig 3.25(a). There was a small increase in Q_{Yo}. The parameter n remained stable during the whole process. There was a 33% decrease of compoment C_c and a 38% increase for compoment R_c, which accounts for the major impedance change from bacteria layer.

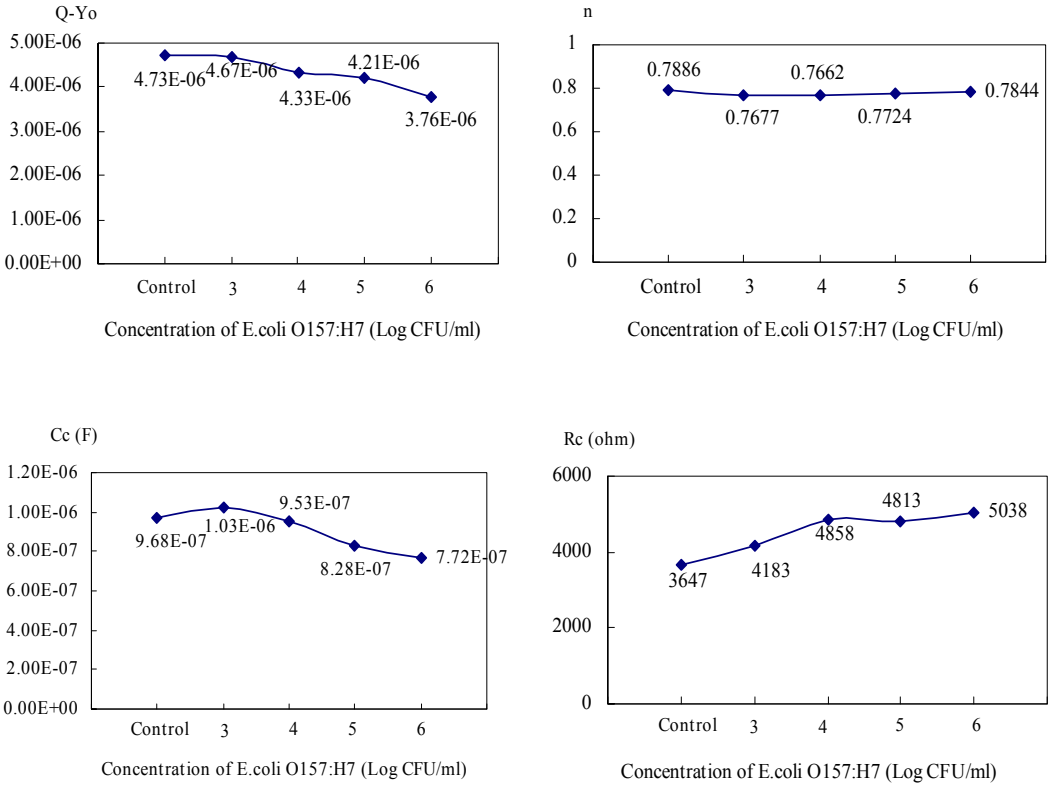

Fig 3.26 Circuit model parameters change with concentrations for samples with only *E.coli O157:H7* on anti-*E.coli O157:H7* antibody modified membrane

However, for the anti-*Staphylococcus aureus* modified nanoporous membrane in chamber B, there was no significant impedance amplitude change between control group and samples with only *E. coli O157:H7* shwon in Fig 3.27. The NIC at 100 Hz was 4.61±0.10 % for concentration of 10^3 CFU/ml, and 5.05±0.32% for 10^4 CFU/ml, 5.55%±0.05% for 10^5 CFU/ml, and 5.96±0.17% for 10^6 CFU/ml. This slight change was caused by physical adsorption of *E. coli O157:H7* cells which were failed to be washed away. Compared with the impedance data in chamber A shown in Fig 3.25, *E. coli O157:H7* could be specifically detected between 10^3 and 10^4 CFU/ml using this system. Fig 3.28 showed the equivalent circuit parameters change with different *E. coli O157:H7* concentrations. All the parameters including Q_{Yo}, n, C_c and

R_c remained almost unchanged, which demonstrated the specificity for detection of *E. coli O157:H7* for this system. Actually, the percentage variation between 10^6CFU/ml and control group for each element in Fig 3.28 are: Q-Yo: 3.25%; n: 0.68%; Cc: 0.78%; Rc: 3.48%, which are very small. Therefore there is almost no change in all elements.

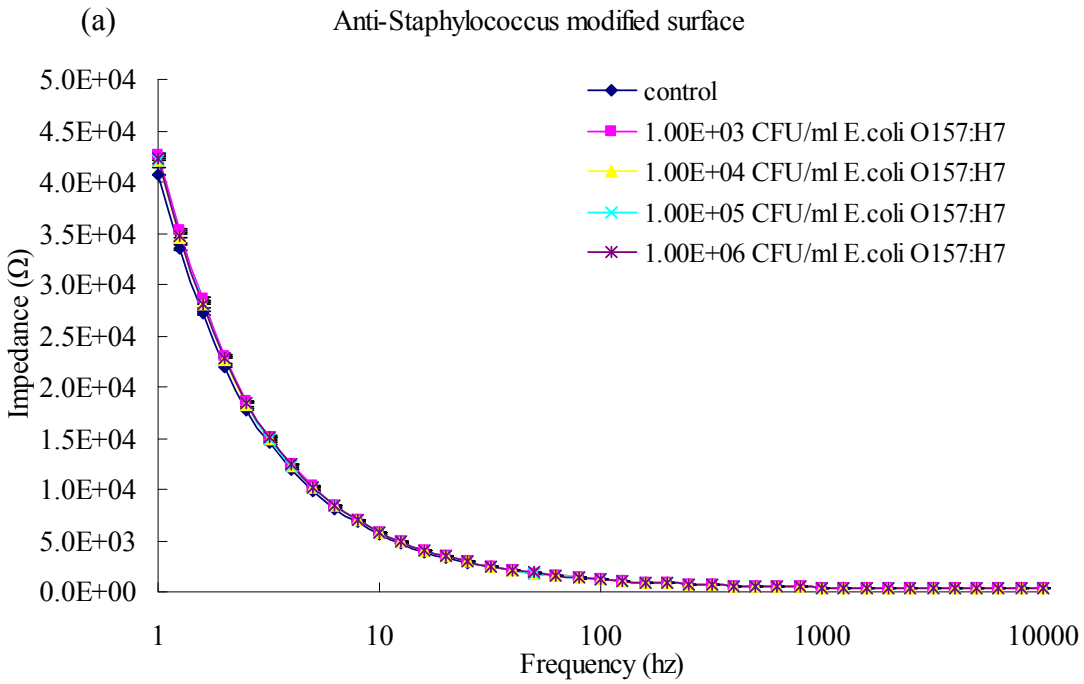

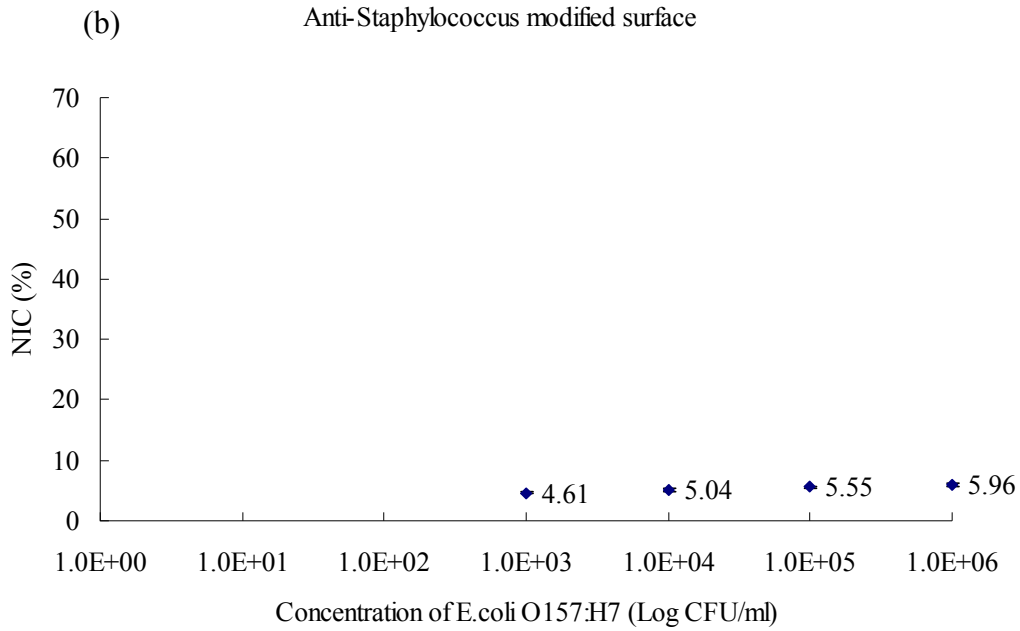

Fig 3.27 (a) Impedance spectra and (b) NIC of samples with only *E.coli O157:H7* from 10^3 to 10^6 CFU/ml on anti-*Staphylococcus aureus* antibody modified nanoporous membrane

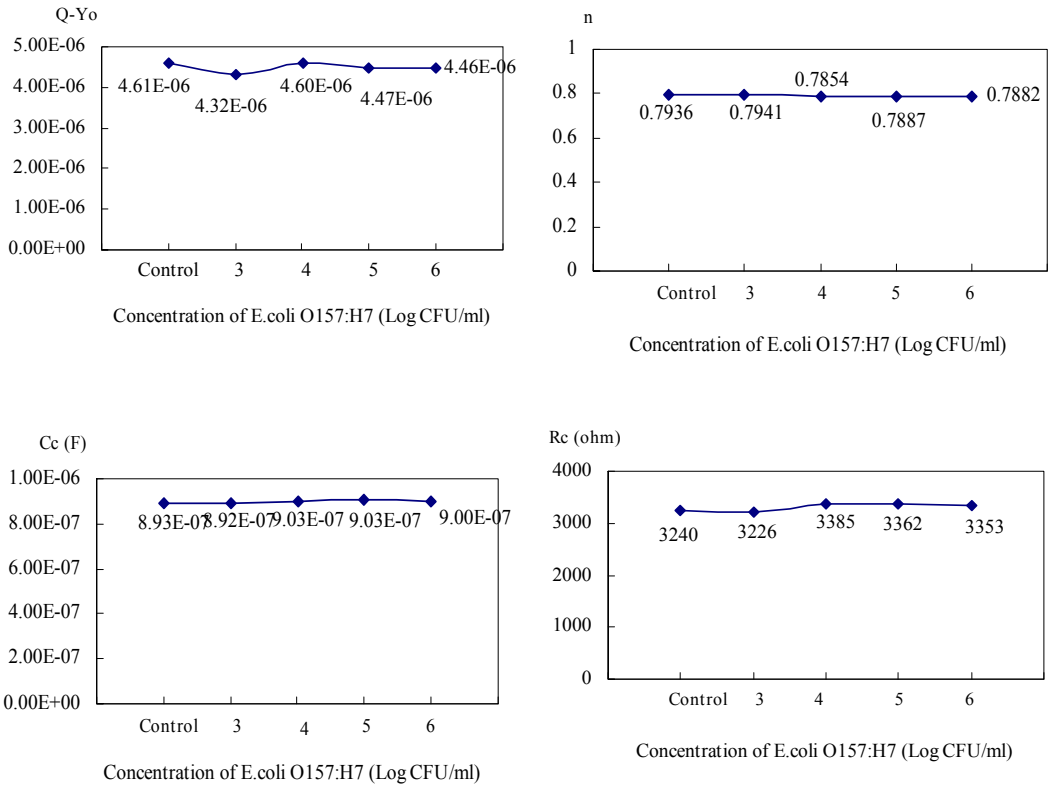

Fig 3.28 Circuit model parameters change with concentrations for samples with only *E.coli O157:H7* on anti-*Staphylococcus aureus* antibody modified membrane

3.5.2 Detection for Samples with only *Staphylococcus aureus*

In order to test the specificity of this multiple bacteria sensing system for *Staphylococcus aureus*, samples with only *Staphylococcus aureus* with different concentrations were injected. Fig 3.29 showed the setup for samples with only *Staphylococcus aureus* in the multiple type bacteria detection system.

Fig 3.30 showed the measured impedance spectra and calculated NIC at 100 Hz with anti-*E.coli O157:H7* antibody modified membrane in chamber A for samples with only *Staphylococcus aureus*. As shown in Fig 3.30(a), there was no obvious impedance amplitude change on the anti-*E.coli* O157:H7 modified surface. As shown in Fig 3.30(b), the NIC at 100 Hz was 2.27±0.31% for 10^3 CFU/ml, and increased to 3.77±0.41% for 10^4 CFU/ml, 6.53±0.74% for 10^5 CFU/ml and 9.20±0.62% for 10^6 CFU/ml. The slight impedance amplitude increas was caused by the unspecific physical adsorption that could not be washed away.

Fig 3.31 showed the fitted equivalent model parameters. Generally, all the parameters including Q_{Yo}, n, C_c and R_c remained almost unchanged, which demonstrated the specificity for detection of *Staphylococcus aureus* for this system. The average values for Q_{Yo} and n are 4.01±0.0566 μF and 0.7985±0.002653, respectively. C_c and R_c are 0.681±0.0326 μF and 4421.2±187.16 ohm, respectively.

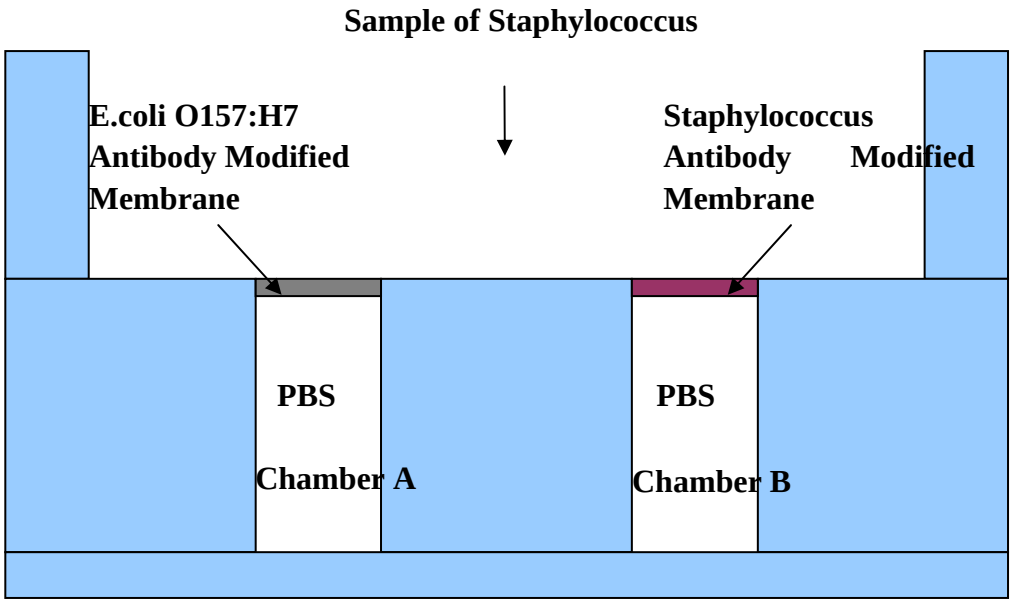

Fig 3.29 Setup of multiple type bacteria detection system for sample with only *Staphylococcus aureus*

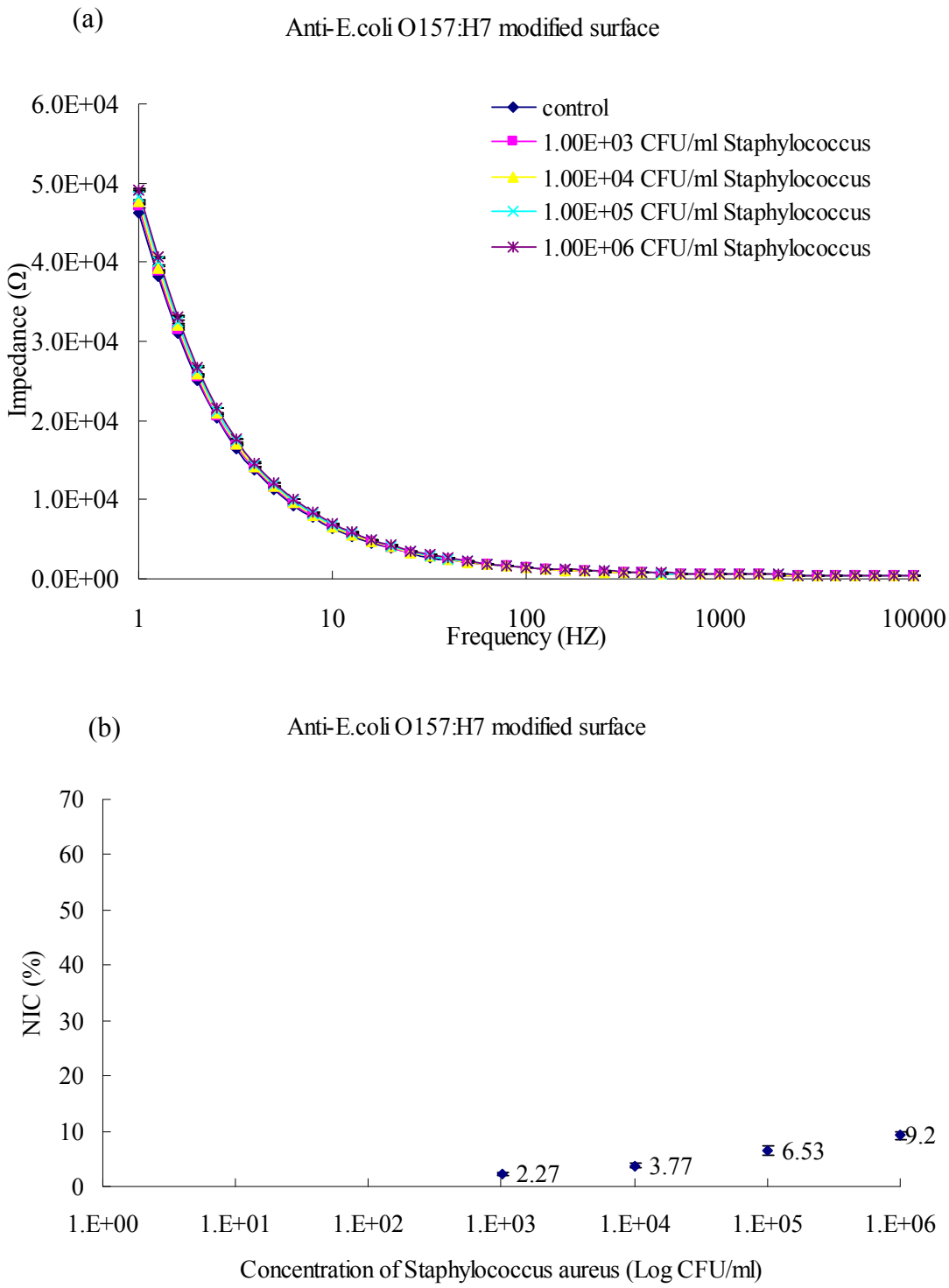

Fig 3.30 (a) Impedance spectra and (b) NIC of samples with only *Staphylococcus aureus* from 10^3 to 10^6 CFU/ml on anti-*E.coli O157:H7* antibody modified nanoporous membrane

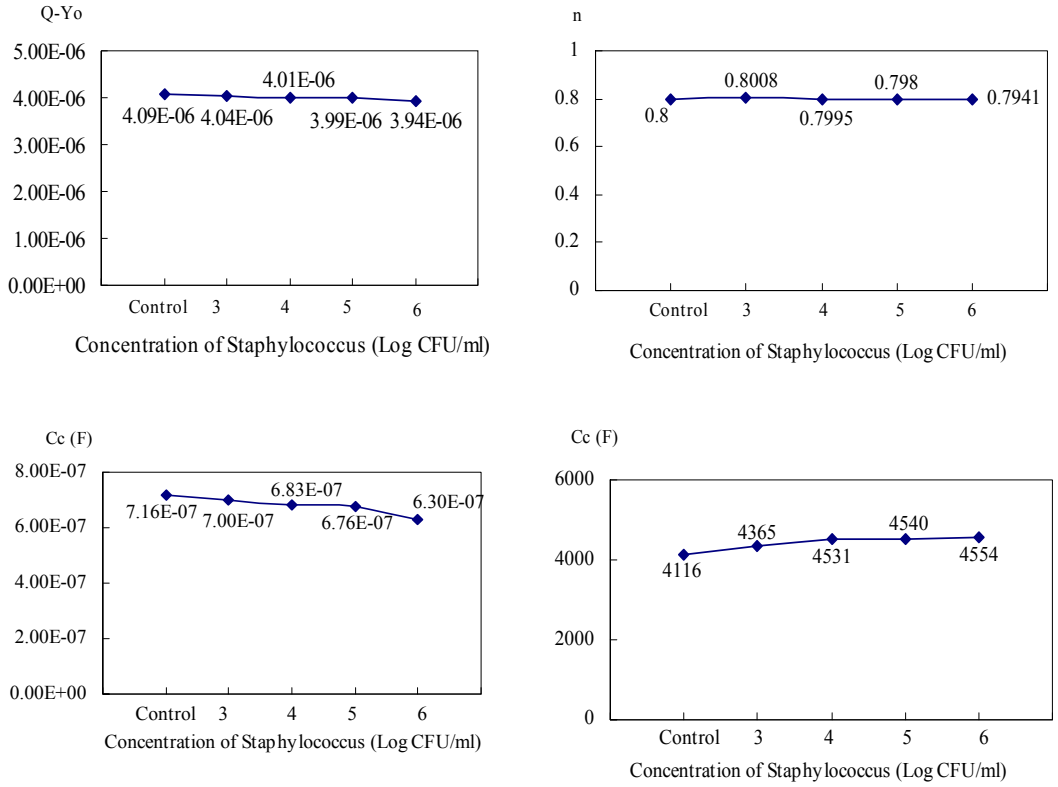

Fig 3.31 Circuit model parameters change with concentrations for samples with only *Staphylococcus aureus* on anti-*E. coli O157:H7* antibody modified membrane

Fig 3.32 showed the measured impedance spectra and calculated NIC at 100 Hz with anti- *Staphylococcus aureus* antibody modified membrane in chamber B for samples with only *Staphylococcus aureus*. The impedance spectra showed a clear upper shift in Fig 3.32(a). As shown in Fig 3.32(b), the NIC at 100 Hz was 17.97±2.93% for 10^3 CFU/ml, and then increased to 25.91±3.71% for 10^4 CFU/ml, 43.11±3.75% for 10^5 CFU/ml and 59.06±4.52% for 10^6 CFU/ml. Compared with unspecific detection impedance data of chamber A shown in Fig 3.30(a), *Staphylococcus aureus* could be

specifically detected around 10^3 CFU/ml using this system. Fig 3.33 showed the fitted equivalent model parameters change with concentrations. Q_{Yo} decreased by around 30% from 4.06×10^{-6} F of control group to 3.08×10^{-6} F of 10^6 CFU/ml which was mainly caused by the non-specific physical adsorption of bacteria on membrane surfaces. There was no obvious change for the parameter n. C_c and R_c showed a decrease of 51.09% and an increase of 67.32% from PBS control group to 10^6 CFU/ml, which were the main contribution to the impedanc amplitude change. The average values for Q_{Yo} and n are 4.01±0.057 μF and 0.80±0.0027, respectively. C_c and R_c are 0.681±0.033 μF and 4421.2±187.16 ohm, respectively.

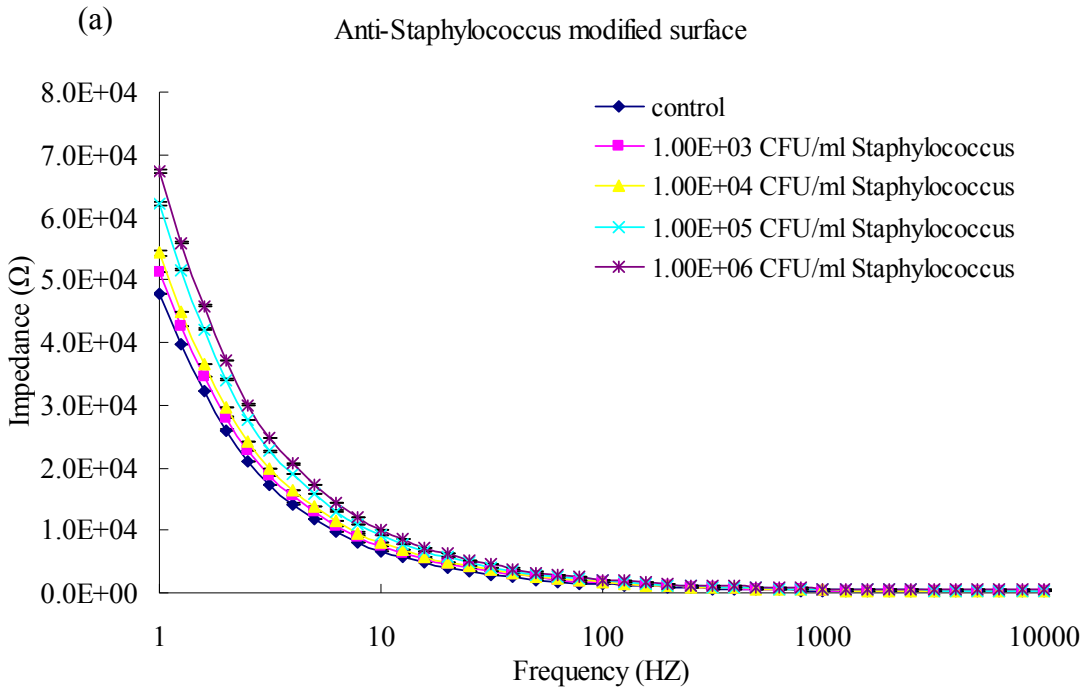

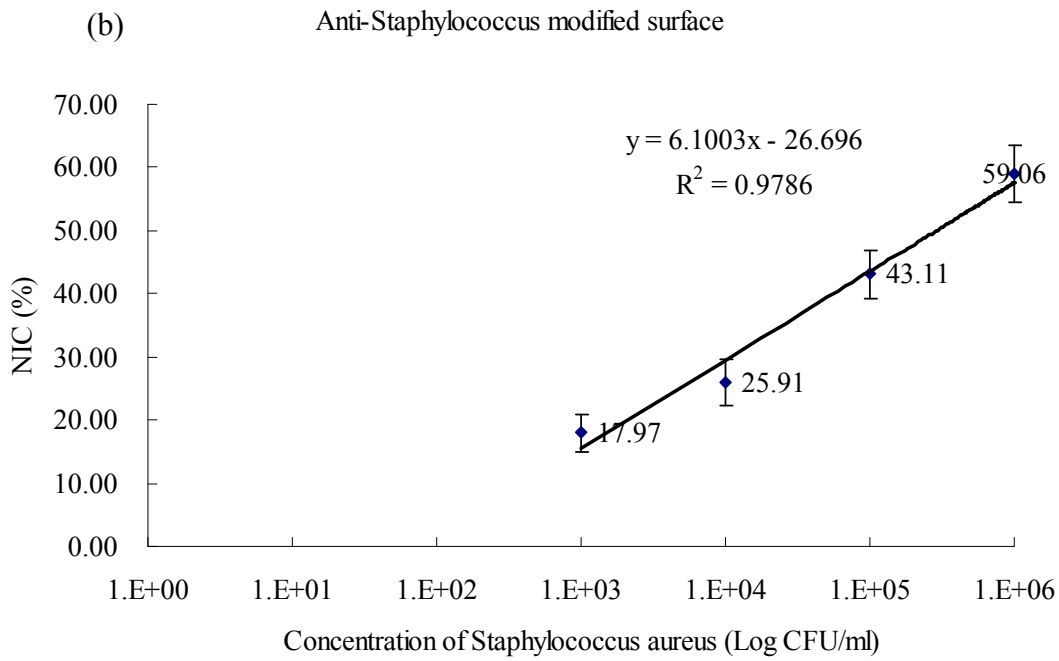

Fig 3.32 (a) Impedance spectra and (b) NIC of samples with only *Staphylococcus aureus* from 10^3 to 10^6 CFU/ml on anti- *Staphylococcus aureus* antibody modified nanoporous membrane

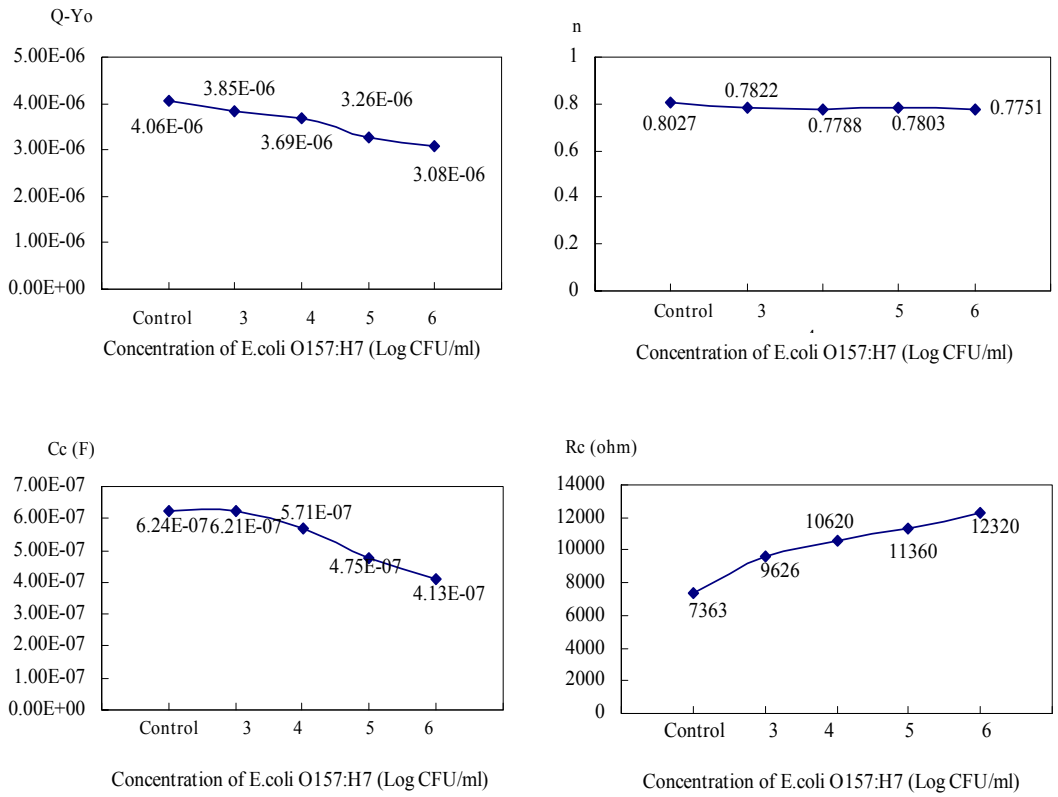

Fig 3.33 Circuit model parameters change with concentrations for samples with only *Staphylococcus aureus* on anti-*Staphylococcus aureus* antibody modified membrane

3.5.3 Detection for Samples with Mixed *E.coli O157:H7* and *Staphylococcus aureus*

E. coli O157:H7 and *Staphylococcus aureus* with the same concentration 10^9 CFU/ml were first mixed together and then diluted by PBS solution to various concenrations from 10^3 to 10^6 CFU/ml. The mixed bacteria samples were then injected into the chip for testing. The setup for this detection was shown in Fig 3.34. The impedance spectra for various concentrations of *E. coli O157:H7* and *Staphylococcus aureus* were recorded respectively, together with PBS control group.

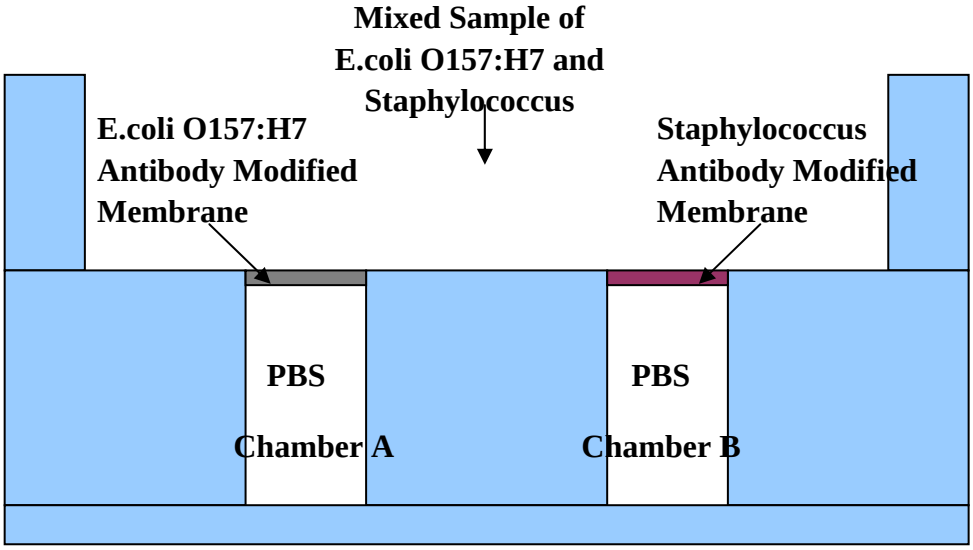

Fig 3.34 Chart of system for mixed bacteria simultaneous detection

Fig 3.35 showed the measured impedance spectra and calculated NIC at 100 Hz with anti-*E.coli O157:H7* antibody modified membrane in chamber A. The impedance spectra were recorded in the frequency range from 1 Hz to 10,000 Hz with mixed bacteria concentration from 10^3 to 10^6 CFU/ml. In Fig 3.35(a), the impedance magnitude increased with the increasing of *E. Coli O157:H7* concentrations in the mixed samples. As shown in Fig 3.35(b), the NIC at 100 Hz increased from 15.94±1.10% for 10^3 CFU/ml to 45.17±1.70% for 10^4 CFU/ml, 82.49±2.54% for 10^5 CFU/ml and finally to 116.17±13.33% for 10^6 CFU/ml. The regression equation of NIC at 100 Hz for mixed bacteria concentration of 10^3-10^6 CFU/ml is $y=14.68x-87.162$ with $R^2=0.9979$.

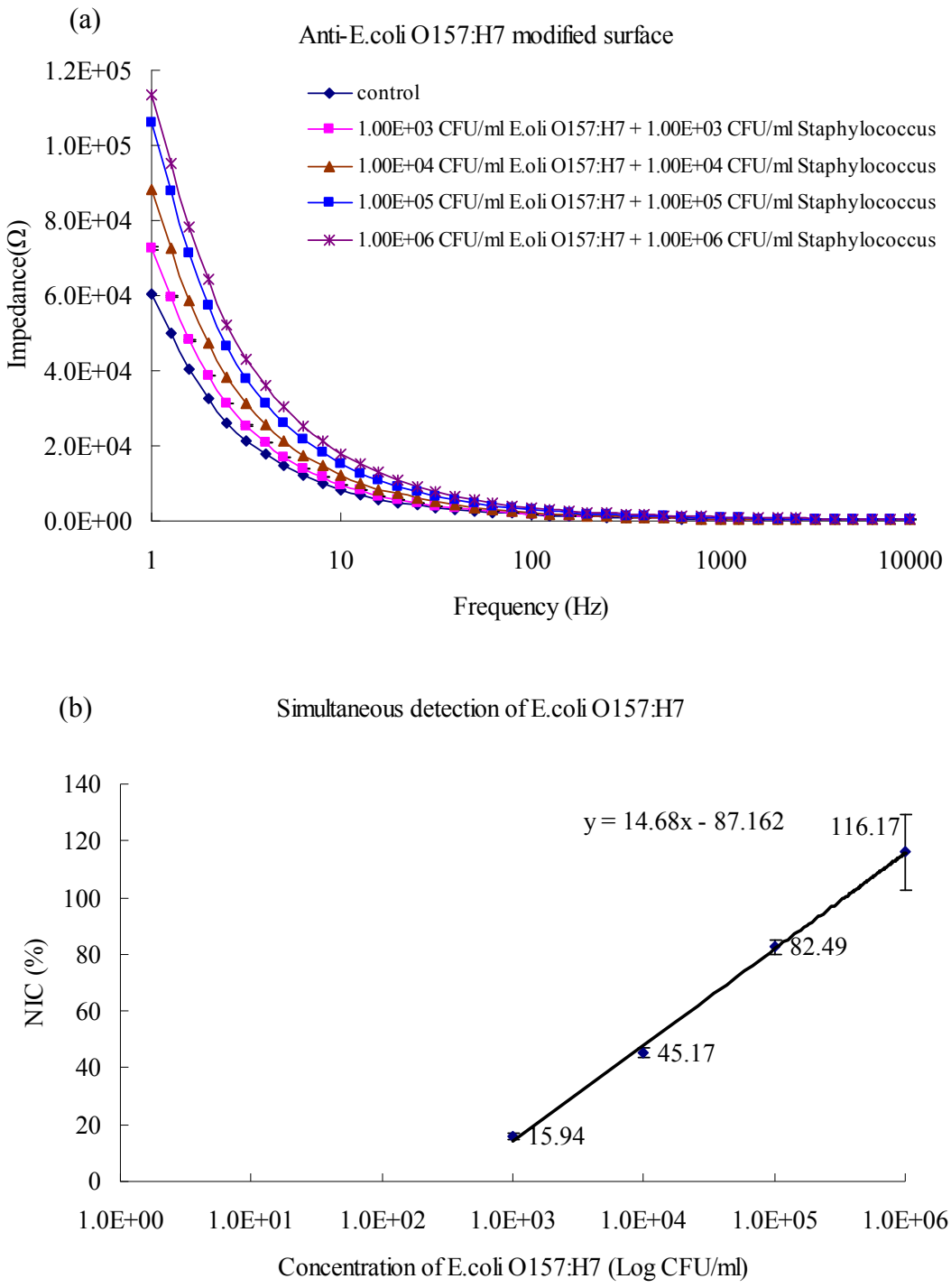

Fig 3.35 (a) Impedance spectra and (b) NIC of *E. coli O157:H7* concentrations in the bacteria mixture samples from 10^3 to 10^6 CFU/ml on anti- *E.coli O157:H7* antibody modified nanoporous membrane

Fig 3.36 showed the equivalent circuit parameters change with *E. coli O157:H7* concentrations in the mixture samples. Q_{Yo} showed a decrease about 40%. The parameter n stayed almost unchanged with the fitted average value around 0.7834± 0.018427. C_c showed an obvious decrease of 76.6% from 6.37×10^{-7} F of control group to 1.49×10^{-7} F of 10^6 CFU/ml. Meanwhile, R_c showed an obvious increase of 195.2% from 5.318 kohm in the control group to 15.7 kohm at the concentrations of 10^6 CFU/ml. This change of C_c and Rc are much larger than the change of Q_{Yo}.

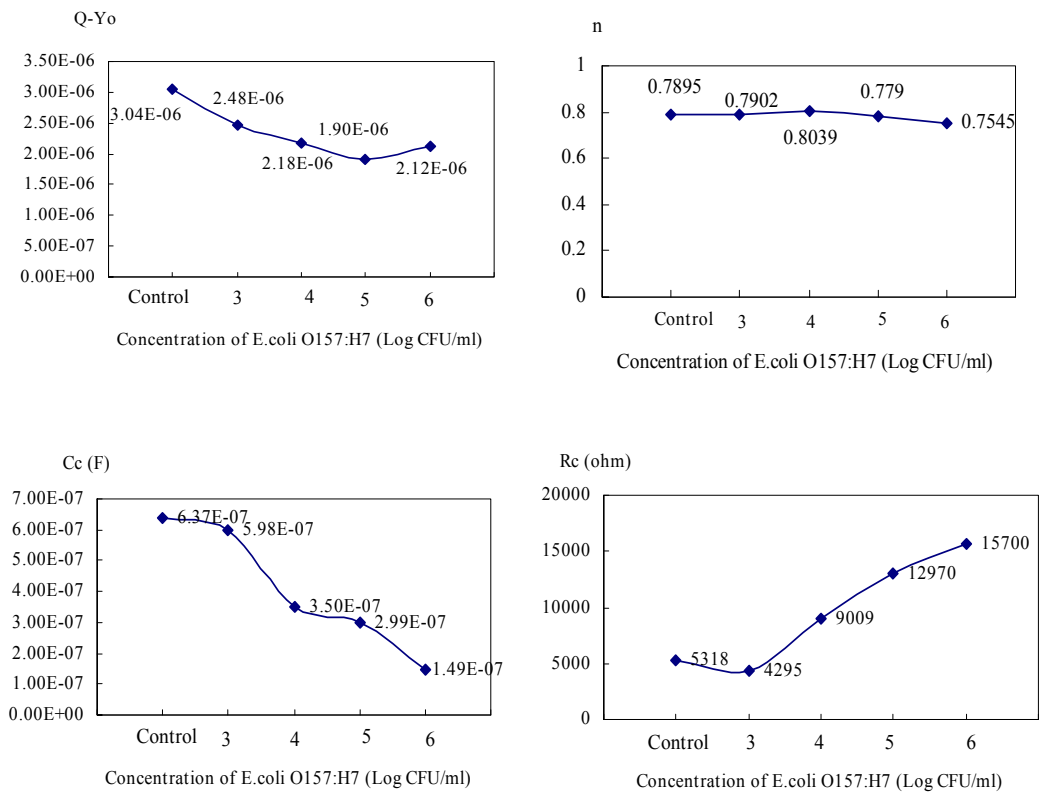

Fig 3.36 Circuit model parameters change with *E. coli O157:H7* concentrations in the bacteria mixture samples on anti-*E. coli O157:H7* antibody modified membrane

Fig 3.37 showed the measured impedance spectra and calculated NIC at 100 Hz with anti-*Staphylococcus aureus* antibody modified membrane in chamber B for the mixed bacteria samples. The impedance spectra were recorded in the frequency

range from 1 Hz to 10,000 Hz with mixed bacteria concentration from 10^3 to 10^6 CFU/ml. In Fig 3.37(a), the impedance magnitude increased with the increasing of *Staphylococcus aureus* concentrations in the mixed samples. As shown in Fig 3.37(b), the NIC at 100 Hz was 2.38±1.26% for 10^3 CFU/ml, and then then increased to 9.19±2.12% for 10^4 CFU/ml, 37.36±2.96% for 10^5 CFU/ml and 58.73±8.18% for concentration of 10^6CFU/ml. The regression equation is y=8.5652x-61.834 with R^2=0.9545.

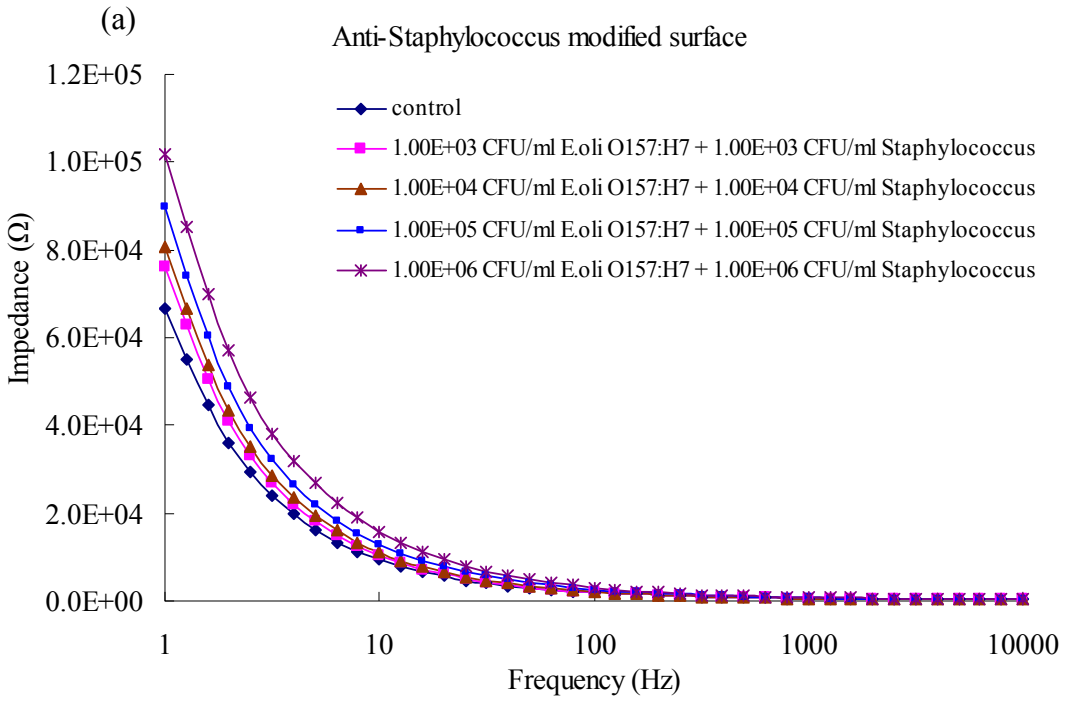

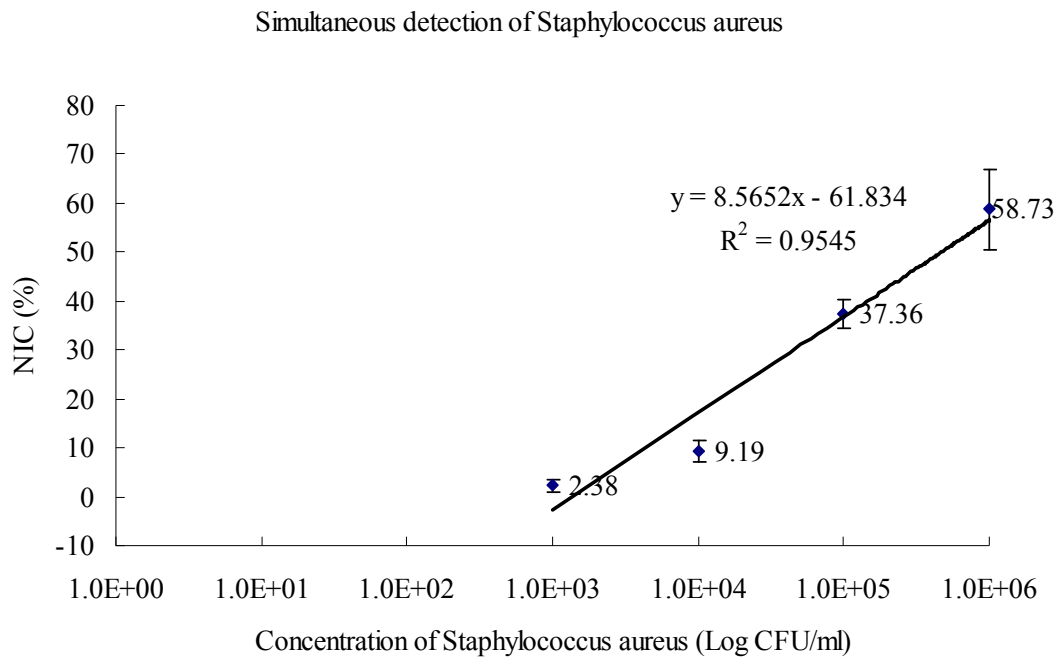

Fig 3.37(a) Impedance spectra and (b) NIC of *Staphylococcus aureus* concentrations in the bacteria mixture samples from 10^3 to 10^6 CFU/ml on anti-*Staphylococcus aureus* antibody modified nanoporous membrane

Fig 3.38 showed the equivalent circuit parameters change with *Staphylococcus aureus* concentrations in the mixture samples. Q_{Yo} showed a decrease of 21.2% from 2.83 μF for PBS control group to 2.23 μF for 10^6 CFU/ml. The average value of n was 0.7865±0.012596. C_c showed a large decrease of 184% from 0.541 μF to 0.19 μF and R_c showed a dramatically increase of 230% from 6.211 kohm to 20.45 kohm.

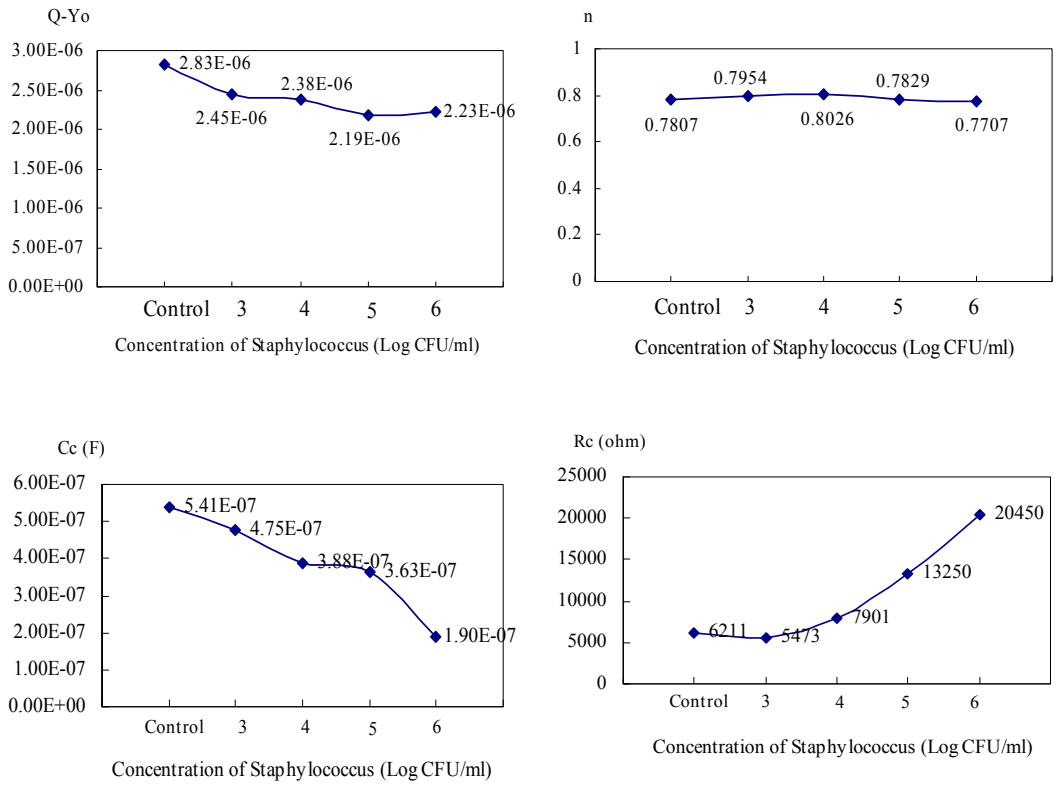

Fig 3.38 Circuit model parameters change with *Staphylococcus aureus* concentrations in bacteria mixture samples on anti-*Staphylococcus aureus* antibody modified membrane

Generally, the great changes of the components C_c and R_c for both *E. coli O157:H7* and *Staphylococcus aureus* detection indicated that the measured impedance amplitude changes were mainly due to the interface capacitance and resistance changes which were caused by the increasing blocked nanopores with more captured bacteria cells.

4 Discussions, Conclusion and Future studies

4.1 Discussions

4.1.1 Antibody Immobilization on Nanoporous Alumina Membranes

Antibody molecules can be immobilized onto nanoporous alumina membrane by physical adsorption and chemical bonding. To achieve the best antibody immobilization efficiency, different approaches were compared. In physical adsorption, antibody molecules were directly adsorbed onto the untreated surface of nanoporous membrane in previous studies (Toh, et al. 2009). But we found that the efficiency was very low. The hydrophilic surface of nanoporous alumina membrane might prevent the immobilization of antibody by physical adsorption. As discussed above, proteins such as antibody were difficult to be adsorbed onto a hydrophilic surface compared with hydrophobic one. In addition, the relatively rough surface of nanoporous membrane during fabrication process might not be appropriate for antibody immobilization.

In this project, both approaches were explored. We compared 3-(Trimethoxysilyl)propyl methacrylate (TPM) silane and GPMS silane modified nanoporous alumina membranes for antibody affinity study. The end group of TPM silane is vinyl group which will not react with antibody. However, the hydrophobic property of TPM silane monolayer can increase antibody physical adsorption.

Therefore, TPM silane modified membranes were used as physical adsorption group and GPMS silane modified membranes were treated as chemical grafting group. It was noticed that the grafting of silane of TPM could change the nanoporous alumina membrane surface from hydrophilic into hydrophobic due to the hydrophobic functional group of TPM. Fig 4.1 showed the scheme of antibody physical adsorption on TPM modified membrane. The antibody immobilization efficiency was increased by using TPM-modified membrane because antibody molecules were happy to adsorb onto the hydrophobic surface. Besides, the smooth, uniform and regular layer on membrane surface formed by of TPM may also be very suitable for antibody immobilization. The TPM-modified membrane was used to capture bacteria, we observed that the TPM-modified membrane could increase the antibody immobilization efficiency to some degree, however, this physical binding via van der walls force might not be firm enough during the flowing conditions such as injection of bacteria samples onto the membrane surface or washing the surface by PBS solution. The antibody molecules might easily detach from the alumina membrane by solution injection. And the efficiency to capture bacteria cells was still low. Moreover, we found that the antibody molecules could only randomly adsorb onto the alumina membrane surface physically without a uniform orientation. The bacteria binding sites of antibody were directionless and not exposed completely to bacteria samples, so some immobilized antibodies might lose the functionality for bacteria capturing.

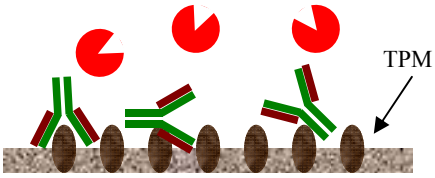

Fig 4.1 Antibody physical adsorption on TPM modified membrane

So, the silane of GPMS was chosen to modify the membrane surface because the GPMS molecule could not only provide a smooth layer but also create functional groups (epoxy group) on nanoporous membrane, which could react with amino groups of antibody and form a chemical bonding. Fig. 4.2 showed the scheme of antibody covalently binding on GPMS modified membrane. This firmly chemical bonding between silane and antibody was strong enough to resist detaching force such as washing and solution injection. In addition, we discovered the GPMS-modified membrane had high bacteria capturing efficiency. It is due to the uniform orientation of immobilized antibodies via chemical bonding. Since the epoxy-amino chemical bonding between silane and antibody is on opposite side of bacteria binding sites, when the chemical bonding is formed near the membrane surface, these bacteria binding sites on antibodies were subjected to samples uniformly and exposed completely. So the bacteria cells have more opportunities to be captured onto membrane surface.

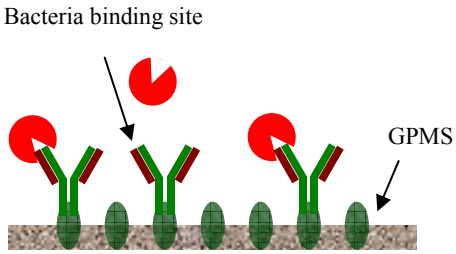

Fig 4.2 Antibody covalently binding on GPMS modified membrane

GPMS concentration is another factor which may affect the antibody immobilization efficiency. We have optimized the GPMS concentration by observing the fluorescence labeled antibodies immobilized on the membranes for various GPMS concentrations. It was found that, with the increasing of concentration of GPMS, fluorescence intensity increased which represented the increased antibody immobilization efficiency. Moreover, when the concentration was larger than the amount of 1%, the fluorescence intensity did not change much. It could be explained as following. Initially, with low GPMS concentration, the GPMS molecules were insufficient to cover the whole membrane surface if concentration was lower than 1%, so there was an increase of intensity with the increasing of GPMS concentration. When GPMS concentration became larger than 1%, the surface was saturated with GPMS molecules and no more GPMS molecules could be grafted on the membrane surface and the amount of fluorescence labeled antibody chemical bonded with GPMS was saturated.

We also found that room temperature was appropriate for GPMS silane modification. When the temperature was too high, the GPMS molecules were easy to volatize and the concentration of GPMS would decrease. On the other hand, when the temperature was too low, the rate of silanization would be influenced. A magnetic stirrer was utilized to make the GPMS solution homogeneous. Because we noticed the GPMS molecules were not uniformly distributed on nanoporous membrane without stirring. Some parts of surface formed a very thick GPMS layer while some

parts nearly had no GPMS molecules. This non-uniform formation would affect the following antibody binding.

There is another important factor that may cause the low antibody immobilization efficiency, which is due to the surplus anhydrous ethanol introduced in the washing step of silane modification. Since these molecules might cover the silane monolayer and prevent the functional silane groups reacting with antibody. Therefore, the silaned nanoporous alumina membranes need to be dried by nitrogen gas and hotplate for at least 8 hours to make the surplus ethanol molecules away from membrane surface completely.

4.1.2 Fabrication of PDMS based Chip

The PDMS chip in this project was fabricated using soft lithography technique. The mixing ratio between silicon elastomer and curing agent determined the mechanical property of PDMS. This influenced the spot punching process for Pt wire electrode localization. If PDMS was too soft, the holes punched by needles were irregular and not smooth, which made it difficult for the insertion of Pt wire electrode through the punched holes. If PDMS was too hard, PDMS elastomer surface was brittle and easy to be destroyed during the punching process with needles. Different ratios of silicon elastomer and curing agent were tried to achieve the optimal mechanical property for punching purpose. The best mixing ratio was 10:1 in this experiment, which could achieve the regular hole shape for best localization of pt wire electrodes.

Moreover, the property of the surface of PDMS device might also influence antibody immobilization. Without treatment, the PDMS device had a hydrophobic surface. When the antibody solution was injected, antibody molecules might be adsorbed onto the hydrophobic surface of PDMS by physical adsorption which would cause the loss of samples before the sensing experiments. So the amount of bacteria cells captured on membrane was reduced and the impedance change might be largely influenced. When PDMS surface was treated by air plasma, the surface of PDMS device had many hydroxyl groups (-OH) and the surface was changed into hydrophilic. This hydrophilic surface could largely avoid antibody adsorption.

4.1.3 Integration of Nanoporous Alumina Membrane into PDMS Device

Since the nanoporous alumina membrane was brittle, it was easy to break the membrane when embedding it into PDMS chamber using tweezers. We used a vacuum sucking pen to handle the membranes. The sealing between nanoporous alumina membrane and PDMS surface was challenging in this project. Since the surfaces of glass slides and PDMS were easy to be bond together after plasma treatment due to the covalent interaction of hydroxyl group between two surfaces. We first tried to covalently bond the membrane to PDMS by plasma. However, it might not help much for boding between nanoporous alumina membrane and PDMS after plasma treatment. There were two possible reasons for that. First of all, the nanopores reduced the contact area between membranes and PDMS surfaces and the

hydroxyl groups on nanoporous membrane were insufficient to make a firm bond. Secondly, the procedure of bonding needs a vacuum environment. Airs on the other side of membrane were easy to penetrate the interface of permeable PDMS and nanoporous membrane through nanopores and destroyed the bonding easily. Nail polish, for the advantage of quick solidification, was also tried to seal the nanoporous membranes and PDMS. It could be dried in 15 minutes and the adhesion between membrane and PDMS seemed good, but when we dropped water on the membrane surface, water would pass through the membrane quickly which meant the sealing was poor. The leakage of water may be caused by the nanopores or the adhesion gap between PDMS and membrane. Finally, we used AB glue for the sealing between nanoporous alumina membrane and PDMS. Although the AB glue was needed to be solidified for 1 hour, the sealing was very good. The water droplet could remain on the membrane surface without any leakage for a long time.

The amount of AB glue was another factor that might influence membrane integration. When the AB glue was too much, the solidification time was too long. When the AB glue was too little, the adhesion between membrane and PDMS was not firm enough and the water droplet could leak easily. Many experiments were tried and finally the membrane could be firmly adhered to PDMS with appropriate amount of AB glue.

4.1.4 Impedance Analysis for Bacteria Detection

Conventional electrochemical methods based on impedance measurement for bacteria detection always involve metal electrodes. The bacteria cells are directly immobilized on the antibody modified electrode surface. However, these methods have some limitations. The metal electrode has the problem of surface polarization during impedance measurement. Especially, when the impedance change related with bacteria is much smaller than the electrode polarization impedance in the low bacteria concentrations, it is difficult to extract the impedance information related with bacteria from total measured impedance. With the electrode based biosensor for bacteria detection, the impedance magnitude increased largely at the frequency of 1000Hz-10000Hz which is high frequency region, showing the effect of electrode polarization, however, for this membrane based biosensor, the impedance stayed relatively stable at 1000Hz, and increase slowly even at the frequency of 100Hz showing its non-conductive property, which can avoid the electrode polarization effectively during impedance measurement. In addition, the nanopores can be covered by the micro-sized bacteria cells, the electrical current will be blocked and the impedance amplitude will be changed. Therefore, we chose this nanopore-blocking impedance sensing system for bacteria detection.

In the impedance measurement, the maximum normalized impedance change (NIC) caused by bacteria was found to be around the frequency of 100 Hz. The possible reason was that, when frequency was in the high frequency range from 1 kHz to 10

kHz, the whole impedance spectrum was dominated by the resistance of bulk solution R_s. However, when frequency range was from 1-10 Hz, the whole impedance was largely determined by the constant phase element (CPE) of interfacial double layer effect on the membrane surface. In the frequency range between 10 Hz -1 kHz, the impedance spectrum was controlled by the components of C_c and R_c which were related to bacteria cell capturing on the membrane surface in parallel within the circuit model. So, when impedance of C_c and R_c equaled to each other, the impedance amplitude change reached the maximum which was around 100 Hz.

In single type specific bacteria detection experiment, the impedance amplitude change for *E. coli O157:H7* with concentration of 10^2 CFU/ml was difficult to be differentiated from that produced in cross bacteria experiment using anti-*Staphylococcus aureus* modified membranes. The possible reason for the small impedance change at this concentration might be due to the insufficient *E. coli O157:H7* cells captured on nanoporous membrane, which could not be distinguished from the nonspecific physical adsorption as a noise background. It was noticed that when concentration of *E. coli O157:H7* increased to 10^3 CFU/ml, the impedance amplitude change was easily distinguished from cross bacteria detection experiment. Thus, it could be concluded that, the sensitivity of single type bacteria detection biosensor for *E. coli O157:H7* was 10^3 CFU/ml. On the other hand, we found that the impedance amplitude change for *Staphylococcus aureus* at 10^2 CFU/ml was large enough to be distinguished from that in cross bacteria detection using anti- *E. coli*

O157:H7 antibody modified membrane. So the sensitivity for *Staphylococcus aureus* in single type bacteria detection system was 10^2 CFU/ml. Although the experiment conditions were tried to keep the same, there were still many factors which might cause the difference for different kinds of bacteria in the same detection system. First of all, the antibody-antigen binding efficiency could not be the same for different kinds of bacteria. In this experiment, *Staphylococcus aureus* might have a higher binding efficiency with anti- *Staphylococcus aureus* antibody. Secondly, even though nanoporous alumina membranes were modified together, the antibody immobilization efficiency might also be different, which was discussed above. Thirdly, the experimental conditions such as the location of electrodes, the injection volume of bacteria samples might also be an important factor to influence the sensitivity. Finally, the number of non-target bacteria cells which were remained on membrane surface after washing could not be controlled exactly for different experiments.

In the single bacteria detection impedance measurement, the sensitivity with concentration of 10^4 CFU/ml seems to be not as good as promised, this is because it's necessary to compare the impedance change between specific bonding and non-specific bonding, Actually, in the single bacteria specific bonding (specific antibody with the target bacteria) the normalized impedance change (NIC) at the concentration of 10^4 CFU/ml are 45% and 60% for *E.coli O157:H7* and *staphylococcus aureus* respectively, even with concentration of 10^3 CFU/ml, the NIC are 20% and 50%. However, the NIC in the non-specific bonding at concentration of

10^4 CFU/ml (antibody with the non-target bacteria) are only 5.54% and 5.30% for *E.coli O157:H7* and *staphylococcus aureus* respectively, this means the two kinds of bacteria with concentration of 10^4 CFU/ml can be easily detected with impedance spectrum, and the sensitivity of this nanoporous membrane based biosensor for *E.coli O157:H7* and *staphylococcus aureus* are 10^3 CFU/ml, which are relatively high.

The cross bacteria detection experiment was performed to test the specificity of the biosensor. When non-target bacteria sample was injected to PDMS chamber, the most possible reason for the small impedance increase is the physical adsorption caused by the non-target bacteria and unexpected particles in sample that were remained on the surface after washing. Few green dots caused by non-specific binding with technique of fluorescence assay could also been observed, which were caused by bacteria physical adsorption. In addition, the injected solution volume, environment temperature and intrinsic limits of impedance might also contribute to the small impedance change. In the experiments, we kept the volume and temperature to be the same for each experiment.

In the simultaneous detection experiment for multiple type bacteria, there were two membranes modified by anti- *E. coli O157:H7* antibody and anti-*Staphylococcus aureus* antibody respectively. Various samples including mixed bacteria sample and single type bacteria samples. The sensitivity for mixed bacteria sample and single type bacteria sample at the same concentration was a little different for both membranes. The possible reason for this phenomenon was that, when bacteria

samples mixed together, there might be assembly and conjugation between two kinds of bacteria cells and the assembled bacteria cells were located onto one kind of membrane which might have higher binding chances, while there were fewer bacteria cells captured on the other membrane. But for single bacteria sample, this phenomenon would not happen. Therefore, the sensitivity could be different for mixed bacteria and single bacteria in the simultaneous detection system.

4.1.5 Limitations of Sensitivity

The sensitivity for *E.coli O157:H7* in the proposed biosensor was10^4 CFU/ml and the sensitivity for *Staphylococcus. aureus* in the proposed biosensor was 10^3 CFU/ml; Meanwhile, the sensitivity for both bacteria in simultaneous detection biosensor were 10^3 CFU/ml for *E.coli O157:H7* and 10^4 CFU/ml for *Staphylococcus. aureus*, and the response time of this nanoporous alumina membrane based biosensor was about 2-3 hours. On the other hand, from result of the non-specific bacteria bonding experiment, the specificity of this proposed biosensor was very good. Compared with the SPR-based biosensor with sensitivity of $10^2 - 10^3$ CFU/mL and response time of 3 hours for *E.coli O157:H7* which was demonstrated by Waswa et al. (2007) and with interdigitated array microelectrode-based impedance biosensor with sensitivity of 8.4×10^4 CFU/mL which was reported by Varshney et al. (2007), the nanoporous alumina membrane has a relatively high sensitivity, good specificity and short response time.

In the experiment, the sensitivity for both *E. coli O157:H7* and *Staphylococcus aureus* was around 10^3-10^4 CFU/ml. This nanoporous alumina membrane based biosensor has some limitations. First of all, the sensitivity is limited by the non-specific binding which may be caused by non-target bacteria or unexpected particle adsorption. These non-specific binding may also introduce impedance change which is comparable to the impedance change induced by the low concentration of target bacteria. Therefore, to confirm the existence of target bacteria, the concentration needs to be increased to lead larger impedance change. Secondly, the sensitivity is limited by the design of PDMS chamber. If the height of PDMS top chamber is smaller, i.e. the nanoporous membrane is closer to the top PDMS device, the bacteria cells on the top of solution are closer to the antibody-modified membrane surface and may have more opportunity to be captured. Furthermore, the distance between the Pt wire electrode and membrane may also influence the sensitivity. According to our experience, if the distance is smaller, the device may be more sensitive to the impedance change on the surface. Finally, the limited binding efficiency of antibody-antigen is also an important factor that influences the sensitivity of this biosensor. This binding efficiency is decided by the natural factors such as the activity of antibody and bacteria. In addition, since the nanoporous alumina membrane has a very high pore density, it is difficult to cover most of the nanopores by bacteria cells even with large bacteria concentration. Part of electrical current can flow through the membrane. So the impedance change is also limited by the high pore density.

4.1.6 Limitation of Response Time

The response time of the proposed biosensor is mainly limited by the activity of bacteria cells and distance between bacteria and antibody and the size of proposed sensor, and the exact reaction rate constant is about 15 minutes for the antibody-antigen reaction. The antibody antigen reaction rate is influenced by many factors such as temperature, PH value and the activity of bacteria.

The response time of the biosensor for bacteria detection is about 2-3 hours and it still can be improved for the purpose of in field detection which needs rapid and real-time detection. The response time is largely limited by the antibody-antigen reaction and the distance from antibody on the membrane to bacteria cells in the solution. For the antibody-antigen reaction, it is decided by the activity of antibody and bacteria which are natural factors. To accelerate the process of bacteria reaching antibodies on the membrane, magnetic nanoparticle driving method can be a good choice. Magnetic nanoparticle has magnetic property and can be functionalized easily. With the help of appropriate silane, the nanoparticle can be conjugated to the bacteria. By applying a magnetic field, not only these nanoparticle conjugated bacteria can be driven to the antibody in a short time and react with it, but also the collision frequency between antibodies and bacteria can be enhanced to increase binding efficiency. The combination of the two mechanisms significantly decreases the response time and improves the bacteria-antibody binding efficiency. Another method to shorten the response time is to decrease the height of PDMS chamber to

make the nanoporous membrane surface and the antibody in the solution much closer to all bacteria cells. With shorter distance between bacteria and antibody, the bacteria cells can be captured by antibody on the membrane more easily and quickly, which will decrease the response time.

4.1.7 Equivalent Circuit Analysis

The equivalent circuit model was chosen based on the electrochemical theory, each component added into the circuit need to make the chi-square lower than before. And after many times modeling, these equivalent circuits could make the chi-square smallest. Therefore, we choose this model as the equivalent circuit for this nanoporous alumina membrane based biosensor. The R & C for *E.coli O157:H7* with highest concentration of 106 CFU/ml are 5038 (Ω) and 7.72E-07 (F), because the Z=R-j*1/wC, and the absolute value of impedance is 5.43*104 Ω, the total impedance of *E.coli O157:H7* at concentration of 106 CFU/ml is 9.0*104 Ω, therefore, the contribution of R & C in parallel is 5.43*104/9.0*104=60.3%, which means the major contribution of total impedance is induced by R & C, which was caused by the bacteria captured on the nanoporous alumina membrane. The other concentrations of bacteria could be calculated in the same way.

4.2 Conclusion

In this project, a PDMS based impedance biosensor integrated with nanoporous alumina membrane was developed for detection pathogenic bacteria of *E. coli O157:H7* and *Staphylococcus aureus* respectively and simultaneously. Surface modification was conducted by the silane monolayer of GPMS with a concentration of 1%, which was applied as a novel linker to connect antibody molecules to nanoporous alumina membrane. Antibodies specific to *E. coli O157:H7* and *Staphylococcus aureus* were used to capture target bacteria cells and give specificity of the bacteria detection system. The effective immobilization of antibody molecules on silane of GPMS modified nanoporous alumina membrane was investigated by approaches of XPS and AFM. In the experiment of impedance spectrum measurement for bacteria detection, the normalized impedance change caused by bacteria showed a maximum value at frequency of 100 Hz. In the single specific bacteria detection experiment, the change of impedance magnitude increased gradually with the bacteria concentrations. Moreover, in the cross bacteria detection experiment, the normalized impedance change remained under 5% for various bacteria concentrations, which demonstrated the specificity of this biosensor. In the simultaneous bacteria detection experiment for multiple type bacteria detection, the impedance changes on *E. coli O157:H7* side and *Staphylococcus aureus* side showed the increase with bacteria concentrations respectively in the mixed bacteria samples. However, when only one kind of bacteria such as *E. coli O157:H7* or *Staphylococcus aureus* added into the system, only the specific antibody side showed an increase of

impedance change. For response time detection experiment, the detection assay for both *E .coli O157:H7* and *Staphylococcus aureus* could be completed in around 3 hours.

4.3 Future studies

Since the sensitivity of the nanoporous alumina membrane based biosensor is not as high as the infectious dosage both for *E .coli O157:H7* and *Staphylococcus aureus*, the improvement of sensitivity is still the key concern in future research. There are two suggested solutions. First of all, since the nanoporous alumina membrane has the property of porosity, bacteria cells with low concentrations can not cover sufficient nanoporous membrane area. Thus, it is necessary to decrease the nanoporous membrane sensing area to increase the sensitivity. With this point of view, it is helpful if the nanoporous membrane is micropatterned by one kind of material which can prevent non-specific adsorption in advance. As is well-known, polyethylene glycol (PEG) is a kind of biomaterial which could easily resist proteins such as antibody. Therefore, it is of great interest to pattern PEG hydrogel on nanoporous membrane in order to prevent non-specific protein binding to insure specificity. At the same time, the patterned PEG layer can define the small sensing area of nanoporous to increase sensitivity for low bacteria concentration detection. Another approach to increase sensitivity is to conjugate microbeads on captured bacteria cells. Since these beads are in micro-scale which is comparable to bacteria cells, they could enlarge the covering area of bacteria cells on the membrane surface and then the

electrical signal change can be enlarged too. Since the specific antibodies can easily be grafted on the surface of microbeads through proper silane modification, the antibody modified microbeads can conjugate onto the bacteria cells which have been captured on the nanoporous alumina membrane and covered more nanopores.

References

[Anon], 1996. Outbreak of Escherichia coli O157:H7 infections associated with drinking unpasteurized commercial apple juice - British Columbia, California, Colorado, and Washington, October 1996 (Reprinted from MMWR, vol 45, pg 975, 1996). Jama-J Am Med Assoc 276(23), 1865-1865.

Ahmed, A.M., Kawamoto, H., Inouye, K., Hashiwata, Y., Sakaki, M., Seno, M., Shimamoto, T., 2005. Genomic analysis of a multidrug-resistant strain of enterohaemorrhagic Escherichia coli O157 : H7 causing a family outbreak in Japan. J Med Microbiol 54(9), 867-872.

Akeson, M., Branton, D. Kasianowicz, J. J., Brandin, E., Deamer, D.W., 1999, Microsecond Time-Scale Discrimination Among Polycytidylic Acid, Polyadenylic Acid, and Polyuridylic Acid as Homopolymers or as Segments Within Single RNA Molecules. Biophys J, 77(6), 3227-3233.

Ali, S.H., 2004. A socio-ecological autopsy of the E-coli O157 : H7 outbreak in Walkerton, Ontario, Canada. Soc Sci Med 58(12), 2601-2612.

Baggett, H.C., Hennessy, T.W., Leman, R.F., Hamlin, C.E., Bruden, D.A., Reasonover, A.L., Sparks, R.D., Donlan, R.M., McAllister, S.K., Martinez, P., Butler, J.C., 2001. Outbreak of community-acquired methicillin-resistant Staphylococcus aureus (MRSA) skin infections among Alaska Natives, 2000. Clin Infect Dis 33(7), 1091-1091.

Bayley, H.. Cremer, P.S., 2001, Stochastic Sensing Based on Nature. Nature, 413, 226-230.

Bell, J.M., Turnidge, J.D., Participants, S.A., 2002. High prevalence of oxacillin-resistant Staphylococcus aureus isolates from hospitalized patients in Asia-Pacific and South Africa: Results from SENTRY antimicrobial surveillance program, 1998-1999. Antimicrob Agents Ch 46(3), 879-881.

Bopp, D.J., Sauders, B.D., Waring, A.L., Ackelsberg, J., Dumas, N., Braun-Howland, E., Dziewulski, D., Wallace, B.J., Kelly, M., Halse, T., Musser, K.A., Smith, P.F., Morse, D.L., Limberger, R.J., 2003. Detection, isolation, and molecular subtyping of Escherichia coli O157 : H7 and Campylobacter jejuni associated with a large waterborne outbreak. J Clin Microbiol 41(1), 174-180.

Borsheim, K.Y., Bratbak, G., Heldal, M., 1990. Enumeration and Biomass Estimation of Planktonic Bacteria and Viruses by Transmission Electron-Microscopy. Appl Environ Microb 56(2), 352-356.

Bruce, M.G., Curtis, M.B., Payne, M.M., Gautom, R.K., Thompson, E.C., Bennett, A.L., Kobayashi, J.I., 2003. Lake-associated outbreak of Escherichia coli O157 : H7 in Clark County, Washington, August 1999. Arch Pediat Adol Med 157(10), 1016-1021.

Campbell, K.M., Vaughn, A.F., Russell, K.L., Smith, B., Jimenez, D.L., Barrozo, C.P., Minarcik, J.R., Crum, N.F., Ryan, M.A.K., 2004. Risk factors for community-associated methicillin-resistant Staphylococcus aureus infections in an outbreak of disease among military trainees in San Diego, California, in 2002. J Clin Microbiol 42(9), 4050-4053.

Caruso, F., Rodda, E., Furlong, D.F., Niikura, K., Okahata, Y., 1997. Quartz crystal microbalance study of DNA immobilization and hybridization for nucleic acid sensor development. Analytical Chemistry 69(11), 2043-2049.

Chan, K.S., Ling, M.L., Hsu, L.Y., Tan, A.L., 2009. Methicillin-Resistant Staphylococcus aureus Throat Colonization Among Healthcare Workers During an Outbreak in Singapore General Hospital. Infect Cont Hosp Ep 30(1), 95-97.

Chan, S.F., Chan, Z.C.Y., 2008. A review of foodborne disease outbreaks from 1996 to 2005 in Hong Kong and its implications on food safety promotion. J Food Safety 28(2), 276-299.

Chemburu, S., Wilkins, E., Abdel-Hamid, I., 2005. Detection of pathogenic bacteria in food samples using highly-dispersed carbon particles. Biosensors & Bioelectronics 21(3), 491-499.

Chen, C.S., Durst, R.A., 2006. Simultaneous detection of Escherichia coli O157 : H7, Salmonella spp. and Listeria monocytogenes with an array-based immunosorbent assay using universal protein G-liposomal nanovesicles. Talanta 69(1), 232-238.

Cui, X.Y., Martin, D.C., 2003. Electrochemical deposition and characterization of poly(3,4-ethylenedioxythiophene) on neural microelectrode arrays. Sensor Actuat B-Chem 89(1-2), 92-102.

d'Azevedo, P.A., Trancesi, R., Sales, T., Monteiro, J., Gales, A.C., Pignatari, A.C., 2008. Outbreak of Staphylococcus hominis subsp novobiosepticus

bloodstream infections in Sao Paulo city, Brazil. J Med Microbiol 57(2), 256-257.

de Boer, E., Beumer, R.R., 1999. Methodology for detection and typing of foodborne microorganisms. International Journal of Food Microbiology 50(1-2), 119-130.

Dundas, S., Todd, W.T.A., Stewart, A.I., Murdoch, P.S., Chaudhuri, A.K.R., Hutchinson, S.J., 2001. The central Scotland Escherichia coli O157 : H7 outbreak: Risk factors for the hemolytic uremic syndrome and death among hospitalized patients. Clin Infect Dis 33(7), 923-931.

Ercole, C., Del Gallo, M., Mosiello, L., Baccella, S., Lepidi, A., 2003. Escherichia coli detection in vegetable food by a potentiometric biosensor. Sensor Actuat B-Chem 91(1-3), 163-168.

Sackmann, E., 1996. Supported Membranes: Scientific and Practical Applications. Science 271(5245), 43-48.

Gau, J.J., Lan, E.H., Dunn, B., Ho, C.M., Woo, J.C.S., 2001. A MEMS based amperometric detector for E-Coli bacteria using self-assembled monolayers. Biosensors & Bioelectronics 16(9-12), 745-755.

Gehring, A.G., Irwin, P.L., Reed, S.A., Tu, S.I., Andreotti, P.E., Akhavan-Tafti, H., Handley, R.S., 2004. Enzyme-linked immunomagnetic chemiluminescent detection of Escherichia coli O157 : H7. J Immunol Methods 293(1-2), 97-106.

Gehring, A.G., Patterson, D.L., Tu, S.I., 1998. Use of a light-addressable potentiometric sensor for the detection of Escherichia coli O157 : H7. Analytical Biochemistry 258(2), 293-298.

Goode, B., O'Reilly, C., Dunn, J., Fullerton, K., Smith, S., Ghneim, G., Keen, J., Durso, L., Davies, M., Montgomery, S., 2009. Outbreak of Escherichia coli O157 H7 Infections After Petting Zoo Visits, North Carolina State Fair, October-November 2004. Arch Pediat Adol Med 163(1), 42-48.

Guerin, F., Buu-Hoi, A., Mainardi, J.L., Kac, G., Colardelle, N., Vaupre, S., Gutmann, L., Podglajen, I., 2000. Outbreak of methicillin-resistant Staphylococcus aureus with reduced susceptibility to glycopeptides in a Parisian hospital. J Clin Microbiol 38(8), 2985-2988.

Gultepe, E., Nagesha, D., Menon, L., 2007. High-throughput assembly of nanoelements in nanoporous alumina templates. Applied Physics Letters 90(16), 163119-163123.

Hilborn, E.D., Mermin, J.H., Mshar, P.A., Hadler, J.L., Voetsch, A., Wojtkunski, C., Swartz, M., Mshar, R., Lambert-Fair, M.A., Farrar, J.A., Glynn, M.K., Slutsker, L., 1999. A multistate outbreak of Escherichia coli O157 : H7 infections associated with consumption of mesclun lettuce. Arch Intern Med 159(15), 1758-1764.

Hilborn, E.D., Mshar, P.A., Fiorentino, T.R., Dembek, Z.F., Barrett, T.J., Howard, R.T., Cartter, M.L., 2000. An outbreak of Escherichia coli O157 : H7 infections and haemolytic uraemic syndrome associated with consumption of unpasteurized apple cider. Epidemiology and Infection 124(1), 31-36.

Ho, P.L., Cheung, C., Mak, G.C., Tse, C.W., Ng, T.K., Cheung, C.H.Y., Que, T.L., Lam, R., Lai, R.W.M., Yung, R.W.H., Yuen, K.Y., 2007. Molecular epidemiology and household transmission of community-associated methicillin-resistant Staphylococcus aureus in Hong Kong. Diagn Micr Infec Dis 57(2), 145-151.

Ho, P.L., Tse, C.W.S., Mak, G.C., Chow, K.H., Ng, T.K., 2004. Community-acquired methicillin-resistant Staphylococcus aureus arrives in Hong Kong. J Antimicrob Chemoth 54(4), 845-846.

Hobson, N.S., Tothill, I., Turner, A.P.F., 1996. Microbial detection. Biosensors & Bioelectronics 11(5), 455-477.

Howell, S.W., Inerowicz, H.D., Regnier, F.E., Reifenberger, R., 2003. Patterned protein microarrays for bacterial detection. Langmuir 19(2), 436-439.

Hu, Y., Zhang, Q., Meitzler, J.C., 1999. Rapid and sensitive detection of Escherichia coli O157 : H7 in bovine faeces by a multiplex PCR. J Appl Microbiol 87(6), 867-876.

Huff, J.L., Lynch, M.P., Nettikadan, S., Johnson, J.C., Vengasandra, S., Henderson, E., 2004. Label-free protein and pathogen detection using the atomic force microscope. J Biomol Screen 9(6), 491-497.

Ip, M., Lyon, D.J., Chio, F., Cheng, A.E., 2004. A longitudinal analysis of methicillin-resistant Staphylococcus aureus in a Hong Kong teaching hospital. Infect Cont Hosp Ep 25(2), 126-129.

Jofre, A., Martin, B., Garriga, M., Hugas, M., Pla, M., Rodriguez-Lazaro, D., Aymerich, T., 2005. Simultaneous detection of Listeria monocytogenes and

Salmonella by multiplex PCR in cooked ham. Food Microbiol 22(1), 109-115.

Johnson, R.P., Durham, R.J., Johnson, S.T., Macdonald, L.A., Jeffrey, S.R., Butman, B.T., 1995. Detection of Escherichia-Coli O157-H7 in Meat by an Enzyme-Linked-Immunosorbent-Assay, Ehec-Tek. Appl Environ Microb 61(1), 386-388.

Jones, T.F., Kellum, M.E., Porter, S.S., Bell, M., Schaffner, W., 2001. An outbreak of community-acquired foodborne illness due to methicillin-resistant Staphylococcus aureus. Clin Infect Dis 33(7), 1106-1106.

Kang, B., Yeo, U., Yoo, K.H., 2010. Anodized aluminum oxide-based capacitance sensors for the direct detection of DNA hybridization. Biosens Bioelectron 25(7), 1592-1596.

Karch, H., Tarr, P.I., Blelaszewska, M., 2005. Enterohaemorrhagic Escherichia coli in human medicine. Int J Med Microbiol 295(6-7), 405-418.

Ke, D.B., Menard, C., Picard, F.J., Boissinot, M., Ouellette, M., Roy, P.H., Bergeron, M.G., 2000. Development of conventional and real-time PCR assays for the rapid detection of group B streptococci. Clin Chem 46(3), 324-331.

Keene, W.E., Sazie, E., Kok, J., Rice, D.H., Hancock, D.D., Balan, V.K., Zhao, T., Doyle, M.P., 1997. An outbreak of Escherichia coli O157:H7 infections traced to jerky made from deer meat. Jama-J Am Med Assoc 277(15), 1229-1231.

Kim, J., Gale, B.K., 2008. Quantitative and qualitative analysis of a microfluidic DNA extraction system using a nanoporous AlOx membrane. Lab Chip 8(9), 1516-1523.

Kim, J., Voelkerding, K.V., Gale, B.K., 2006. Patterning of a nanoporous membrane for multi-sample DNA extraction. J Micromech Microeng 16(1), 33-39.

Kotewicz, M.L., Mammel, M.K., LeClerc, J.E., Cebula, T.A., 2008. Optical mapping and 454 sequencing of Escherichia coli O157:H7 isolates linked to the US 2006 spinach-associated outbreak. Microbiol-Sgm 154, 3518-3528.

Krambeck, C., Krambeck, H.J., Overbeck, J., 1981. Microcomputer-Assisted Biomass Determination of Plankton Bacteria on Scanning Electron-Micrographs. Appl Environ Microb 42(1), 142-149.

Larssen, K.W., Jacobsen, T., Bergh, K., Tvete, P., Kvello, E., Scheel, O., 2005. Outbreak of methicillin-resistant Staphylococcus aureus in two nursing homes in Central Norway. J Hosp Infect 60(4), 312-316.

Lazcka, O., Del Campo, F.J., Munoz, F.X., 2007. Pathogen detection: A perspective of traditional methods and biosensors. Biosensors & Bioelectronics 22(7), 1205-1217.

Leonard, P., Hearty, S., Brennan, J., Dunne, L., Quinn, J., Chakraborty, T., O'Kennedy, R., 2003. Advances in biosensors for detection of pathogens in food and water. Enzyme Microb Tech 32(1), 3-13.

Leung, P.H.M., Yam, W.C., Ng, W.W.S., Peiris, J.S.M., 2001. The prevalence and characterization of verotoxin-producing Escherichia coli isolated from cattle

and pigs in an abattoir in Hong Kong. Epidemiology and Infection 126(2), 173-179.

Levine, M.M., Xu, J., Kaper, J.B., Lior, H., Prado, V., Tall, B., Nataro, J., Karch, H., Wachsmuth, K., 1987. A DNA Probe to Identify Enterohemorrhagic Escherichia-Coli of O157-H7 and Other Serotypes That Cause Hemorrhagic Colitis and Hemolytic Uremic Syndrome. Journal of Infectious Diseases 156(1), 175-182.

Liechti, K.M., Schnapp, S.T., Swadener, J.G., 1997. Contact angle and contact mechanics of a glass/epoxy interface. Int J Fracture 86(4), 361-374.

Loferer-Krossbacher, M., Klima, J., Psenner, R., 1998. Determination of bacterial cell dry mass by transmission electron microscopy and densitometric image analysis. Appl Environ Microb 64(2), 688-694.

MacDonald, D.M., Fyfe, M., Paccagnella, A., Trinidad, A., Louie, K., Patrick, D., 2004. Escherichia coli O157 : H7 outbreak linked to salami, British Columbia, Canada, 1999. Epidemiology and Infection 132(2), 283-289.

Magliulo, M., Simoni, P., Guardigli, M., Michelini, E., Luciani, M., Lelli, R., Roda, A., 2007. A rapid multiplexed chemiluminescent immunoassay for the detection of Escherichia coli O157 : H7, Yersinia enterocolitica, salmonella typhimurium, and Listeria monocytogenes pathogen bacteria. J Agr Food Chem 55(13), 4933-4939.

Mao, X.L., Yang, L.J., Su, X.L., Li, Y.B., 2006. A nanoparticle amplification based quartz crystal microbalance DNA sensor for detection of Escherichia coli O157 : H7. Biosensors & Bioelectronics 21(7), 1178-1185.

Mead, P.S., Slutsker, L., Dietz, V., McCaig, L.F., Bresee, J.S., Shapiro, C., Griffin, P.M., Tauxe, R.V., 2000. Food-related illness and death in the United States (Reprinted from Emerging Infectious Diseases). J Environ Health 62(7), 9-18.

Michino, H., Araki, K., Minami, S., Takaya, S., Sakai, N., Miyazaki, M., Ono, A., Yanagawa, H., 1999. Massive outbreak of Escherichia coli O157 : H7 infection in schoolchildren in Sakai City, Japan, associated with consumption of white radish sprouts. Am J Epidemiol 150(8), 787-796.

Miwa, N., Kawamura, A., Masuda, T., Akiyama, M., 2001. An outbreak of food poisoning due to egg yolk reaction-negative Staphylococcus aureus. International Journal of Food Microbiology 64(3), 361-366.

Mo, X.T., Zhou, Y.P., Lei, H., Deng, L., 2002. Microbalance-DNA probe method for the detection of specific bacteria in water. Enzyme Microb Tech 30(5), 583-589.

Mouallem, R.M., Fukuda, J.M., Levy, J.M., Mangat, R.K., Gastanaduy, A.S., 2003. Staphylococcus Aureus food poisoning outbreak associated with spaghetti and meat sauce. Pediatric Research 53(4), 126a-126a.

Nema, V., Agrawal, R., Kamboj, D.V., Goel, A.K., Singh, L., 2007. Isolation and characterization of heat resistant enterotoxigenic Staphylococcus aureus from a food poisoning outbreak in Indian subcontinent. International Journal of Food Microbiology 117(1), 29-35.

O'Brien, F.G., Lim, T.T., Chong, F.N., Coombs, G.W., Enright, M.C., Robinson, D.A., Monk, A., Said-Salim, B., Kreiswirth, B.N., Grubb, W.B., 2004.

Diversity among community isolates of methicillin-resistant Staphylococcus aureus in Australia. J Clin Microbiol 42(7), 3185-3190.

Obrien, A.D., Melton, A.R., Schmitt, C.K., Mckee, M.L., Batts, M.L., Griffin, D.E., 1993. Profile of Escherichia-Coli O157-H7 Pathogen Responsible for Hamburger-Borne Outbreak of Hemorrhagic Colitis and Hemolytic-Uremic Syndrome in Washington. J Clin Microbiol 31(10), 2799-2801.

POPSIC,http://www.popsci.com/science/article/2010-04/using-super-small-sensor-measure-rate-cell-growth-first-time.

Pyle, B.H., Broadaway, S.C., McFeters, G.A., 1999. Sensitive detection of Escherichia coli O157 : H7 in food and water by immunomagnetic separation and solid-phase laser cytometry. Appl Environ Microb 65(5), 1966-1972.

Radke, S.A., Alocilja, E.C., 2005. A high density microelectrode array biosensor for detection of E-coli O157 : H7. Biosens Bioelectron 20(8), 1662-1667.

Riley, L.W., Remis, R.S., Helgerson, S.D., Mcgee, H.B., Wells, J.G., Davis, B.R., Hebert, R.J., Olcott, E.S., Johnson, L.M., Hargrett, N.T., Blake, P.A., Cohen, M.L., 1983. Hemorrhagic Colitis Associated with a Rare Escherichia-Coli Serotype. New Engl J Med 308(12), 681-685.

Rodrigue, D.C., Mast, E.E., Greene, K.D., Davis, J.P., Hutchinson, M.A., Wells, J.G., Barrett, T.J., Griffin, P.M., 1995. A University Outbreak of Escherichia-Coli O157/H7 Infections Associated with Roast Beef and an Unusually Benign Clinical Course. Journal of Infectious Diseases 172(4), 1122-1125.

Romer, W., Steinem, C., 2004, Impedance analysis and single-channel recordings on nano-black lipid membranes based on porous alumina. Biophys J 86(2), 955-965

Ronkainen, N.J., Halsall, H.B., Heineman, W.R., 2010. Electrochemical biosensors. Chem Soc Rev 39(5), 1747-1763.

Sartz, L., De Jong, B., Hjertqvist, M., Plym-Forshell, L., Asterlund, R., Loefdahl, S., Osterman, B., Stahl, A., Eriksson, E., Hansson, H.B., Karpman, D., 2008. An outbreak of Escherichia coli O157 : H7 infection in southern Sweden associated with consumption of fermented sausage; aspects of sausage production that increase the risk of contamination. Epidemiology and Infection 136(3), 370-380.

Schlosser, G., Kacer, P., Kuzma, M., Szilagyi, Z., Sorrentino, A., Manzo, C., Pizzano, R., Malorni, L., Pocsfalvi, G., 2007. Coupling immunomagnetic separation on magnetic beads with matrix-assisted laser desorption ionization-time of flight mass spectrometry for detection of staphylococcal enterotoxin B. Appl Environ Microb 73(21), 6945-6952.

Schmitt, M., Schulerschmid, U., Schmidtlorenz, W., 1990. Temperature Limits of Growth, Tnase and Enterotoxin Production of Staphylococcus-Aureus Strains Isolated from Foods. International Journal of Food Microbiology 11(1), 1-20.

Su, X.L., Li, Y.B., 2004. A self-assembled monolayer-based piezoelectric immunosensor for rapid detection of Escherichia coli O157 : H7. Biosensors & Bioelectronics 19(6), 563-574.

Subramanian, A., Irudayaraj, J., Ryan, T., 2006. A mixed self-assembled monolayer-based surface plasmon immunosensor for detection of E-coli O157 : H7. Biosensors & Bioelectronics 21(7), 998-1006.

Suehiro, J., Hatano, T., Shutou, M., Hara, M., 2005. Improvement of electric pulse shape for electropermeabilization-assisted dielectrophoretic impedance measurement for high sensitive bacteria detection. Sensor Actuat B-Chem 109(2), 209-215.

Swaminathan, B., Feng, P., 1994. Rapid Detection of Food-Borne Pathogenic Bacteria. Annu Rev Microbiol 48, 401-426.

Swan, E.E.L., Popat, K.C., Grimes, C.A., Desai, T.A., 2005. Fabrication and evaluation of nanoporous alumina membranes for osteoblast culture. J Biomed Mater Res A 72A(3), 288-295.

Tsang, H.F., Tsui, L.K., 2007. Epidemiology of CA-MRSA and the HKSAR's Public Health Response. Medical Bulletin 12(12).

Velusamy, V., Arshak, K., Korostynska, O., Oliwa, K., Adley, C., 2010. An overview of foodborne pathogen detection: In the perspective of biosensors. Biotechnol Adv 28(2), 232-254.

Vlassiouk, I., Krasnoslobodtsev, A., Smirnov, S., Germann, M., 2004. "Direct" detection and separation of DNA using nanoporous alumina filters. Langmuir 20(23), 9913-9915.

Vlassiouk, I., Takmakov, P., Smirnov, S., 2005. Sensing DNA hybridization via ionic conductance through a nanoporous electrode. Langmuir 21(11), 4776-4778.

Wagenvoort, J.H.T., Toenbreker, H.M.J., Heck, M.E.O.C., van Leeuwen, W.J., Wannet, W.J.B., 2000. Hospital outbreak of methicillin-resistant Staphylococcus aureus followed by an in vivo change to a mecA-negative mutant with loss of epidemicity. Eur J Clin Microbiol 19(12), 976-977.

Wang, X., Smirnov, S., 2009. Label-Free DNA Sensor Based on Surface Charge Modulated Ionic Conductance. Acs Nano 3(4), 1004-1010.

Waswa, J., Irudayaraj, J., DebRoy, C., 2007. Direct detection of E-Coli O157 : H7 in selected food systems by a surface plasmon resonance biosensor. Lwt-Food Sci Technol 40(2), 187-192.

Wells, J.G., Davis, B.R., Wachsmuth, I.K., Riley, L.W., Remis, R.S., Sokolow, R., Morris, G.K., 1983. Laboratory Investigation of Hemorrhagic Colitis Outbreaks Associated with a Rare Escherichia-Coli Serotype. J Clin Microbiol 18(3), 512-520.

Williams, R.C., Isaacs, S., Decou, M.L., Richardson, E.A., Buffett, M.C., Slinger, R.W., Brodsky, M.H., Ciebin, B.W., Ellis, A., Hockin, A., 2000. Illness outbreak associated with Escherichia coli O157 : H7 in Genoa salami. Can Med Assoc J 162(10), 1409-1413.

Wolfrum, B., Mourzina, Y., Sommerhage, F., Offenhausser, A., 2006. Suspended nanoporous membranes as interfaces for neuronal biohybrid systems. Nano Lett 6(3), 453-457.

Xiong, G., Elam, J.W., Feng, H., Han, C.Y., Wang, H.H., Iton, L.E., Curtiss, L.A., Pellin, M.J., Kung, M., Kung, H., Stair, P.C., 2005. Effect of atomic layer

deposition coatings on the surface structure of anodic aluminum oxide membranes. Journal of Physical Chemistry B 109(29), 14059-14063.

Yang, L., Bashir, R., 2008. Electrical/electrochemical impedance for rapid detection of foodborne pathogenic bacteria. Biotechnol Adv 26(2), 135-150.

Yang, L.J., Li, Y.B., 2005. AFM and impedance spectroscopy characterization of the immobilization of antibodies on indium-tin oxide electrode through self-assembled monolayer of epoxysilane and their capture of Escherichia coli O157 : H7. Biosensors & Bioelectronics 20(7), 1407-1416.

Yang, L.J., Li, Y.B., Erf, G.F., 2004a. Interdigitated array microelectrode-based electrochemical impedance immunosensor for detection of Escherichia coli O157 : H7. Anal Chem 76(4), 1107-1113.

Yang, L.J., Li, Y.B., Griffis, C.L., Johnson, M.G., 2004b. Interdigitated microelectrode (IME) impedance sensor for the detection of viable Salmonella typhimurium. Biosens Bioelectron 19(10), 1139-1147.

Yang, L.J., Ruan, C.M., Li, Y.B., 2003. Detection of viable Salmonella typhimurium by impedance measurement of electrode capacitance and medium resistance. Biosens Bioelectron 19(5), 495-502.

Yu, J.J., Liu, Z.B., Yang, M., Mak, A., 2009. Nanoporous membrane-based cell chip for the study of anti-cancer drug effect of retinoic acid with impedance spectroscopy. Talanta 80(1), 189-194.

List of Publications

Journal Paper:

1. **Tan**, **F.,** Leung, P.H.M, Liu, Z.B., Zhang, Y., Xiao, L.D., Ye, W.W., Zhang X., Li Y. and Yang, M., A PDMS microfluidic impedance immunosensor for E. coli O157:H7 and Staphylococcus aureus detection via antibody- immobilized nanoporous membrane, Sensors and Actuators B-Chemical, 159(1), 328-335, (2011) (IF: 3.368)
2. Yang, M, and **Tan, F.,** Nanoporous membrane based biosensing application, Nanolife, (Invited review paper, In press)

Conference Proceedings

1. Tan F., Yu, J.J., Leung, P.H.M., Mo Yang., Rapid detection of bacteria with nanoporous alumina membrane based microfluidic chip, the World Congress on Biosensors 2010, Glasgow, Scotland, UK May 26-28, 2010